Hindcast tidal inlet Eastern Scheldt

Storms December 2001 and December 2003

Final Report

CG/1461/07542/A

20 December 2007

SVASEK HYDRAULICS

Schiehaven 13G
3024 EC Rotterdam
P.O.Box 91
3000 AB Rotterdam
The Netherlands
Ⓣ +31 - 10 - 467 13 61
Ⓕ +31 - 10 - 467 45 59
Ⓔ info@svasek.com
Ⓘ www.svasek.com

Document title	Hindcast tidal inlet Eastern Scheldt Storms December 2001 and December 2003
Short document title	Hindcast tidal inlet Eastern Scheldt
Status	Final Report
Date	20 December 2007
Project name	SWAN Hindcast tidal inlet Eastern Scheldt
Project number	1461
Client	WL | Delft Hydraulics
Reference	CG/1461/07542/A

Author Marloes van den Boomgaard, Caroline Gautier

CONTENTS

LIST OF TABLES

LIST OF FIGURES

LIST OF APPENDICES

1 INTRODUCTION

1.1 General

This report concerns the hindcast study of the SWAN wave model for two storms in the inlet of the Eastern Scheldt, including the selection of the storms. For this project Svašek Hydraulics is subcontractor to WL | Delft Hydraulics (subcontract with ref MCI-27367/H4918.27/JG dd October 12th, 2007). The overall client is Rijkswaterstaat. The project is part of the project “Strength and Loading of Coastal Structures" (SBW: Sterkte en Belasting Waterkeringen).

The work has been carried out by Marloes van den Boomgaard en Caroline Gautier. From WL | Delft Hydraulics, Jacco Groeneweg is involved.

1.2 Background

The SBW-project has the task of improving the models and methods used to derive the waves within the Hydraulic Boundary Conditions (HBC) for the primary sea defences along the Wadden Sea coast.

Among other activities this is achieved by performing hindcasts with the SWAN wave model of storm events in the Wadden Sea (for instance Alkyon 2007 , Royal Haskoning 2006 , WL| Delft Hydraulics, 2006).

In order to get more confidence in the performance of SWAN, additional hindcasts in comparable areas outside the Wadden Sea are carried out. The inlet of the Eastern Scheldt in the south west of the Netherlands is such an area, characterised by banks, tidal channels and shallow foreshore. Furthermore, waves have been monitored there since the 1980's.

The aim of this study is the performance of SWAN with respect to the wave penetration of combined swell and wind sea into the inlet of the Eastern Scheldt.

1.3 Approach

The study consists of three parts:
A) Data inventarisation and storm selection
B) SWAN hindcast
C) Analysis SWAN results and comparison with wave observations

ad A: Data inventarisation and storm selection
During the last three decades, wave observations have been carried out for the inlet of the Eastern Scheldt. Out of a number of severe storms two suitable storms are selected, based on the availability of wave data, additional metadata (wind, water levels, bathymetry) and particularly - as requested by the client - the occurrence of both swell and wind sea.

ad B: SWAN hindcast
For the SWAN hindcasts the model schematization is set up, wave boundary conditions is defined, the metadata are collected (bathymetry, wind, currents, water levels) and the input files are made. Next, the SWAN simulations are executed.

ad C: Analysis of SWAN results and comparison with wave observations
The results of the SWAN simulations are analysed and the results are compared with the observed waves. The comparison is both statistically and visually (graphs and scatter plots). Attention has been paid to the combination of swell and wind waves.

1.4 Set up of the report

An overview of the measurements is given in Chapter 2. In Chapter 3 the selection of the storm events is described. The set up of the SWAN simulations is subject of Chapter 4, and the results are presented in Chapter 5. In Chapter 6 the comparison of the simulations and the observations is given. In Chapter 7 additional simulations are described with alternative settings. Finally, in Chapter 8 conclusions are drawn and recommendations are given.

2 MEASUREMENTS

2.1 Introduction

This study focusses on the question: To what extent does the numerical wave model SWAN simulate the wave penetration of combined swell and wind sea into the inlet of the Eastern Scheldt correctly?

In order to determine the reliability of the performance of SWAN in such situations, wave measurements near the inlet Eastern Scheldt are required as input for the model and for the comparison between measurements and model results afterwards. Besides wave measurements, also wind and water level observations are used in this study.

A description of the measurements used in this study is given in this chapter.

2.2 Measurements

2.2.1 General

During the last three decades, wave and wind observations have been carried out in and near the inlet of the Eastern Scheldt. The main source of the hydrometeo observations used in this study is the Monitoring System ZEGE (ZEeuwse GEtijdewateren) by Hydrometeo Centre Zeeland (HMCZ). This system started in 1980 and aims at the automatic collection, processing and validation of hydraulic and meteorological variables (wind, water temperature, salinity, water levels and wave parameters). It is run by order of the Directorate Zeeland of Rijkswaterstaat in the Netherlands. The system consists of 72 measurement locations (see figure 2.1). All data can be downloaded for free at www.hmcz.nl.

Apart from the ZEGE-data, data at locations Europlatform (EUR) and Lichteiland Goeree (LEG) (data received from Koos Doekes, RIKZ) is used. Three-hourly wind and wave data from the DONAR database were provided, completed with 10 minute wave spectra of the "Year database" of the North Sea Monitoring System.

2.2.2 Measurement locations

Measurement locations of monitoring system ZEGE

Figure 2.1 shows the 72 measurement locations of the monitoring system ZEGE. Note that not all locations provide wave data. First the area of interest is roughly selected (see blue square in Figure 2.1). This selection is based on the aim of this study (the performance of SWAN for the wave penetration of combined swell and wind sea into the inlet of the Eastern Scheldt. Subsequently the availability of the data in the area of interest is verified. Only at four locations long term wave measurements are carried out (see green circles in Figure 2.1). At some of these locations, wind and water level observations are available too, see Table 2.1.

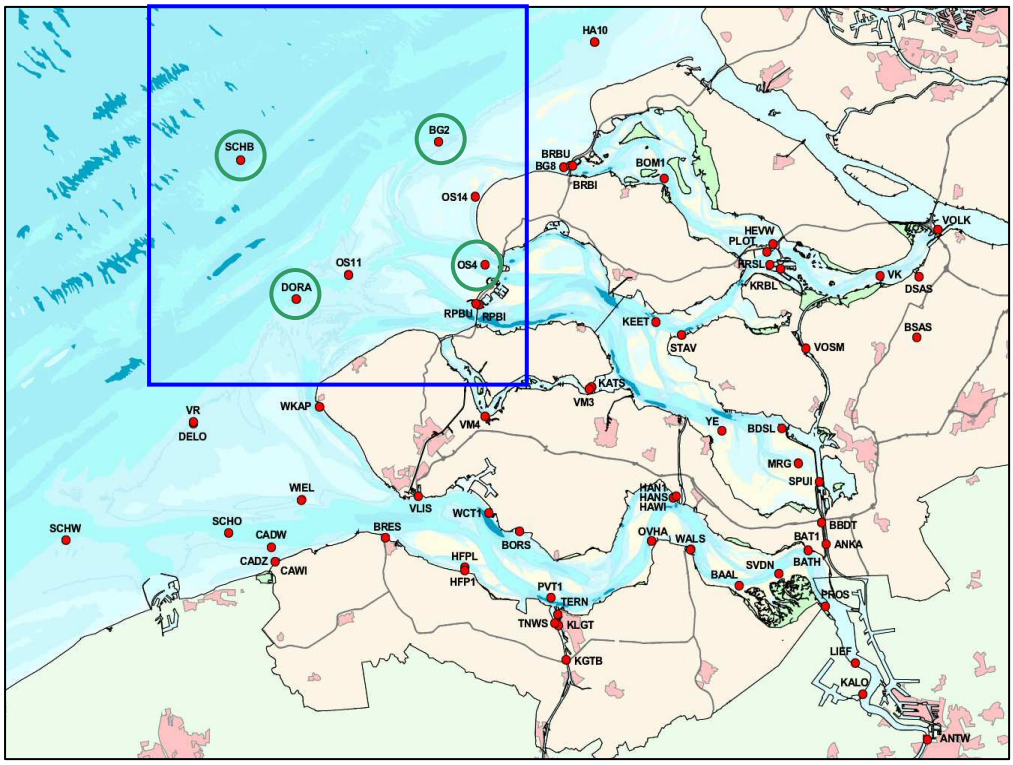

Figure 2.1: Measurement locations ZEGE (circles indicate suitable wave observations)

Additional measurement locations

Figure 2.2 shows the wave measurement locations (near the eastern Scheldt only) of the North sea Monitoring System. Again first the area of interest is roughly selected (see blue square in Figure 2.2). Three locations are in the area of interest, but the location “SCHB” is already selected in ZEGE. For this reason only two measurement locations are selected for this study (see green circles in Figure 2.2). At some of these locations, wind and water level observations are available as well, see Table 2.1.

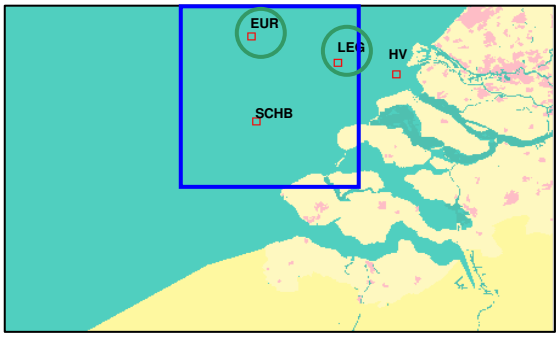

Figure 2.2: Available DONAR measurement locations near the Eastern Scheldt

Figure 2.3 shows the selected measurement locations. The color of the dots indicates the type of measurement.

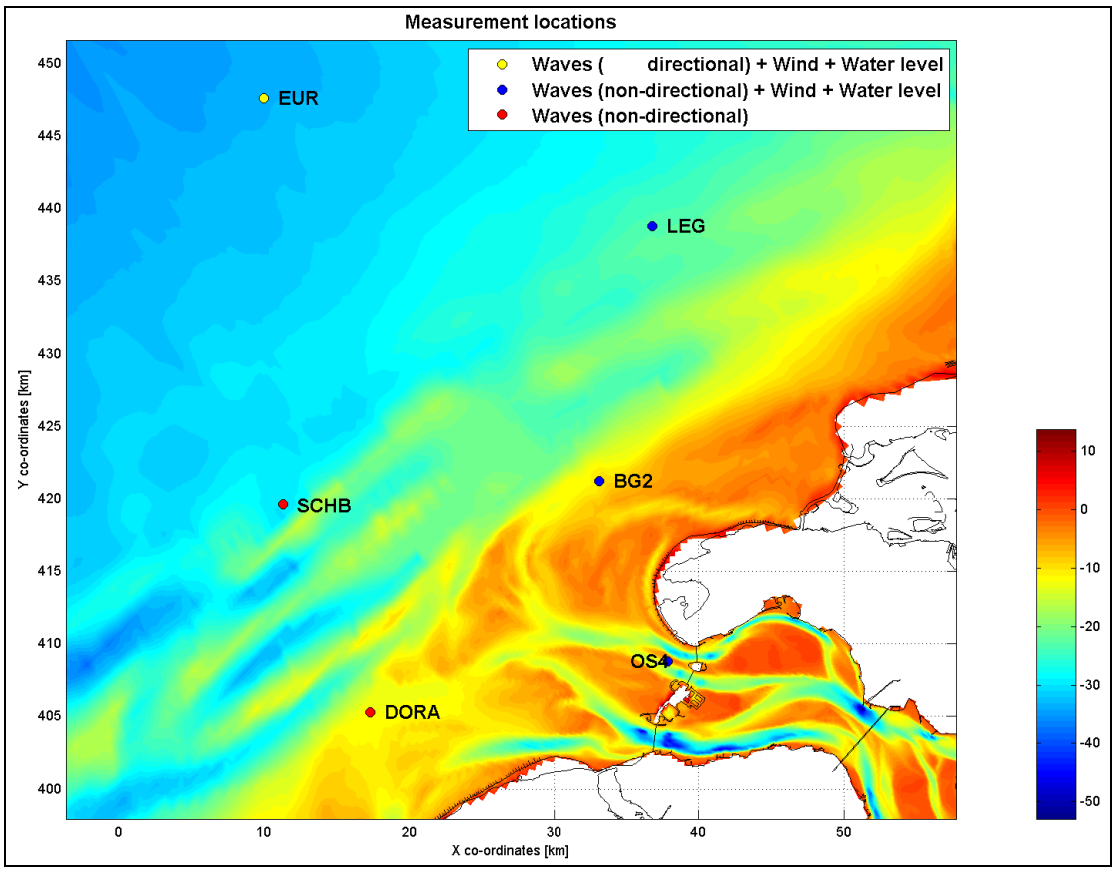

Figure 2.3: Selected measurement locations including the type of measurement

The exact position of the selected measurement locations, the kind of observation(s), the type of wave instrument and the local depths can be found in Table 2.1.

Location		Wave Instruments	X Coordinate (RD) [m]	Y Coordinate (RD) [m]	Depth [NAP +m]	Source	Wave measurements	Wind measurements	Water level
Europlatform	(EUR)	Directional waverider	9963	447601		North Sea	x	x	x
Lichtereiland Goeree	(LEG)	Saab radar.	36779	438793		North Sea	x	x	x
Schouwenbank	(SCHB)	Directional waverider	11332	419605	-20	ZEGE	x		
Brouwershavensche Gat 2	(BG2)	Step gauge	33140	421239	-11.32	ZEGE	x	x	x
Domburger Rassen	(DORA)	Non directional waverider	17325	405275	-12	ZEGE	x		
Oosterschelde 4	(OS4)	Step gauge ?	37837	408813	-9.25	ZEGE	x	x	x

Table 2.1: The measurement locations used in this study

2.2.3 Data files and parameters

At the four wave locations SCHB, BG2, DORA and OS4, the 1d-wave spectra (0-1.0 Hz) are available and several parameters. The time step is 30 minutes. There is no information on wave direction. The following wave data files are available:

- GHR2-files
- GSO2-files

A description of these data files can be found in Appendices 2.1 and 2.2.

At LEG the 1d-wave spectra and spectral wave parameters are available. There is no information on wave direction. At EUR, also directional wave information is available.

Wind data

For the locations BG2 and OS4 wind observations are available, both wind direction and several types of wind velocity among which the 10 minute scalar mean, corrected to 10 m above the sea surface. The time step is 10 minutes. The following wind data files are used from ZEGE:

- WNr2-files
- WIO2-files

A description of these data files is presented in Appendix 2.3.

Also at LEG and EUR wind velocity and wind direction is available.

Water level data

Water level observations with a 10 minute time step are available at BG2 and OS4. The following water level data files are used:

- WTr2-files
- WTO2-files

Appendix 2.3 shows a description of these data files.

Also at EUR and LEG water level observations are available.

3 STORM SELECTION

3.1 Approach

During the last three decades, wave observations have been carried out near the inlet of the Eastern Scheldt. Two suitable storms are selected, based on the availability of wave data, additional metadata (wind, water levels, bathymetry) and particularly - as requested by the client – the simultaneous occurrence of both swell and wind sea.

The selection of storm events consists of a primary rough selection followed by the final detail selection.

For the rough selection KNMI's list with high wind velocities over period 1982-2002 for station 312 (Oosterschelde) is used (see Appendix 3.1). Besides, "stormflitsen" by the SVSD were checked as well as a previous hindcast study in the Western Scheldt (Svašek Hydraulics, 2003) and the measurement report Western Scheldt 2003-2006 (Svašek Hydraulics, 2006). To prevent time consuming searches for older metadata it was decided to consider storms from 1990. The rough selection resulted into eight storms, see Table 3.1.

		position in KNMI's wind velocity list*	hindcast Western Scheldt (Svasek 2003)	measurement report Western Scheldt
1	23-29 Jan 1990	1		
2	23-28 Feb 1990	4		
3	26-30 May 2000	6	yes	
4	25-30 Dec 2001		yes	
5	25-28 Oct 2002	2	yes	
6	20-24 Dec 2003			yes
7	7-10 Feb 2004			yes
8	10-15 Feb 2005			yes

Table 3.1: Rough storm selection

Next, the availability of data of these storms was checked, and the 1d-wave spectra were checked on the presences of sea and swell waves (double peaked spectra).

The following criteria are defined:
- At least four locations with wave data east of and including SCHB must be available.
- Wave data at SCHB or nearby must be available (for boundary conditions)
- Wave data at BG2 or nearby (OS13) must be available
- At least one wave location near the Eastern Scheldt storm surge barrier must be available (OS4).
- Preferably wind coming from the north western quadrant (which makes it easier to position the computational grids in accordance with both wind direction and the depth contours (for uniform upwave boundary condition).
- A rather uniform wind velocity and wind direction in a time frame around the selected instant.
- Preferably a double peaked 1d-wave spectrum, if possible with a swell period larger than 10 seconds.

- In general high waves, preferably Hs>=1.0 m near the storm surge barrier (OS4).
- Some variation in water level and tidal phase between the selected moments.
- Wave spectra (2d) must be available at Europlatform (for offshore wave boundary conditions)

It turned out that double peaked spectra are rare, especially at the deeper wave locations. Most spectra with two peaks hold only a small amount of energy, and are therefore not suitable for hindcasting, three examples are presented in Appendix 3.2.

Unfortunately the perfect spectrum combing high swell with severe wind sea has not been found. However, two storms have been selected, each with three interesting moments (MET), see paragraph 3.2 and 3.3.

25- 30 December 2001:	26 December 2001 09:00
	26 December 2001 12:00
	29 December 2001 15:00
20-24 December 2003:	21 December 2003 13:30
	21 December 2003 16:00
	23 December 2003 02:30

3.2 Storm A: period 25 – 30 December 2001

In Figure 3.1 the development of the wave height H_{m0} for all the measurement locations, the water level at OS4, the magnitude of the current velocity at BG2 and the wind characteristics at BG2 are shown graphically. A detailed presentation of the time series and wave spectra of this storm can be found in Appendices 3.3 and 3.4.

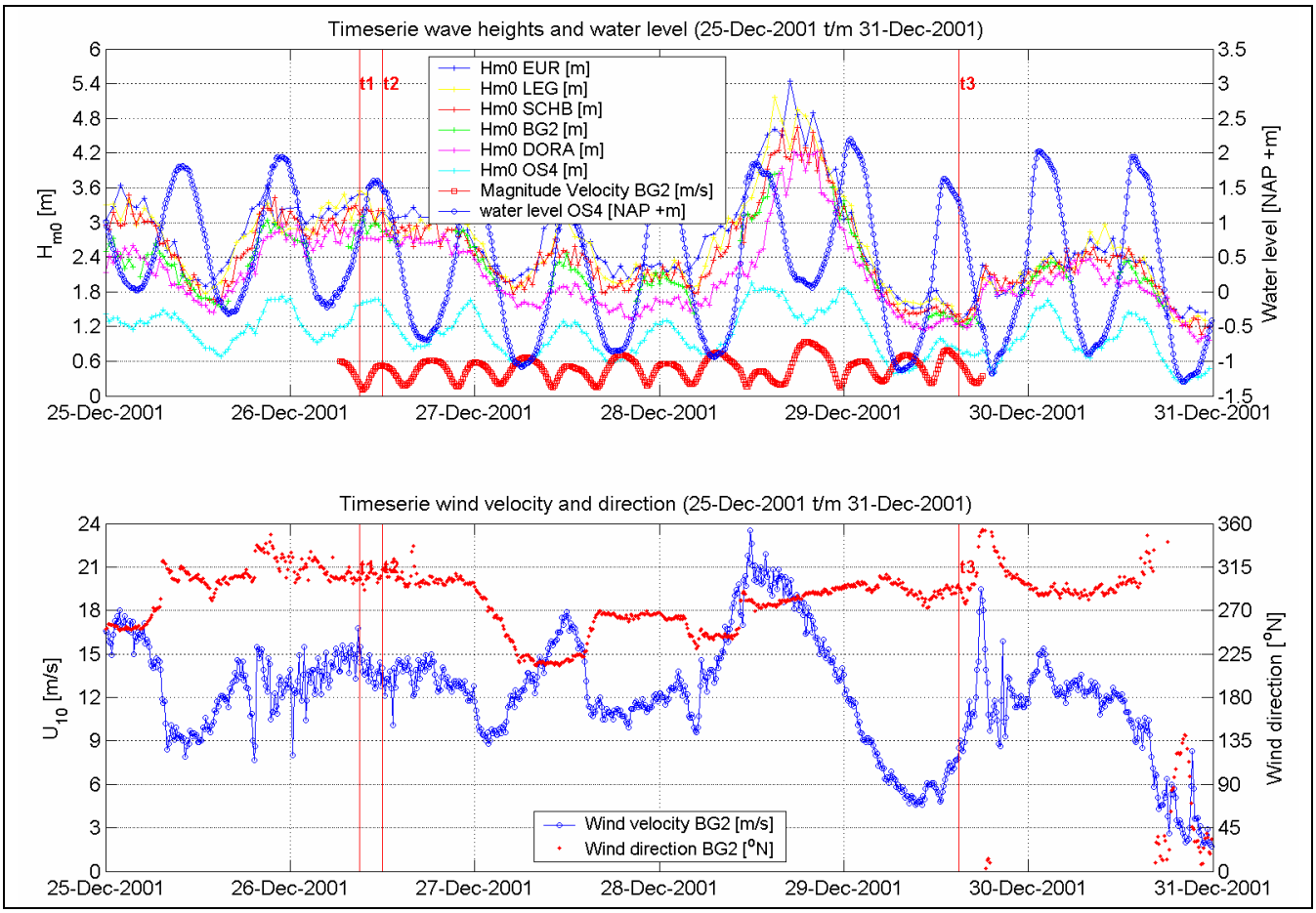

Figure 3.1 Time series of H_{m0}, water level, magnitude of the current velocity, wind of Storm December 2001

The storm of December 2001 reached maxima at the 28th of almost 24 m/s wind velocity and 5.4 m significant wave height at Europlatform (EUR). The selected moments are less severe, but rather chosen on spectral shape. Wave data is continuously available at five stations (EUR, LEG, SWB, DORA and OS4). At BG2 some wave data is missing during low water. Wave heights at OS4 vary with tide.

The three interesting moments of this storm are described below.

t1: 26 Dec 2001; 9:00

The constant wind is approximately 15 m/s from 310°. Both at SWB and at BG2 the wave spectrum has a main energy peak at approximately 8 seconds and a smaller low-frequency peak at approximately 14 seconds. Significant wave height for SWB is 3.1 m and at OS4 1.6 m. Water levels are rising thanks to a flood current at OS4. At BG2 it is more or less slack tide.

t2: 26 Dec 2001; 12:00

This is only 3 hours after the first simulation time. Wind has reduced slightly to 14 m/s, the direction is 307°. The spectra of both SWB and BG2 show a small energy peak at approximately 14 seconds, and a main peak at approximately 8 seconds. Note however that this shape is no longer visible at the most eastern station OS4. The significant wave height at SWB is 3.2 m and at OS4 1.6 m. At OS4 it is high water, and the current velocity is negligible. At BG2 flood velocities are approximately 0.5 m/s, to the northeast.

t3: 29 Dec 2001; 15:00

At this moment, the storm seems to be over. The wind has reduced to only 8 m/s, with a direction of 295°. As a result, the waves are much lower than during the other two moments (the significant wave height, at SWB and OS4 is 1.4 m respectively 0.8 m). However, the reason for selecting this time is the spectral shape at SWB and BG2, with a main peak at approximately 8 seconds, and a smaller peak at approximately 2 seconds. The tidal phase is more or less equal to t2; slack tide and high water at OS4 and flood flow at BG2.

3.3 Storm period 20 – 24 December 2003

In Figure 3.2 the development of the wave height H_{m0} for all the measurement locations, the water level at OS4, the magnitude of the current velocity at BG2 and the wind characteristics at BG2 are shown graphically. A detailed presentation of the time series and wave spectra of this storm can be found in Appendix 3.5 and 3.6.

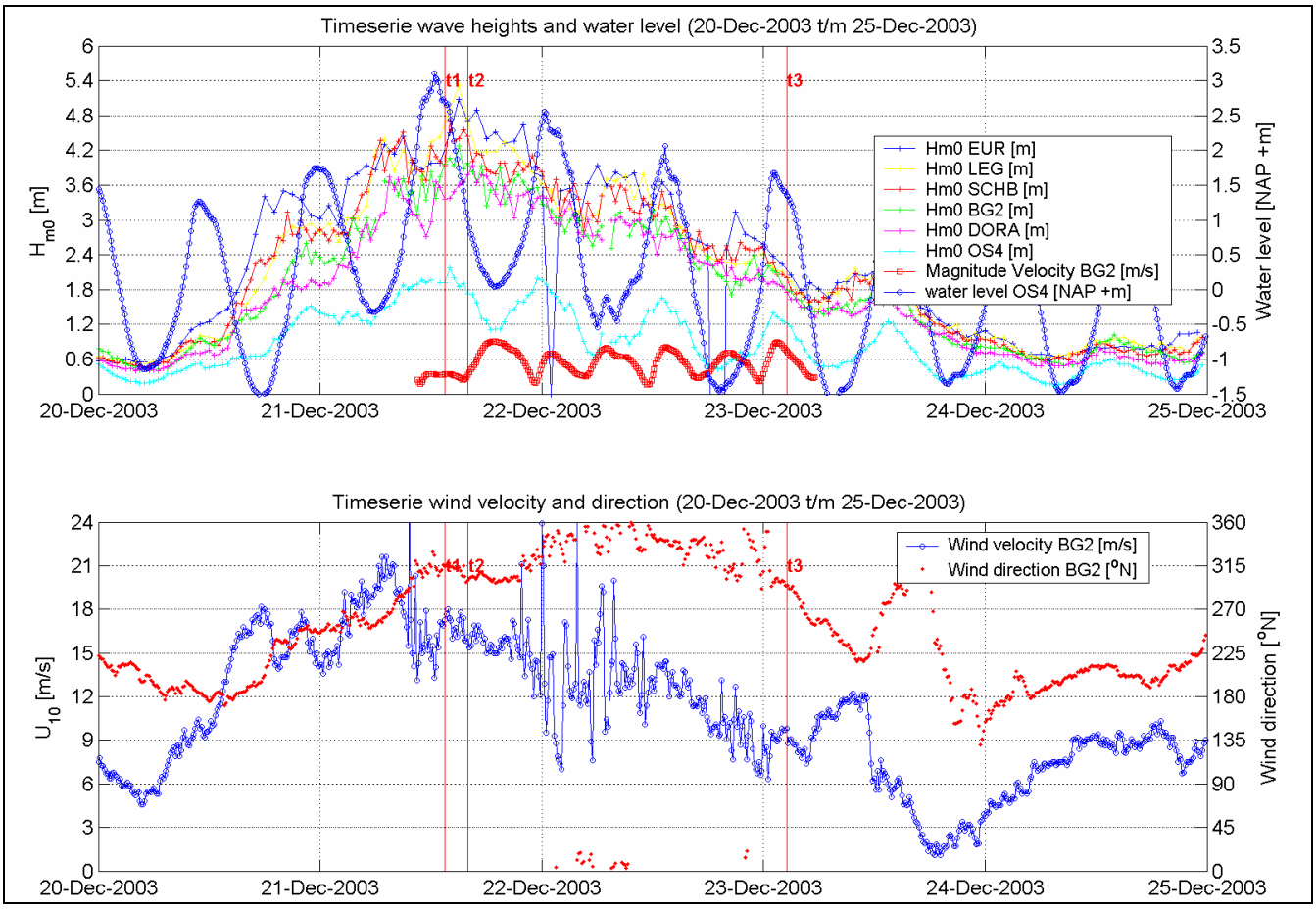

Figure 3.2 Time series of H_{m0}, water level, magnitude of the current velocity, wind of Storm December 2003

The (north-) north western storm caused high water levels and high waves. This combination gave especially at the most eastern location OS4 relatively high waves.

During this event the Eastern Scheldt barrier has been closed from 9:00 to 16:00 on December 21st, 2003.

The three interesting moments of this storm are described below.

t1: 21 Dec 2003; 13:30
The wind is approximately 16 m/s and has turned from S to NW during the last 24 hours. The significant wave height at SCHB is almost 4 m. At OS4 it is still 1.9 m. The water level has just had its maximum at OS4 (>NAP+3 m), the current velocity is small.

t2: 21 Dec 2003; 16:00

Wind speed and direction is almost the same as t1 which is only a few hours earlier, but the water level has decreased. Therefore, the wave height at OS4 has reduced from 1.9 m to 1.7 m while the western wave stations show larger waves than at the previous simulation moment. At SCHB the H_{m0} is 4.4 m. Both at SCHB and BG2 the energy spectrum shows peaks at 12 s and 8 s. At OS4 the flow is maximum (for that tide; approximately 0.5 m/s) and directed out of the estuary (going to approximately 300°), water levels are falling.

t3: 23 Dec 2003; 2:30

At this moment the wind comes rather from WNW and has dropped to approximately 9 m/s. The significant wave heights at SCHW and OS4 are respectively 2.0 m and 1.2 m. At OS4 it is slack tide, the currents at BG2 are to the NE.

4 SWAN SIMULATIONS

4.1 Introduction

This chapter describes the model setup, including the choice of the computational grids (section 4.2), the used physics (section 4.3), the boundary conditions (section 4.4), the bathymetry (section 4.5), the water level and current fields (section 4.6), the wind (section 4.7), and the model output (section 4.8).

4.2 Computation grids

In order to establish the performance of the numerical wave model SWAN, especially the penetration of the wave energy of combined swell and wind sea into the inlet of the Eastern Scheldt, a comparison of the SWAN results with the measurements is needed. This means a finer grid resolution in the areas with higher bottom gradients. Because of the limitations of the SWAN model nesting of the grids is required. Therefore five computational grids are used for the SWAN simulations (See Table 4.1 and Figure 4.1):

	Computational grid	Resolution	X length [m]	Y length [m]	Number of grids
1	North Sea (N)	400 m x 200 m	106800	24600	268 x 124
2	Coast (K)	200 m x 200 m	94000	28800	471 x 145
3	BG2 (B)	50 m x 50 m	15000	20000	301 x 401
4	DORA (D)	50 m x 50 m	15000	20000	301 x 401
5	Fine (F)	20 m x 20 m	4300	6000	216 x 301

Table 4.1: Definition of the computational grids

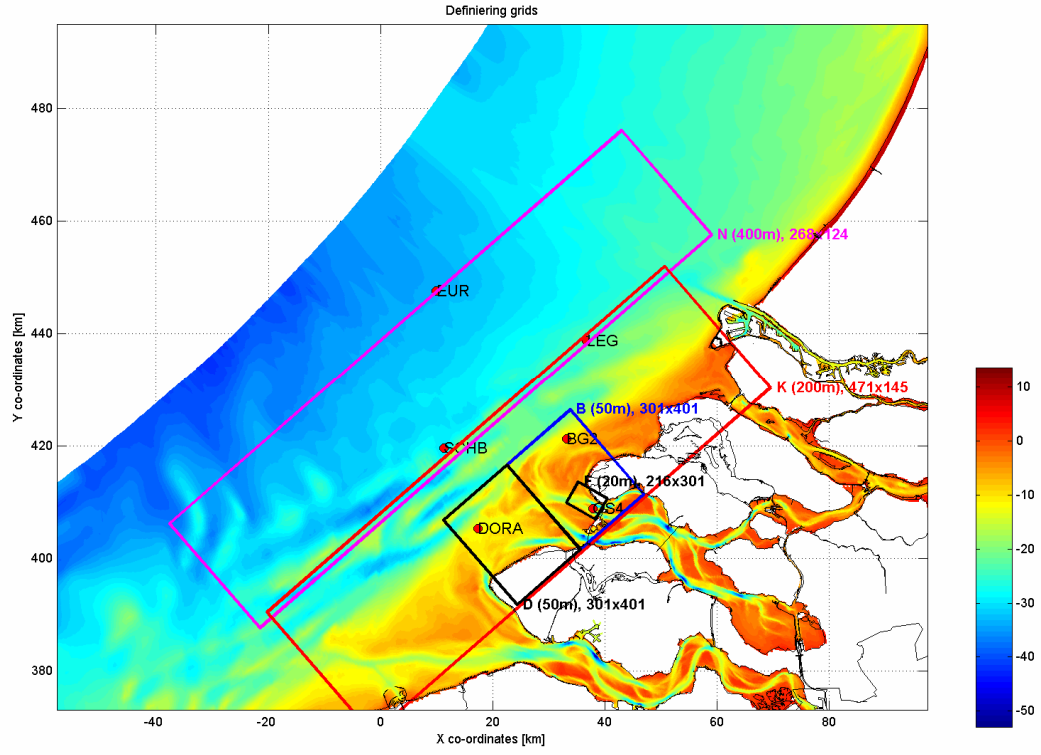

Figure 4.1: The Computational grids

The considerations which have led to these five computational grids are:

Coastal grid (K)
First the K-grid is defined which contains the area of interest and the offshore boundary near the measurement locations SCHB and LEG, which have been used for the boundary conditions (see paragraph 4.4).

The orientation of this grid is set parallel to the deep water depth contour lines (see figure 4.1), to avoid strong variations in wave conditions along the boundary due to bathymetry changes. Besides this orientation is nearly perpendicular to the wind directions of the selected moments which lies between 295-310^{o} N.

Only the northwest border of this K-grid is used as an input boundary for the simulations. Therefore the length of this northwest border is determined in such a way that the northeastern and southwestern boundaries do not affect the three nested grids (B, D and F).

The resolution of this grid is set to 200 m x 200 m. The simulations with this K-grid generate the boundary conditions for the nested B- and D-grids.

Since the interest is in combined swell and wind sea, not a parametrised spectrum but a fully 2d-spectra is needed at the offshore boundary. Unfortunately, no directional information is available at the locations SCHB and LEG. To compute the wave direction at SCHB and LEG an extra grid is developed. This grid is the North Sea grid (N) and has an offshore deep water boundary through Europlatform (EUR). At this location 2d-spectra are available.

North Sea grid (N)
This grid is only used to obtain wave directional information at the locations SCHB and LEG. The orientation of this N-grid is equal to the orientation of the K-grid (for the same reasons). The resolution in y-direction (SE to NW) is 200 m. In x-direction (SW to NE) the bathymetric variations are less and the resolution is set to 400 m.

The 2d-spectra measured at EUR are imposed at the offshore boundary. As for grid K-grid no boundary conditions are applied on the northeast and southwest boundary. Therefore the length of the deepwater boundary is determined in such a way that the erroneous boundary conditions at the northeastern and southwestern sides of the domain have no influence on the results at SCHB and LEG.

The wave directions computed at SCHB and LEG are added to the measured 1d-spectra at SCHB and LEG which gives the 2d-spectra. These 2d-spectra are used as boundary conditions for the simulations with the K-grid (see paragraph 4.4).

BG2 and DORA grid (B & D)
For wave simulations at the measuring locations DORA and BG2 a computational resolution of 50 m x 50 m is applied. Hereto, the nested grids B & D are defined, which

receive their boundary conditions from the coarser run on the K-grid. Besides, this finer resolution was needed for the transition between the K-grid (200m x 200m) and the F-grid (20 m x 20 m).

The B-grid computes the boundaries for the detail grid at OS4. The purpose of the D-grid is not only to compute the waves at location DORA for comparison with the observations, but also to obtain the wave field in the entire area in front of the barrier.

Fine Grid (F)
This grid is located in the mouth of the Eastern Scheldt. The bottom gradients in this area are large and for a good comparison of the measured data in OS4 with the SWAN results a fine resolution is needed which is chosen to be 20 m x 20 m. The orientation of this grid is selected to be in line with the channel (see Figure 4.1). The boundary conditions of this F-grid are obtained from the coarser B-grid.

4.3 Physical settings

The simulations are performed with the third-generation wave model SWAN, which is developed by the Technical University Delft. The most recent version 40.51AB is used for the SWAN simulations. For details see the SWAN User Manual.

The following physical settings are applied:

- GEN3 WESTH
  The computations run in third-generation mode for wind input, quadruplet interaction and whitecapping. Whitecapping is simulated according to the formulation proposed by Van der Westhuijsen et al. (2007), with nonlinear saturation-based whitecapping (Alves and Banner, 2003) combined with wind input of Yan (1978).

- QUAD
  The non-linear quadruplet wave-wave interactions are activated in the computations, which is the default formulation in SWAN (DIA).

- TRIAD trfac=0.05
  The wave-wave interaction is activated in the computations using the Lumped Triad Approximation (LTA method). The default values of Triad are used.

- BREAKING alpha=1 gamma=0.73
  The depth-induced wave breaking is modeled according to Battjes and Janssen (1978), which is default in SWAN

- FRICTION JONSWAP CFJON=0.067
  The bottom friction is activated in the computations using the JONSWAP formulation. The default values are used.

4.4 Numerical settings

- The spectral directions cover the full circle and the spectral directional resolution is set to 10 ° (36 sectors).
- The frequency range is going from 0.03 Hz to 1.0 Hz with 37 frequencies.
- The convergence criteria are set to rather strict criteria (this is recommended in WL| Delft Hydraulics, September 2007). The following command is applied:

  NUM STOPC 0.00 0.01 0.001 99.5 STAT mxitst = 80 alfa =0.0

  which means that SWAN stops the iteration process if the relative change in the local significant wave height from one iteration to the next is less than 0.01 and the curvature of the iteration curve of H_{m0} normalized with H_{m0} is less than 0.001:

$$\frac{\left|H_{m0}^{n}(i,j)-H_{m0}^{n-1}(i,j)\right|}{H_{m0}^{n-1}(i,j)}<0.01$$

  and

$$\frac{\left|H_{m0}^{n}-(H_{m0}^{n-1}+H_{m0}^{n-2})\right|+H_{m0}}{2H_{m0}^{n}}<0.001, \qquad \text{n=3, 4,.....}$$

  These conditions must be satisfied in at least 99.5% of all wet grid points before the iterative process stops or the maximum number of iterations is achieved. The maximum number of iterations is set to 80. Under-relaxation is not applied (alfa=0), because this could stop the process too early.

4.5 Boundary conditions

Figure 4.2 shows the position within the five computational grids where wave boundary conditions are applied.

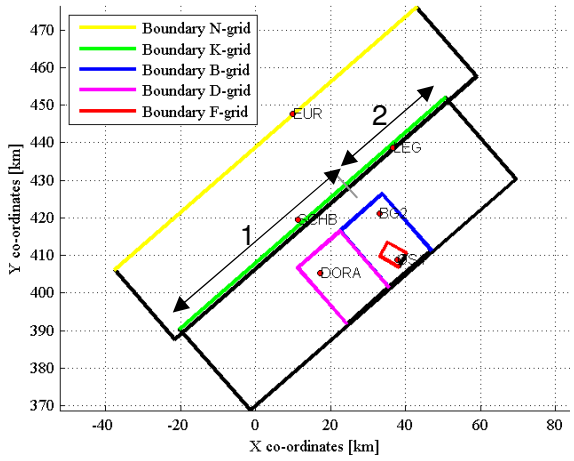

Figure 4.2: The locations of the used wave boundaries

The SWAN computations are carried out in a train of nested grids, each providing wave boundary conditions for the next computational grid. The F-grid receives the boundary conditions from the B-grid. The B-grid and D-grid both get their boundary conditions from the K-grid. Part of the boundary conditions for the K-grid is provided by the computations on the N-grid.

The K-grid is the first one in the train. Its deep water boundary is close to the measurement locations Schouwenbank (SCHB) and Lichteiland Goeree (LEG). These wave observations are applied as boundary conditions for this grid. However, since no observed wave directions are available here, an additional SWAN run is defined to compute the wave directions at the deep water boundary of the K-grid. Combining the computed directions and the observed 1d-energy density makes it possible to apply 2d-spectra as boundary conditions of the deep water side of the K-grid.

The offshore boundary of the K-grid consists of two parts, indicated by the arrows in figure 4.2. The boundary of the first part consists of the measured 1d-spectra at SCHB filled up with the directional information obtained from the simulations with the N-grid. The boundary of the second part consists of the measured 1d-spectra at LEG filled up with the directional information obtained from the simulations with the N-grid. The discontinuity that the two different sections on the upwave boundary cause is small and disappears quite soon within the computation on the K-grid. It could have been prevented by letting SWAN compute the spectrum between LEG and SCHB with a spectral interpolation technique (see SWAN user manual).

The N-grid has an offshore deep water boundary (blue line) through Europlatform. At this location observed 2d-spectra are available. However, the representations of observed and computed spectral information differ. The measured spectra are provided as energy density, mean wave direction θ and directional spreading σ as a function of frequency. These frequencies are linearly distributed in the interval 0.01 (or sometimes 0.03) Hz - 0.5 Hz with a resolution of 0.01 Hz. The SWAN spectra are given as a function of frequency and direction, where the frequencies are geometrically distributed in the interval 0.03 Hz – 1.0 Hz and the directions are steps of 10° distributed over the full circle. The measured spectra have been transformed to 2d-spectra in the same format as the computed spectra.

The process to transform the measured 2d-spectra to the fully 2d-spectra is as follows, based on WL| Delft Hydraulics (September 2007). First, the measured energy density, mean direction and directional spreading are interpolated to the frequency domain of SWAN. The directional distribution per frequency is reconstructed using a directional distribution:

$$D(\theta) = A_s \cos^{2s}(\theta - \theta_o)$$

Where

A_s = a normalisation coefficient $A_s = 1/2\sqrt{\pi}.\Gamma(s+1)/\mathrm{T}(s+1/2)$

θ_o = the frequency dependent mean wave direction

s = the spreadings factor $s = 2/\sigma^2 - 1$

σ = the directional spreading

Γ = the gamma function

The 2d-spectra are written to a data file in the SWAN format. Note that the interpolation from the measured frequencies to the SWAN-frequencies may introduce small inaccuracies in the order of 1 or 2 cm and peaks may be smoothed, see Appendix 4.1.

To add directions to the observed 1d-spectra at SCHB and LEG, the observed energy per frequency is distributed over the directions with the same proportions as SWAN computed at these locations.

4.6 Bathymetry

The bathymetry for the inlet of the Eastern Scheldt and surrounding area is obtained from various files and sources in order to cover the whole area of interest with the most recent data for the years of the selected storms (2001 and 2003). The following sources/files are used:

1. depth soundings preformed by RIKZ in 2001 (gr2001.asc)
2. depth soundings preformed by RIKZ in 2004 (gr2004.asc)
3. Data from the Kuststrook model

The bathymetry of these files is shown in Appendix 4.2. It should be noted that the data in the files are not covering the same areas. Therefore the bathymetry of both storms is generated hierarchically:

Storm A (2001): First the file with data nearest (in time) to the 2001-storm event is used, i.e. gr2001.asc. The data of the Kuststrook model is supplemented to cover the whole area.

Storm B (2004): First the file with data nearest (in time) to the 2003-storm event is used, i.e. gr2004.asc. Subsequently, this bathymetry is complemented with the bathymetrical data of 2001 (gr2001.asc). The data of the Kuststrook model is used to fill remaining gaps in the computational area.

The final bathymetry of the computational grids can be found in Appendix 4.3.A and 4.3.B for storms A and B respectively.

4.7 Water level and current fields

The water levels and currents are included in the SWAN computations, using non-uniform fields resulting from WAQUA simulations provided by RIKZ. The WAQUA simulations have been carried out on the "Kuststrook-fijn" grid and the boundary conditions have been generated using Kalman-filtering by Kuststrook-grof.

A graphical presentation of the obtained current fields can be found in Appendix 4.4. The water level fields are presented in Appendix 4.5.A and 4.5.B for storms A and B respectively.

As a check the computed water levels have been compared with water level observations at BG2 and OS4, and they agree well, see Appendix 4.6.

4.8 Wind

Each of the SWAN simulations is performed with a constant uniform wind speed and wind direction over the entire computational domain (grids K, D, B and F). The applied wind speeds and directions are based on visual averaging of the observed wind timeseries at LEG, BG2 and OS4 during a few hours before the selected moments. Visual averaging was preferred so that out layers are not taken into account and a more or less constant value can be determined. It should be noted that this wind is not always as constant as wished for stationary computations, see Appendix 4.7.

For the northern N-grid the wind as measured at EUR is representative. Far offshore the wind tends to be slightly higher than the wind at the other measurement locations. Table 4.2 shows the applied wind speed and direction for the different moments in the two storms.

	Storm A (December 2001)				**Storm B (December 2003)**			
	N-grid		K, D, B, F-grids		N-grid		K, D, B, F-grids	
	Wind velocity	Wind direction	Wind velocity	Wind direction	Wind velocity	Wind direction	Wind velocity	Wind direction
T1	16 m/s	310 °	15 m/s	305 °	18 m/s	317°	16 m/s	315 °
T2	13 m/s	315 °	13 m/s	312 °	17 m/s	300 °	15 m/s	300 °
T3	9 m/s	280 °	8 m/s	293 °	9 m/s	295 °	9 m/s	295 °

Table 4.2: The applied wind speed and direction for the different SWAN simulations

4.9 Output

Every simulation is characterised by a unique name, depending on the computed storm, time, physical or numerical settings and the computational grid. The simulation with the name AK2f refers to the computation of Storm A with the computational grid K for the second selected moment in storm A (see sections 3.3). The letter “f” refers to the physical and numerical settings as described in section 4.3 and 4.4 and these are the base settings in this study. This extra letter is needed because additional simulations with changes in the physical or numerical settings are performed in this study in order to investigate the sensitivity of some settings. These additional simulations are elaborated in chapter 7.

In order to see the development of the wave parameters along specific lines 6 curves are defined over which output is generated by SWAN. The starting point of each curve is defined at the offshore boundary of the N-grid and the end point of each curve is chosen at the coast or at the southeast boundary of the computational grid. The 6 curves are shown graphically in appendix 4.8.

Besides, three point-files are defined in order to see the swan output in specific locations, e.g.:

1) obs.pnt
   A file with the 6 measurement locations (EUR, LEG, SCHB, BG2, DORA, OS4). The wave parameters at these locations are requested in order to compare simulated waves with the observed waves at these locations.
2) dam.pnt
   A file with 9 output locations close to the Eastern Scheldt storm surge barrier
3) pnt.pnt
   A file with 8 output locations located on curve 6, which has the same direction as the deep channel near OS4 (see appendix 4.6)

Appendix 4.8 shows the defined curves and output points of the points-files.

For every simulation the following output is generated:
1. Spatial distribution of different wave parameters
2. Tables with wave parameters
3. 1d-spectra
4. 2d-spectra
5. Test output

Ad. 1
The spatial distribution (block files) of different wave parameters is generated as output. The following 17 parameters are written into block files:
XP, YP, DEP, HS, HSWELL, RTP, TM01, TM02, TMM10, DIR, DSPR, WLENGTH, DHSIGN, DRTM01, VEL, WATLEV, WIND.
A description of these wave parameters can be found in the SWAN user manual of SWAN.

Ad. 2
For each simulation tables are produced for the defined curves and point files (see appendix 4.6). Each table consists of the following wave parameters XP, YP, DEP, HS, HSWELL, RTP, TMM10, TM01, TM02, FSPR, DIR, DSPR, WLENGTH, TPS, DHSIGN, DRTM01, WATLEV, WIND, VEL.

Ad. 3
All the simulations provide 1d-spectra at the specific locations in the defined point-files.

Ad. 4
The simulations on the computational grids K and B provide 2d-spectra at the wave boundaries of the nested grids (see section 4.5). Besides all the computational grids generate 2d-spectra at all the specific locations in the point-files.

Ad. 5
In order to check the convergence behavior of the simulations extra test output is generated for the 6 measurement locations by using the TEST command. The test output produces intermediate results of the SWAN simulations, like the values of the wave height H_{m0} and wave period T_{m01} for each iteration.

5 SWAN RESULTS

5.1 Introduction

This chapter gives an overview of the results of the SWAN simulations. The comparison of the SWAN results and the observed wave data is not discussed in this chapter but in the next chapter (6) which also contains the wave spectra, both computed and observed.

In the appendices plots of the SWAN output are given. Both block-file plots on the computational grids are given, and wave parameters along curve 3 (from the deep water boundary of the K-grid to location OS4). In the appendices with block files the figure at the top shows the results of the simulation with the K-grid. In the middle figure the results of the simulations with the B- and D-grid are combined. At the bottom the results are presented of the simulation with the finest grid F.

The following plots are available:
Appendix 5.1: Convergence behavior H_{m0} and T_{m01} per simulated storm moment (SWAN test output)
Appendix 5.2 Iteration process on wet grid points for storm A and B (SWAN print file)
Appendix 5.3: significant wave height per simulated storm moment (SWAN block output)
Appendix 5.4: wave period $T_{m-1,0}$ per simulated storm moment (SWAN block output)
Appendix 5.5: 2d-energy density spectra
Appendix 5.6: SWAN parameters (H_{m0}, mean wave direction, $T_{m-1,0}$, Depth) on curve 3

5.2 Convergence behavior

The convergence behavior of these SWAN simulations is controlled by the curvature criterion (see section 4.4).

The actual convergence behavior of the simulations is checked using the TEST output. Appendix 5.1 presents per SWAN simulation per storm and per selected moment the values of the normalised wave height H_{m0} and wave period T_{m01} for each iteration. The normalisation is carried out by dividing the values with the values obtained in the last iteration per location.

Besides, a check was performed by using the PRINT files. One of the things written to this file is for each iteration the percentage of the wet grid point which has enough accuracy. Appendix 5.2 visualises this iteration process on the wet grid points of storm A and B.
Table 5.1 shows the number of iterations for the different SWAN simulations:

	Number of iterations of the SWAN simulations							
	Storm A				Storm B			
Moment	K-grid	B-grid	D-grid	F-grid	K-grid	B-grid	D-grid	F-grid
T1	24	39	17	30	37	36	16	12
T2	21	37	15	16	19	32	15	20
T3	80 (97.16%)	80 (98.91%)	28	15	80 (96.68 %)	80 (99.11%)	53	26

Table 5.1: Number of iterations of the SWAN simulations

Inspection of all the figures and table 5.1 showed that generally a sufficient number of iterations is performed. But for four simulations (t3 of Storm A and B for grid K and B) the convergence behavior after 80 iterations is still less than. It is clearly visible that for these simulations the convergence behavior is not univocal**,** but fluctuates from "hopeful" to "bad luck" (see appendices 5.7 and 5.8).

Based on the DHSIGN - and DRTM01- block files (presenting the difference in wave height and wave period as computed in the last two iterations; not shown here) the convergence in the area of interest is sufficient and therefore the results of these simulations are accepted.

5.3 Storm December 2001

The spatial distribution of the wave variables H_{m0} and $T_{m-1,0}$ of storm A can be found in respectively Appendix 5.3.A and Appendix 5.4.A. The development of different parameters (H_{m0}, wave direction, $T_{m-1,0}$, depth) along curve 3 is shown in Appendix 5.6.A.

It is convenient that the wind direction is more or less perpendicular to the depth contours so that there is not much variation in waves along the up wave boundary and the area with disturbed side effects is limited.

time t1

The current is weak because it is more or less slack tide, near the surge barrier velocities are only 0.3 m/s. The water level is around NAP+1.25 m at OS4 and NAP+1 m at BG2 (see appendix 4.5.A).

The offshore wave height is approximately 3.2 m. Wave breaking on the shallow outer delta causes dissipation of energy resulting in lower wave heights near the coast. The developments of the significant wave height along curve 3 (see appendix 5.6.A1) show that the reduction of the wave height starts gradually after 10 km. A significant and quick reduction of the wave height by 1.2 m is visible after approximately 14 km where the water depth reaches NAP - 5 m. After this quick reduction the wave height fluctuates between 1.7 m to 1.3 m. This fluctuation is caused by the banks and the deep channels which curve 3 crosses.

The wave direction is influenced by refraction due to local bottom gradients. The first changes of the wave direction along curve 3 are visible after approximately 14 km and at approximately 17 km the wave direction changes very fast with 50 degrees (from northwest to west). Further along curve 3, the wave direction turns to 320 ^{o} again, which probably is caused by refraction to the sides of the channel.

time t2

This moment has a lot of similarity with the selected moment t1 of storm A. Only the current velocities differ significantly, mainly in direction. At BG2 the flow velocities are approximately 0.5 m/s and are going to the northeast. At OS4 (near the surge barrier) the flow velocity is almost zero. The water level at both locations OS4 and BG2 is

around NAP+ 1.5 m. The offshore wave height is 3.2 m. The development of the significant wave height along curve 3 is almost the same as described at t1 it only differs on the following points:
- no increase of the wave height in the beginning of curve 3
- the significant rotation of the wave direction is 10 degrees less (330 to 290)
- the significant wave height at the end of the curve is 0.2 m lower.
- overall, the wave period along the curve is a little bit higher.

time t3
The flood current velocity offshore (near the offshore boundary of the K-grid) is the highest of the three selected moments of this storm and reaches a flow velocity of approximately 1 m/s. The flow velocity at OS4 is almost zero and at BG2 the flood velocity is approximately 0.6 m/s. The water level at both locations OS4 and BG2 is around NAP+ 1.3 m.

The wave heights at t3 are by far the lowest of the three selected moments. At BG2 the H_{m0} is approximately 1.2 m. The offshore wave height is 1.4 m which reduces gradually along curve 3 to 1.2 m at 14 km. The significant and quick reduction is missing at this moment, because of the lower waves, which won't break at these water depths. The wave height at the end of curve 3 is approximately 0.3 m. The shape of the development of the wave period is as from 14 km comparable with the other two moments.

5.4 Storm December 2003

The spatial distribution of H_{m0} and $T_{m-1,0}$ of storm B can be found in respectively Appendix 5.3.B and Appendix 5.4.B. The development of different parameters (H_{m0}, wave direction, $T_{m-1,0}$, depth) along curve 3 is shown in Appendix 5.6.B.

time t1
The flood currents (to the NE on the North Sea and to the east near the Eastern Scheldt surge barrier) are weak. The water levels are high, at OS4 around NAP+2.75 m and at BG2 around NAP+2.5 m.

The first 10 km there is hardly any change in wave height, period and direction, as the water depth varies from circa 30 to 15 m. Next, at the ebb delta where the water depth reduces to circa 5 m, wave energy is dissipated. The wave direction is influenced by refraction due to local bottom gradients. Starting with a wave height of circa 4 m at the upwave boundary of the K-grid, the wave height reduces as the waves propagate to the coast. In front of the Eastern Scheldt surge barrier, the significant wave height is approximately 1.5 m.

time t2
At moment t2 of storm B the waves are highest, well above 4 m and the $T_{m-1,0}$ is almost 9 s. There is an ebb current which reaches 1 m/s near the surge barrier. The water level at OS4 is around NAP+1.5 m and at BG2 around NAP +1.25 m. In this case the influence of the ebb delta is even larger than at t1, because of the lower water levels and hence smaller water depth. Here, between circa 10 and 15 km along curve 3, wave heights reduce considerably from ca 4.4 to 1.5 m. In the next 10 km (ending at OS4) the

wave height just varies with some 0.5 m. In this part there is no clear relation with the bathymetry visible in the curve plot of appendix 5.6.B2.
Where the wave height starts to reduce the wave period Tm-1,0 first shows some increase before reducing too. However, the period reduces more gradually than the wave height.
The wave direction varies considerably along curve 3, between 275 and 350°.

The spatial distribution of the significant wave height in front of the surge barrier (lower plot in Appendix 5.3.B2) shows the shoaling of the waves on the strong opposing current. The strong local increase in significant wave height is only observed for this moment, being the only moment with an opposing current.

time t3
At t3 the wind and wave conditions are less severe than in the previous two times. The significant wave height is ca. 2 m at the offshore boundary of the K-grid and ca 0.80 m at OS4. The ebb delta has less effect on these smaller waves than in t1 and t2. Between 10 and 15 km on curve 3 the wave height reduces now only some 30% whereas the reduction in t2 was rather 65%.

In the deeper parts of the computational area the current velocities are by far the strongest of the three selected moments of this storm. The current velocity at BG2 is around 0.8 m/s (at t1 and t2 it is around 0.3 m/s). The current velocity near the surge barrier the current velocity is weak and comparable with the current at t1. The velocity at OS4 is around 0.2 m/s.

The water level is around NAP+1.5 m at OS4 and NAP+ 1.25 m at BG2

6 COMPARISON MEASURED AND SIMULATED WAVE DATA

6.1 Introduction

The comparison of the SWAN results and the measured wave data concentrates on the 1d-spectra (Appendix 6.1 & 6.2), wave parameters H_{m0} and $T_{m-1,0}$ in scatter plots (Appendix 6.4) and several statistical parameters for H_{m0}, $T_{m-1,0}$, T_p and T_{m02} (Appendix 6.5 and 6.6). Additional plots of detailed SWAN block files surrounding OS4 can be found in Appendix 6.3.

Furthermore, Appendix 6.7 presents for the measuring locations the observed and computed wave parameters for each simulated moment. If a location is present in more than one computational grid, then only the result of the finest computational grid is considered.

Both the measured and simulated integral wave parameters have been computed from the 1d- spectra, both integrated over the frequency domain of [0.03 Hz – 1.0 Hz].

Note that t1, t2 and t3 refer to the simulated moment within the storm.

6.2 1d-Wave spectra

Appendix 6.1A and B show the measured and computed wave spectra for storm A and B. The three columns refer to the moment within the storm and the four rows represent the locations SCHB, BG2, DORA and OS4. The red dots indicate the computed wave direction which unfortunately can not be confirmed by observations.

• Storm A

Storm A is characterised by double peaked spectra at the offshore location SCHB. According to SWAN the direction where the longer waves come from is circa 330° whereas the shorter waves (5 seconds and less) tend to come rather from 270-310°, corresponding with the local wind direction.

Since SCHB is on the upwave boundary of the computational grid, it is not surprising that SWAN agrees well with the measurements here. Differences in spectral shape are mainly due to different frequency resolutions.

At BG2, some 12 km from the boundary, the spectral shape - including position of the peaks - is represented fairly well. At t1 SWAN overestimates the wave height. SWAN computes even higher waves than at SCHB whereas the measurements show a slight decrease in wave height. At t2 and t3 the difference (2 respectively 1 cm) is less than 1%. At this location the low frequency peak is slightly overestimated, resulting in an overestimation of wave period $T_{m-1,0.}$ (also indicated in the plots of appendix 6.1).

For DORA, which is approximately 18 km from the boundary holds more or less the same as for BG2: Good representation of spectral shape, very good agreement of significant wave height for t2 and t3 and an overestimation by SWAN for t1. The energy at the lower peak frequency is not overestimated anymore. At t1 and t2 the amount of energy at the low frequency peak is almost similar as measured, but at t3 the energy at

the low frequency peak is half the measured energy. Still, the period $T_{m-1,0}$ is represented well by SWAN.

At OS4 the amount of wave energy is only a quarter of the amount of energy at SCHB, and the wave height has been halved. Still the representation in terms of significant wave height is very good for t1 and t3 (1 cm difference) and reasonable for t2. The wave period $T_{m-1,0}$ differs significantly (around 1 s difference).

However, the shape of the computed spectra does not agree with the observations. The high frequency flank is represented quite well but for the frequencies below 0.2 Hz (5 seconds) SWAN strongly underpredicts the amount of wave energy. SWAN does compute a small energy peak (0.1 m^2/Hz) at approximately 0.08 Hz, but according to the observations this should be 4 times as high. This holds for all 3 simulated moments. It is obvious that OS4 is the most difficult location of the four considered.

Here, the waves coming from the North Sea propagated over a shallow foreshore for a couple of kilometers and passed large bottom gradients and strong current gradients. Nearshore processes like refraction, triads, bottom friction and possibly wave breaking have had their influence on the spectrum. Furthermore, its position on the slope of the channel makes a good representation harder.

In order to observe the development of the spectral shape in more detail the 1d-wave spectra of five points along curve 6 have been plotted in Appendix 6.2.A&B for t3. It is clearly visible that the energy at the low frequency reduces significantly from point 5 to 4, but the spectra are still double peaked with much more energy at the low frequency in comparison with the energy at the higher frequency peak. At point 3 the energy at the low frequency peak is less than half the energy at point 4. The higher frequency peak is still of the magnitude originally computed at SCHB. The spectra at 2 and at OS4 are similar. The low frequency peak has almost disappeared and the high frequency peak has reduced slightly.

Additional attention has been paid to OS4 by checking the spatial variation of depth, significant wave height and period Tm-1,0, see Appendix 6.3 (storm A only). The left-hand pictures show the water depth and one can see OS4 on the northern side of the channel. Gradients are about 1:40. The grid size of the computational grid is 20 x 20 m. Considering a circle with 100 m radius and OS4 in the center, the maximum variation in Hs is about 0.1 m (plots in middle column) and in period 0.5 s (right hand pictures). Based on this variation in parameters, it is unlikely that within this circle SWAN computes spectra that agree considerably better with the observations than the presented spectra do. The variations are sufficiently small to consider the measuring location of OS4 as suitable.

Also in previous studies it was observed that SWAN tends to underestimate the wave energy at the lower frequencies and hence the wave period (for instance Svašek Hydraulics 2003). It seems that SWAN exaggerates the triad interactions, as also noticed in ref WL | Delft Hydraulics September 2007 "Storm hindcasts for Wadden Sea". In Chapter 7 additional attention will be paid to the triads.

• Storm B

Strom B has been selected for its high waves (4.44 m at SCHB), but the shape of the spectra is in most cases simpler than in storm A.

Starting at t1, even at SCHB some differences in observed and computed spectra can be seen. This is mainly due to the different frequency resolutions. The observed steep peaks at 0.1 Hz and 0.13 Hz have been smoothed during the interpolation to the SWAN input spectrum. The total amount of energy however, is more or less equal in the observed and the SWAN spectrum.
At BG2 and DORA SWAN simulates the spectral shape at t1 quite well. But at OS4 which is furthest from the upwave boundary, SWAN underestimates the wave energy with frequencies below ca. 0.15 Hz considerably. The significant wave height is represented well here at t1. The wave period $T_{m-1,0}$ differs at OS4 with 0.7s (ca 10%).

The double peaked spectra measured at SCHB can be observed in the SWAN results as well. The measured spectra at BG2 and DORA are still more or less double peaked but the SWAN spectra consist of only one peak. This peak is at both locations close to the low frequency peak of the measured spectra. The maximum energy at this frequency is comparable with the measurements. This can also be observed in the small difference in the wave period $T_{m-1,0}$. The total amount of energy is slightly overestimated by SWAN, resulting in a small overestimation of wave heights (H_{m0}) at BG2 and DORA. At OS4 SWAN misses again a significant amount of low frequent energy resulting in an underestimation of both wave height and period. At t2 also the strong ebb current may play a role in SWANs minor performance here.

At t3 the waves at SCHB are circa half as high as during t1 and t2. At BG2 SWAN computes more wave energy than the observations show. In addition SWAN computes a single peaked spectrum at DORA instead of the double peaked spectrum measured. The SWAN wave height (H_{mo}) at DORA is in agreement with the measured wave height H_{m0}. Finally at OS4 we see again a severe underestimation of the lower frequencies resulting in a wave height and period that is much smaller than observed.

Appendix 6.2B shows the 1d-spectra of five points along curve 6 for the third selected moment of this storm. The development of the spectra along the curve is comparable with the development of the spectra along curve 6 of the third moment of storm A (Appendix 6.2.A). The low frequency peak is underestimated more and more along the curve. The energy at the higher frequency peak hardly changes and is more in agreement with the measured peak. This is visible in the wave period $T_{m-1,0}$ as well.

6.3 Scatter plots

The scatter plots can be found in Appendix 6.4.a (H_{m0}) and 6.4.b ($T_{m-1,0}$). The dashed line is the line y = x and the black line is the fit given by y = ax + b. Also the correlation coefficient r is given.

As the different markers in the scatter plots represent the various wave locations, one can see whether one location is represented better than the other.

• H_{m0}

The representation of the significant wave height by SWAN is very good, not only for the higher waves (closer to the upwave boundary) but also for the lower waves. In general the higher waves (above 3 m) are slightly overestimated whereas the lower waves are slightly underestimated.

There is no obvious sign that one of the measurement locations is represented in terms of significant wave height far better or worse than the other.

The correlation coefficient r and the values of a and b are for storm A and B almost similar.

• $T_{m-1,0}$

The agreement between SWAN and observations for the spectral period $T_{m-1,0}$ is not so good. Mainly because of SWAN's underestimation of period at OS4 by circa 1.5 seconds the fit through the data points is far from the line y = x and the correlation coefficient is only 0.93 respectively 0.91. At the other stations the performance of SWAN with respect to the wave period $T_{m-1,0}$ is quite good. There is not much difference between the scatter plots of storm A and B.

6.4 Statistical analysis

Appendix 6.5 gives a number of statistical parameters for the wave parameters H_{m0}, T_p, $T_{m-1,0}$ and T_{m02}. In the lower table both storms are taken together. The other two tables are for storm A and storm B respectively. The number of observations (4 locations x 3 times = 12 per storm) is small for proper statistical analysis.

A description of the statistical parameters can be found in Appendix 6.6.

• H_{m0}

As seen before in this chapter, the agreement between SWAN results and observations is very good for the significant wave height. The bias (difference between the mean of SWAN and the mean of the observations divided by the latter) is only 0.2%. The standard deviation is 6.5%. The mean absolute error is 3.9%.

• T_p

Of the four wave parameters considered T_p is represented the least, which is not surprising having seen the wave spectra (Appendix 6.1). The peak period is not such a suitable parameter to assess the performance for, especially with the "grassy" observed spectra at OS4. The bias is -9.5% (indicating underestimation of SWAN) and the mean absolute error is 16.2%. The standard deviation is large with 22.6% and the correlation coefficient is very small being 0.46.

• $T_{m-1,0}$

The bias, mean absolute error and correlation coefficient seem to be quite good (resp -2.6%, 7.6% and 0.93) but the large standard deviation (10.5%) indicates that SWAN still has difficulties with the prediction of the wave period.

• T_{m02}

This wave parameter is included in the statistical analysis in order to see whether the better representation of the higher frequencies than the lower frequencies (see Appendix 6.1 and Paragraph 6.2) results in good statistical values for the T_{m02}. Indeed the standard deviation (7.7%), mean absolute error (6.8%) and correlation coefficient (0.96) are better for T_{m02} than for the other types of periods. The bias (-2.9%) is almost equal to the bias of $T_{m-1,0.}$

7 ADDITIONAL SIMULATIONS

7.1 Introduction

Chapter 6 showed that the spectra at location OS4 differ significantly from the measured spectra. In order to see if it is possible to compute a spectrum at OS4 which is more in line with the measured spectrum additional simulations are performed, by changing some numerical or physical settings. These simulations are described in this chapter. They differ from the base computations in bottom friction (Paragraph 7.2), triads (Paragraph 7.3) and directional resolution (Paragraph 7.4).

7.2 Bottom friction (case g)

In the base case of this study (case f) the dissipation by bottom friction is modeled by the JONSWAP formulation, which is a semi-empirical expression. The proportionality coefficient of the bottom friction is set to 0.067 m^2s^{-3}, which is advised for wind sea.

All the simulations with this base case show a disagreement of the shape of the computed and the observed spectra at OS4 (see Appendix 6.1). The high frequency flanks are represented quite well but at the low frequencies the wave energy is underestimated by SWAN. This may be due to the relatively high bottom friction.

For this reason a new case “g” is generated. Only the bottom friction coefficient is changed in this case by comparison with the base case. The proportionality coefficient of the bottom friction is set to 0.038 m^2s^{-3}, which is advised for swell conditions (see SWAN user manual). With this lower bottom friction especially the low-frequency waves are dissipated less.

The results of this case (g) are visualised by the measured and computed wave spectra of storm A and B and are presented in Appendix 7.1. The three columns refer to the moment within the storm and the four rows represent the locations SCHB, BG2, DORA and OS4. The red dots indicate the computed wave direction.

As expected the reduction of the bottom friction coefficient only affects the results inshore. The energy at the high frequent flanks is approximately equal to the energy computed with the base case. The energy at the low frequency is slightly higher than in the base case, but still far from the amount of wave energy observed at the low frequency.

It can be concluded that the simulations with the lower bottom friction coefficient come closer to the observations for both storms, regarding spectral shape. Still the performance of SWAN for these cases is mediocre and the computed amount of energy at the low frequencies is still too low.

Appendix 7.2 shows the scatter plots for these runs, and appendix 7.3 the statistical parameters. According to the statistical parameters the $T_{m-1,0}$ has improved (bias -0.4% and MAE 6.3%) but the H_{m0} is less good than in the base case (bias now 2.6% instead of 0.2% in base case).

7.3 Triads (case e)

In the base case f the triad wave - wave interactions are activated. Previous studies (ref WL | Delft Hydraulics September 2007, Svasek 2003)) recognized that SWAN in shallow areas exaggerates the triad interactions.

For this reason case e is generated, where the triad wave- wave interactions are deactivated. Case e consists only of the simulations for the third selected moment of A.

The results of this case (e) are visualised by the measured and computed wave spectra of storm A and B and are presented in Appendix 7.4. From appendix 7.4 can be concluded that the traid wave –wave interactions have hardly any influence on the computed SWAN spectra of this study.

7.4 Directional resolution (case d)

In the base case of this study (case f) the spectral directional resolution was set to 10 degrees (=36 bins).

An additional computation is produced with a higher directional resolution in order to see if the simulations converge faster (case d). Looking at the results of the base case it could be concluded that the convergence behavior of the third selected moment of storm A is weak. Therefore the simulations of this specific moment is simulated once again, but with a higher directional resolution of 4 degrees (=90 bins).

The results of this case (d) are visualised by the measured and computed wave spectra of storm A and B and are presented in Appendix 7.4. The figures show that a higher directional resolution hardly changes the amount of energy at the first frequency peak. The amount of energy at the second frequency peak differs only at the locations BG2, DORA and OS4.

The shape of the spectra at the different locations is in very close agreement with the SWAN spectra of the base case (f). Only in OS4 a very small difference is visible. The amount of energy at the low frequency peak is slightly more compared to the base case, resulting in a higher wave height.

The number of iterations of this selected moment needed with the base case and case d (with higher directional resolution) case are shown in table 7.1

	t3 Storm A	
	Base case f (10°)	Case d (4°)
K-grid	80 (97.16%)	65
B-grid	80 (98.91%)	80 (98.97%)
D-grid	28	18
F-grid	15	13

Table 7.1: number of iterations for case f and d

The convergence behavior of the simulations with the higher directional resolution needs overall less iterations (accept for grid B) but the total computational time (larger matrix) is longer.

It could be concluded that a higher directional resolution in SWAN does not result in better representation of the observations. It needs overall less iterations but the total computational time (2.5 times as much directional bins) is longer.

8 CONCLUSIONS AND RECOMMENDATIONS

8.1 Conclusions

Performance SWAN

- At OS4 SWAN underestimates the wave energy at the lower frequencies (<0.2 Hz) resulting in a severe underestimation of wave period and a slight underestimation of wave height. The evolution of the spectrum over a ray from offshore to the nearshore location OS4 shows that the energy dissipation at the primary peak is strongly overpredicted. Consequently, the low-frequency energy at locations on the shallow foreshore, like OS4, is strongly underpredicted.

- Reducing the friction coefficient from 0.067 to 0.038 leads to improved predictions in this study, regarding the spectral shape. Still the performance of SWAN for these cases is mediocre and the computed amount of energy at the low frequencies is too low.

- The influence of triad wave- wave interaction is limited on t3 of storm A.

- There is not much difference in SWAN's performance for storm A (selected on combined swell and wind sea) and B (selected on high waves)

- High water levels ease the penetration of swell to OS4 both in the SWAN simulations and in the observations, see the spectra of t1 of storm B (Appendix 6.1.B).

- Following the development of the SWAN wave spectra along curve 6 from SCHB to OS4, it can be noticed that the wave energy at the lower frequencies (<0.2 Hz) dissipates considerably (too much according to the observations at OS4) while the energy at the higher frequencies changes less (see Appendix 6.2).

Convergence behavior

- In general the simulations converge far before the maximum number of iterations of 80. Some simulations, however, are still not converged after the maximum number of iterations. These situations occur during t3 (lower waves, lower wind, stronger currents) for both storms. The number of required iterations is very high (above 80) due to the weaker forcing and stronger currents. In the iteration process of storm A t3 we see that the convergence behavior is not unambiguous, but convergence and divergence follow each other.

- In most cases a higher resolution in direction needed less iterations but the total computational time was longer.

Storm selection

- Double peaked spectra with a significant amount of energy are rare in the deep water wave observations of SCHB, DORA and BG2. During the storm selection, more value has been devoted to double peakedness than to stationary wind.

- It must be realised that this study has only one nearshore (OS4) and two deeper (BG2 and DORA) measuring locations available to check the performance of SWAN. This is considerably less than most recent hindcast studies (i.e. Amelander Zeegat, Westerschelde).

8.2 Recommendations

- It must be investigated why SWAN dissipates too much energy at the lower frequencies.
- It is recommended to do more sensitivity runs to check the influence of currents, triads, friction, wind velocity.
- Check why higher directional resolution in SWAN does not result in better representation of the observations.

REFERENCES

Alkyon (January 2007a)
" Analysis SWAN hindcast tidal inlet of Ameland: Storm events of 8 February 2004 and 2, 8 January 2005"
Report A1725, January 2007.

Alkyon (January 2007b)
"Analysis SWAN hindcast tidal inlet of Ameland: Storms of 17 December 2005 and 9 February 2006".
Report A1725, January 2007.

Alves, J.H.G.M. and M.L. Banner (2003)
"Performance of a saturation-based dissipation-rate source term in modeling the fetch limited evolution of wind waves"
Journal of Physc. Oceanogr, 33, 1274-1298, 2003

Battjes, J.A. and J.P.F.M. Janssen (1978)
"Energy loss and set-up due to breaking of random waves"
Proc. 16th Int. Conf. on Coastal Engineering, 569-588, 1978

Delft University of Technology, Faculty of Civil Engineering and Geosciences
"SWAN User Manual (SWAN Cycle III version 40.51AB)"
2007

Royal Haskoning (December 2006)
"Hindcast tidal inlet of Ameland. Storms 17 December 2005 and 9 February 2006".
Report 9S2639.A0, December 2006.

Svašek Hydraulics (June 2003)
"Betrouwbaarheid SWAN in de Westerschelde, vergelijking golfberekeningen en metingen"
Ref 9M5697/R03035/CG/Rott2b, Juni 2003

Svašek Hydraulics (December 2006)
"Rapportage veldmetingen Westerschelde"
Ref: MvdB/06691/1407, December 2006

Yan, L (1987)
"An improved wind input source term for third generation ocean wave modeling."
Technical report, Rep. No. 87-8, Royal Dutch Meteor. Inst., 1987

Westhuysen, A van der (October 2007).
"Advances in the spectral modeling of wind waves in the nearshore"
Phd, Delft University of Technology, 16 October 2007

WL| Delft Hydraulics (August 2006)
"Storm hindcasts Norderneyer Seegat and Amelander Zeegat"
Report H4803.11, August 2006.

WL| Delft Hydraulics (September 2007)
"Storm hindcasts for Wadden Sea: Hindcasts in inlet systems of Ameland, Norderney and Lunenburg"
Rapport H4918.20, September 2007

GHr2-file (waves)

Gegevenssoort	GHr2	
Omschrijving	Golfparameters niveau 2 (0-1000 mHz)	
Sublokatie	N.v.t.	
Aantal kanalen	128	
Tijdstap van inwinning	30 min.	
Datatype	Integer	
Kanaalnummer	Omschrijving	Eenheid
1	H3 Gemiddelde hoogte van het $^1/_3$ deel hoogste golven	cm
2	H10 Gemiddelde hoogte van het $^1/_{10}$ deel hoogste golven	cm
3	H50 Gemiddelde hoogte van het $^1/_{50}$ deel hoogste golven	cm
4	GGH Gemiddelde golfhoogte	cm
5	HMAX Maximale golfhoogte	cm
6	SPGH Spreiding van de golfhoogte	cm
7	TM02 Periodeparameter berekend uit het spectum 0.03-1.0 Hz	0.1 s
8	TMAX Maximale golfperiode	0.1 s
9	GGT Gemiddelde golfperiode	0.1 s
10	SPGT Spreiding van de golfperiode	0.1 s
11	T3 Gemiddelde van het hoogste $^1/_3$ deel van de golfperioden	0.1 s
12	TH3 Gem. periode van de golven waaruit de H3 bepaald is.	0.1 s
13	AG Aantal golven	-
14	AV Aantal vrijheidsgraden	-
15	HCM Kamhoogte	cm
16	HS7 Sign. golfhoogte uit 10 mHZ spectrum van 0.03-0.1425 Hz	cm
17	Hm0 Sign. golfhoogte uit 10 mHz spectrum van 0.03-1.000 Hz	cm
18	TE1 Energie van 0.2 - 1.0 Hz	cm^2
19	TE2 Energie van 0.1 - 0.2 Hz	cm^2
20	E10 Energie van 0.0 - 0.1 Hz	cm^2
21	FP Piekfrequentie	GS 0.01 Hz !)
22	THMAX Periode van de hoogste golf	0.1 s
23	Nwt_zP Quotient som golfperiodes en verwerkingsperiode (*1000)	-
24	Tm-10 Min-eerste moment periode (M_{-1}/M_0)	0.1 s
25	TE0 Energie van 0.5 - 1.0 Hz	.
26	Vormparameter beta van het model-spektrum	.
27	Vormparameter gamma van het model-spektrum	.
28	Czz10(0) Energiedichtheid 0.000-0.005 Hz	$cm^2 * s$
29	Czz10(1) Energiedichtheid 0.005-0.015 Hz	$cm^2 * s$
30	Czz10(2) Energiedichtheid 0.015-0.025 Hz	$cm^2 * s$
.	.	.
.	.	.
127	Czz10(99) Energiedichtheid 0.985-0.995 Hz	$cm^2 * s$

GSO2-file (waves)

Gegevenssoort		
Omschrijving	Golfparameters	
Sublokatie	N.v.t.	
Aantal kanalen	128	
inwinning	30 min.	
Datatype	Integer	
Kanaalnummer	Omschrijving	Eenheid
1	H3 Gemiddelde hoogte van het $^1/_3$ deel hoogste golven	cm
2	H10 Gemiddelde hoogte van het $^1/_{10}$ deel hoogste golven	cm
3	H50 Gemiddelde hoogte van het $^1/_{50}$ deel hoogste golven	cm
4	GGH Gemiddelde golfhoogte	cm
5	HMAX Maximale golfhoogte	cm
6	SPGH Spreiding van de golfhoogte	cm
7	TM02 Periodeparameter berekend uit het spectum 0.03-0.7Hz	0.1 s
8	TMAX Maximale golfperiode	0.1 s
9	GGT Gemiddelde golfperiode	0.1 s
10	SPGT Spreiding van de golfperiode	0.1 s
11	T3 Gemiddelde van het hoogste $^1/_3$ deel van de golfperioden	0.1 s
12	TH3 Gem. periode van de golven waaruit de H3 bepaald is.	0.1 s
13	AG Aantal golven	-
14	AV Aantal vrijheidsgraden	-
15	AF Aantal fouten	-
16	BW Bewerkt aantal waarnemingen	-
17	E01 Totale energie van 0.0-1.0 Hz	cm^2
18	TE1 Energie van 0.2 - 1.0 Hz	cm^2
19	TE2 Energie van 0.1 - 0.2 Hz	cm^2
20	E10 Energie van 0.0 - 0.1 Hz	cm^2
21	FP Piekfrequentie	GH 0.001
22	Dummy	-
23	FPZ Piekfrequentie zeegang	0.01 Hz
24	FPD Piekfrequentie deining	0.01 Hz
25	Dummy	-
26	Dummy	-
27	Beta Spektrum vormparameter beta van modelspektrum	-
28	Gamma Spektrum vormparameter gamma van modelspektrum	-
29	GS0 Energiedichtheid 0.000-0.005 Hz	10 cm^2 * s
30	GS1 Energiedichtheid 0.005-0.015 Hz	10 cm^2 * s
.	.	.
.	.	.
127	GS98 Energiedichtheid 0.975-0.985 Hz	10 cm^2 * s
128	GS99 Energiedichtheid 0.985-0.995 Hz	10 cm^2 * s

WTr2-file (water levels)

Gegevenssoort	wt	
Omschrijving	Waterstand	
Sublokatie	N.v.t.	
Aantal kanalen	1	
Tijdstap van inwinning	1 min.	
Datatype	Integer	
Kanaalnummer	Omschrijving	Eenheid
1	1 min. gemiddelde waterhoogte	NAP

WNr2-file (water levels)

Gegevenssoort	WN	
Omschrijving	Windgegevens	
Sublokatie	N.v.t.	
Aantal kanalen	8	
Tijdstap van inwinnig	10	
Datatype	Integer	
Kanaalnummer	Omschrijving	Eenheid
1	WS10 10-min. scalair gemiddelde windsnelheid	dm/s
2	WR10 10-min. gemiddelde windrichting	tov Nrd.
3	WS10MXS3 Max. 3-sec. windstoot in de afgelopen 10 min. max. van deze windstoten is deze parameter.	dm/s
4	gecorrigeerd naar 10 m boven het zeeoppervlak	dm/s
5	minuten gecorrigeerd naar 10 m boven het zeeoppervlak	dm/s
6	afgelopen 10 min.	dm/s
7	in de afgelopen 10 min.	dm/s
8	afgelopen 10 min.	dm/s

WIO2-file (wind)

Gegevenssoort	WI	
Omschrijving	Windgegevens	
Sublokatie	N.v.t.	
Aantal kanalen	3	
Tijdstap van inwinnig	10	
Datatype	Integer	
Kanaalnummer	Omschrijving	Eenheid
1	Windsnelheid	dm/s
2	Windrichting	tov Nrd.
3	Windstoot	dm/s

	Date	Hour (GMT)	Wind direction (degrees)	Wind speed (m/s)
1	1990, January 25	16	230	26.6
2	2002, October 27	14	260	24.9
3	1987, October 16	7	220	24.7
4	1990, February 28	23	320	24.7
5	1983, November 27	3	240	24.2
6	2000, May 28	10	240	22.9
7	1986, October 20	14	280	22.8
8	1986, January 19	19	300	22.4
9	1992, November 11	13	300	22.4
10	1990, February 26	9	240	22.3
11	1984, November 23	23	250	22.3
12	1986, December 18	24	280	22.3
13	2000, December 13	4	240	21.9
14	1999, December 3	10	210	21.9
15	1999, December 25	1	190	21.8
16	1990, January 28	9	230	21.7
17	1993, November 14	12	280	21.7
18	1994, April 1	8	240	21.7
19	2001, November 8	15	360	21.4
20	1993, January 24	3	230	21.3

20 highest wind speed events of station 312, Eastern Scheldt selected by the knmi

(www.knmi.nl/samenw/hydra/cgi-bin/top$_x$.cgi?stn=312)

APPENDIX 3.1
1461
17-Dec-2007

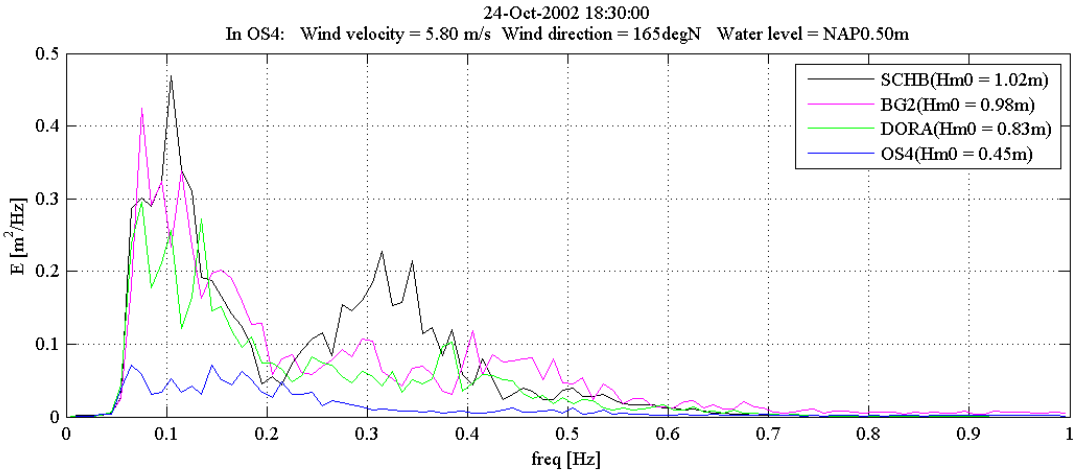

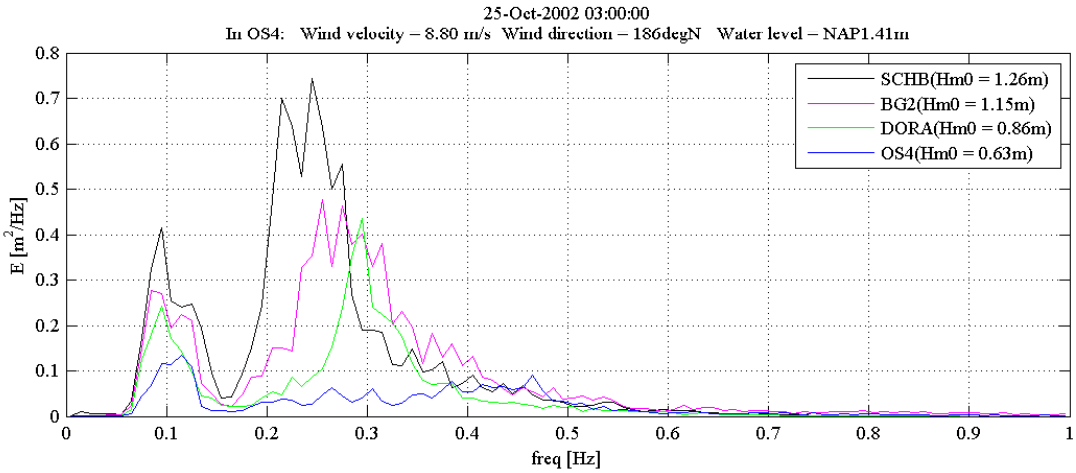

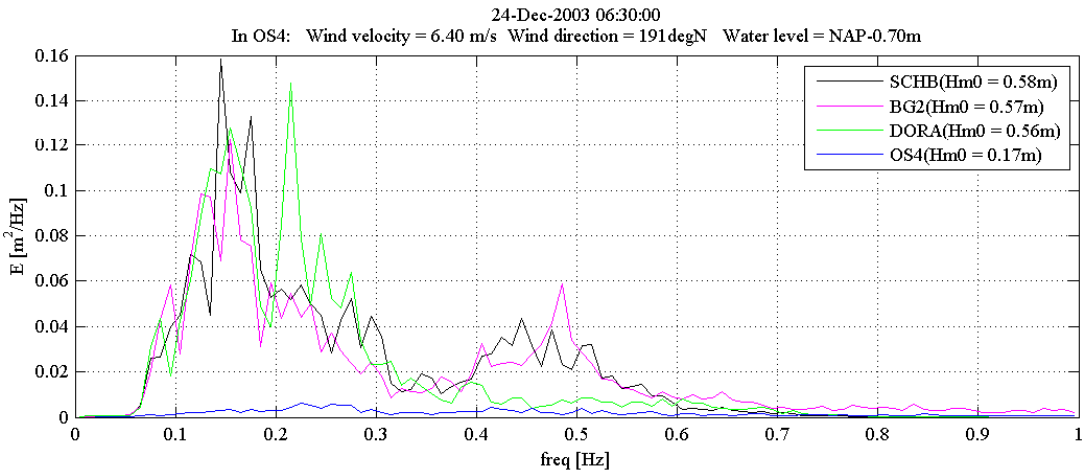

SVASEK HYDRAULICS

Examples of double peaked spectra, but low energy

APPENDIX 3.2
1461
19-Dec-2007

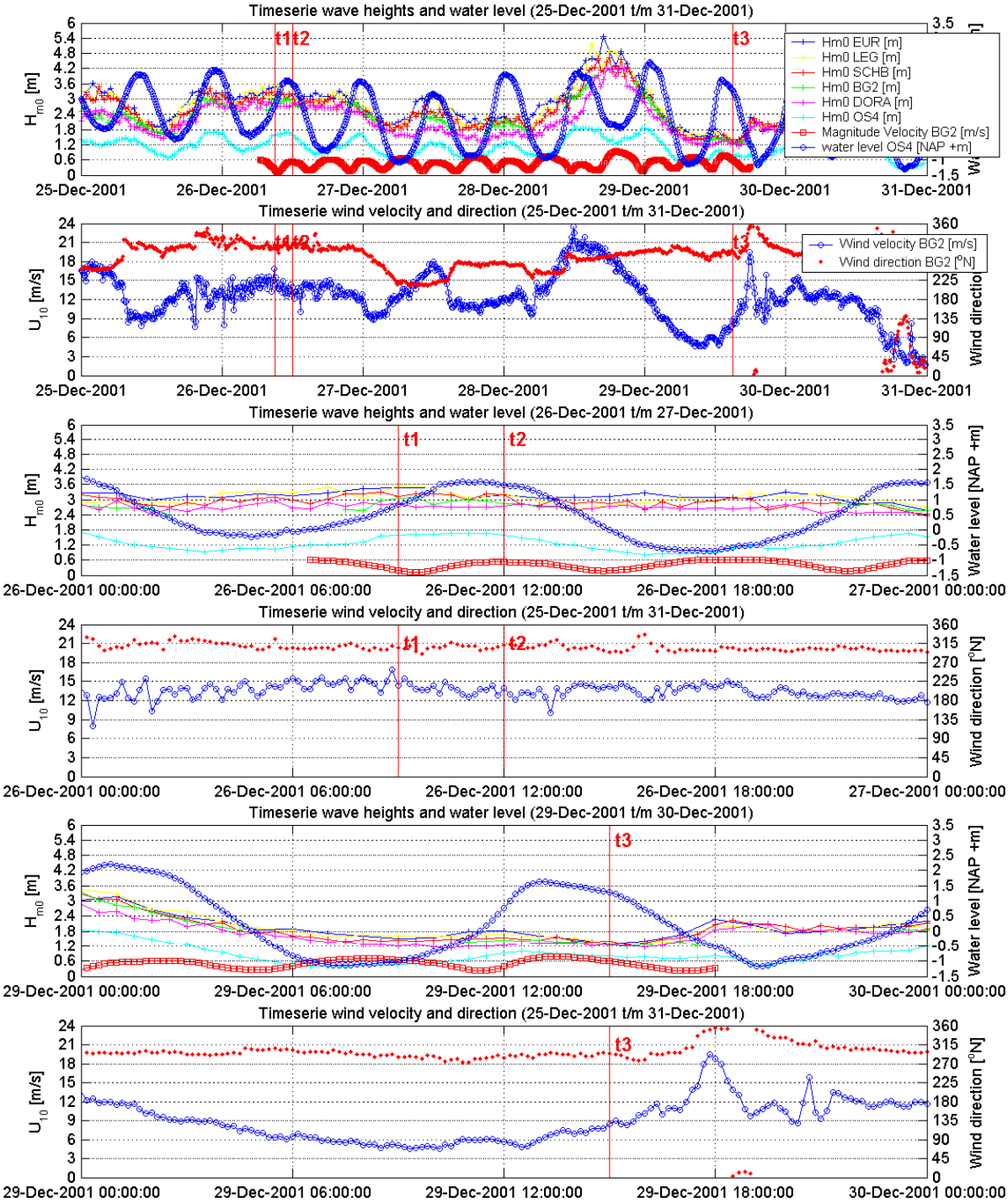
Timeserie wave heights and water level (25-Dec-2001 t/m 31-Dec-2001)
H_m0 [m]
Water level [NAP +m]
t1 t2
t3
Hm0 EUR [m]
Hm0 LEG [m]
Hm0 SCHB [m]
Hm0 BG2 [m]
Hm0 DORA [m]
Hm0 OS4 [m]
Magnitude Velocity BG2 [m/s]
water level OS4 [NAP +m]
25-Dec-2001
26-Dec-2001
27-Dec-2001
28-Dec-2001
29-Dec-2001
30-Dec-2001
31-Dec-2001
Timeserie wind velocity and direction (25-Dec-2001 t/m 31-Dec-2001)
U_10 [m/s]
Wind direction
Wind velocity BG2 [m/s]
Wind direction BG2 [°N]
Timeserie wave heights and water level (26-Dec-2001 t/m 27-Dec-2001)
t1
t2
26-Dec-2001 00:00:00
26-Dec-2001 06:00:00
26-Dec-2001 12:00:00
26-Dec-2001 18:00:00
27-Dec-2001 00:00:00
Timeserie wind velocity and direction (25-Dec-2001 t/m 31-Dec-2001)
Wind direction [°N]
Timeserie wave heights and water level (29-Dec-2001 t/m 30-Dec-2001)
t3
29-Dec-2001 00:00:00
29-Dec-2001 06:00:00
29-Dec-2001 12:00:00
29-Dec-2001 18:00:00
30-Dec-2001 00:00:00
Timeserie wind velocity and direction (25-Dec-2001 t/m 31-Dec-2001)

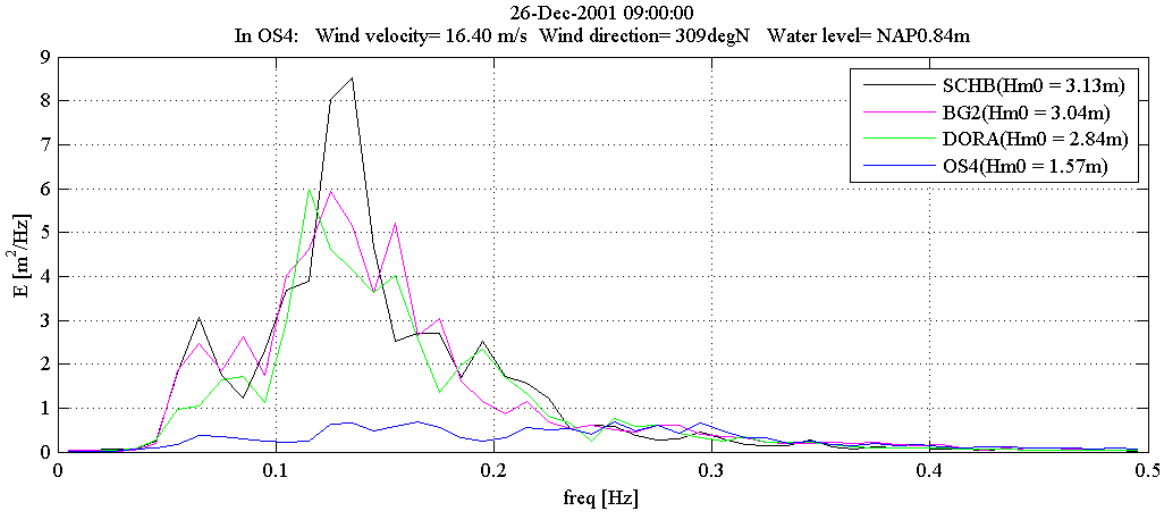
26-Dec-2001 09:00:00
In OS4: Wind velocity= 16.40 m/s Wind direction= 309degN Water level= NAP0.84m
SCHB(Hm0 = 3.13m)
BG2(Hm0 = 3.04m)
DORA(Hm0 = 2.84m)
OS4(Hm0 = 1.57m)
E [m²/Hz]
freq [Hz]

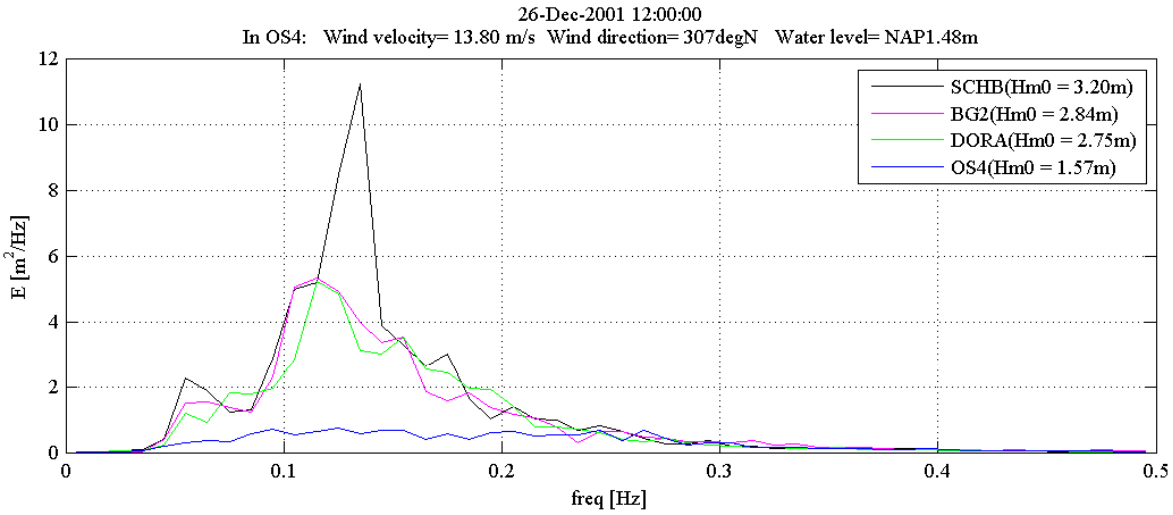
26-Dec-2001 12:00:00
In OS4: Wind velocity= 13.80 m/s Wind direction= 307degN Water level= NAP1.48m
SCHB(Hm0 = 3.20m)
BG2(Hm0 = 2.84m)
DORA(Hm0 = 2.75m)
OS4(Hm0 = 1.57m)
E [m²/Hz]
freq [Hz]

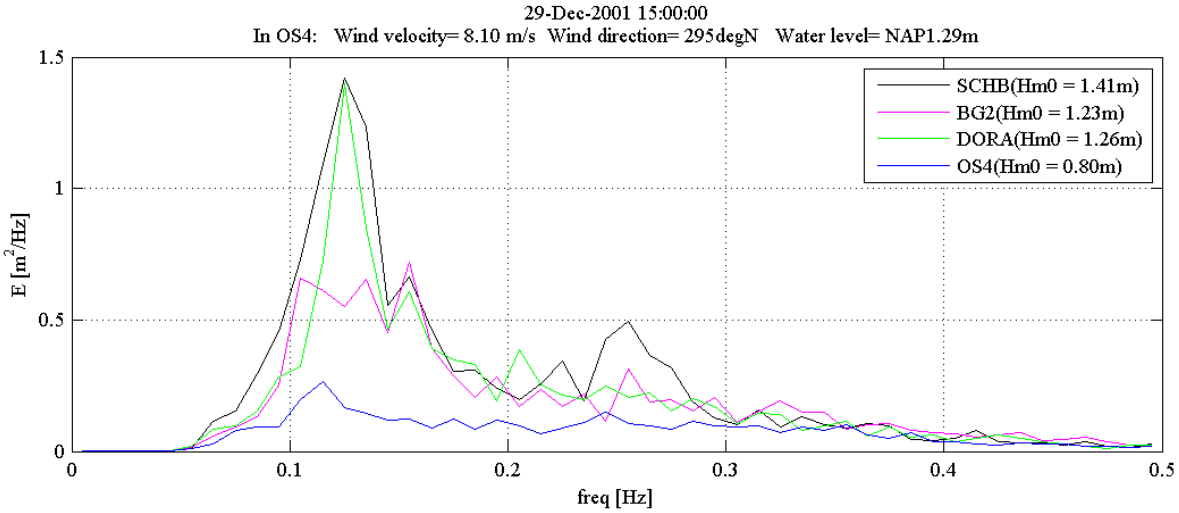
29-Dec-2001 15:00:00
In OS4: Wind velocity= 8.10 m/s Wind direction= 295degN Water level= NAP1.29m
SCHB(Hm0 = 1.41m)
BG2(Hm0 = 1.23m)
DORA(Hm0 = 1.26m)
OS4(Hm0 = 0.80m)
E [m²/Hz]
freq [Hz]

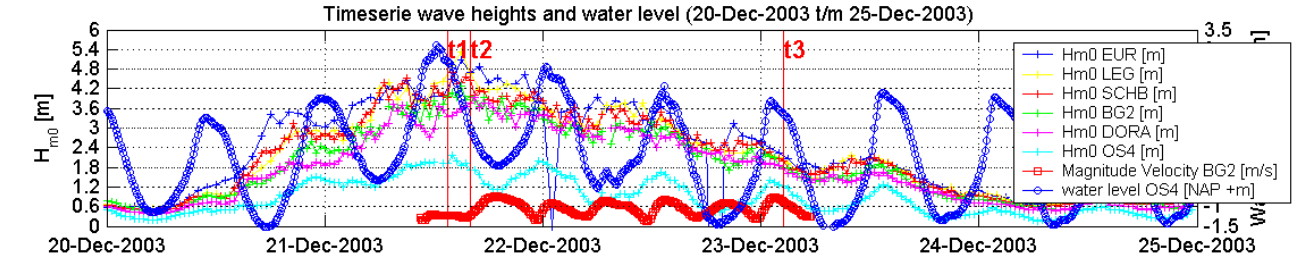
Timeserie wave heights and water level (20-Dec-2003 t/m 25-Dec-2003)
H_m0 [m]
t1 t2
t3
Hm0 EUR [m]
Hm0 LEG [m]
Hm0 SCHB [m]
Hm0 BG2 [m]
Hm0 DORA [m]
Hm0 OS4 [m]
Magnitude Velocity BG2 [m/s]
water level OS4 [NAP +m]
20-Dec-2003
21-Dec-2003
22-Dec-2003
23-Dec-2003
24-Dec-2003
25-Dec-2003

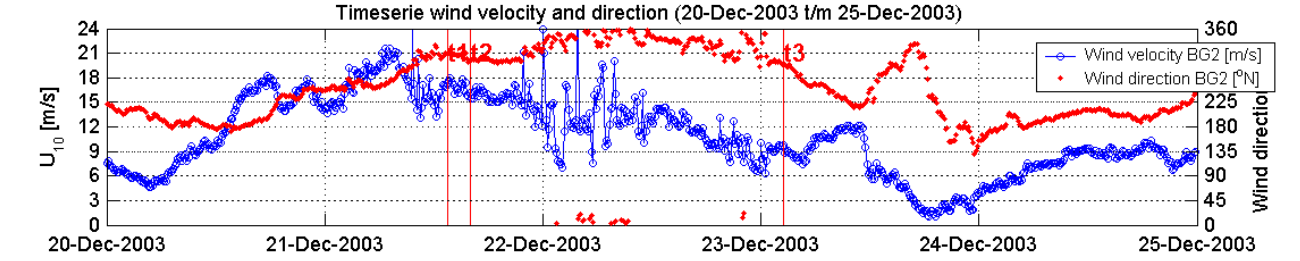
Timeserie wind velocity and direction (20-Dec-2003 t/m 25-Dec-2003)
U_10 [m/s]
Wind direction
t1 t2
t3
Wind velocity BG2 [m/s]
Wind direction BG2 [°N]
20-Dec-2003
21-Dec-2003
22-Dec-2003
23-Dec-2003
24-Dec-2003
25-Dec-2003

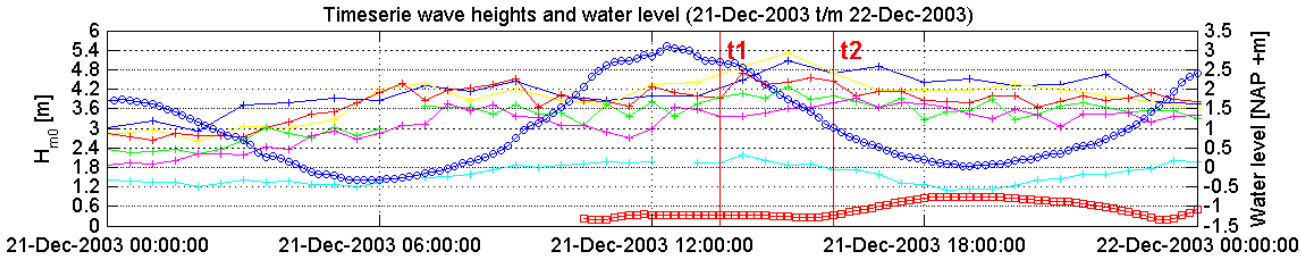
Timeserie wave heights and water level (21-Dec-2003 t/m 22-Dec-2003)
H_m0 [m]
Water level [NAP +m]
t1
t2
21-Dec-2003 00:00:00
21-Dec-2003 06:00:00
21-Dec-2003 12:00:00
21-Dec-2003 18:00:00
22-Dec-2003 00:00:00

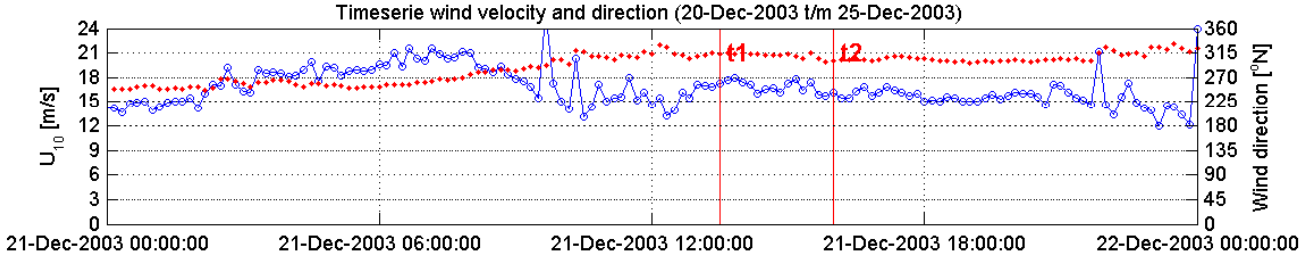
Timeserie wind velocity and direction (20-Dec-2003 t/m 25-Dec-2003)
U_10 [m/s]
Wind direction [°N]
t1
t2
21-Dec-2003 00:00:00
21-Dec-2003 06:00:00
21-Dec-2003 12:00:00
21-Dec-2003 18:00:00
22-Dec-2003 00:00:00

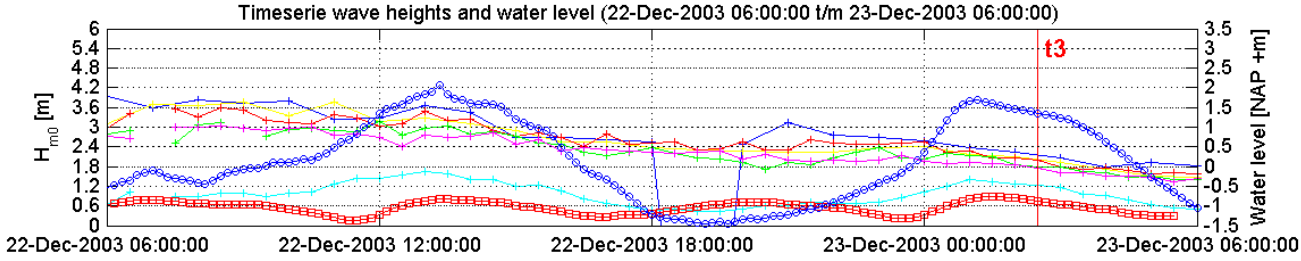
Timeserie wave heights and water level (22-Dec-2003 06:00:00 t/m 23-Dec-2003 06:00:00)
H_m0 [m]
Water level [NAP +m]
t3
22-Dec-2003 06:00:00
22-Dec-2003 12:00:00
22-Dec-2003 18:00:00
23-Dec-2003 00:00:00
23-Dec-2003 06:00:00

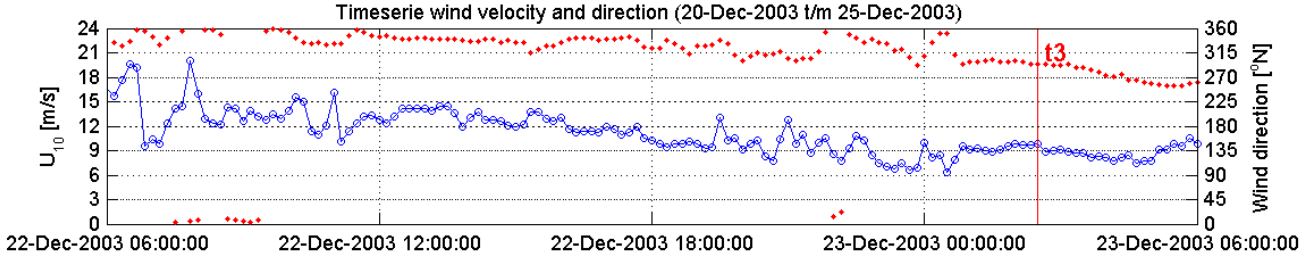
Timeserie wind velocity and direction (20-Dec-2003 t/m 25-Dec-2003)
U_10 [m/s]
Wind direction [°N]
t3
22-Dec-2003 06:00:00
22-Dec-2003 12:00:00
22-Dec-2003 18:00:00
23-Dec-2003 00:00:00
23-Dec-2003 06:00:00

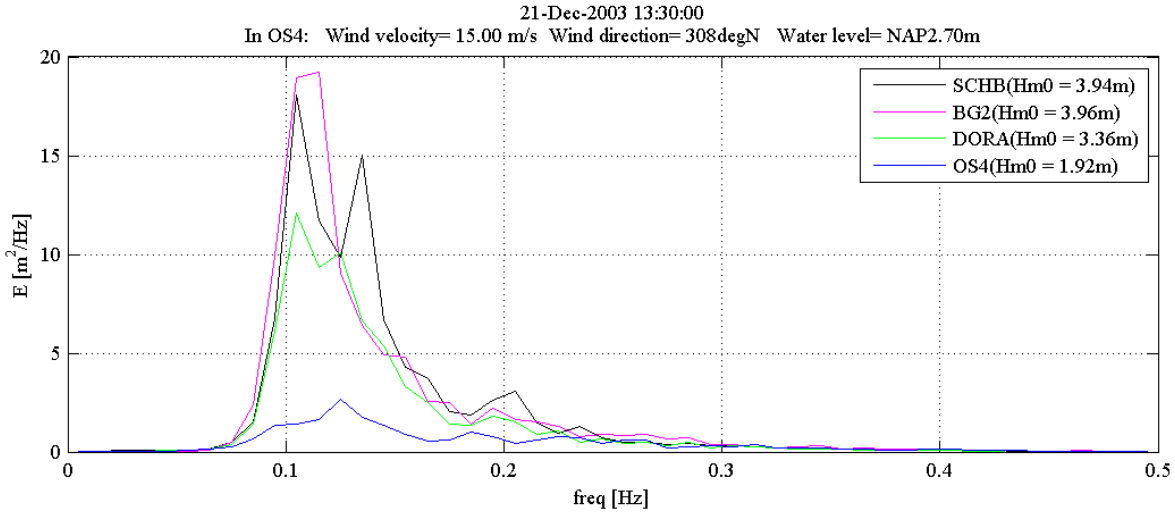
21-Dec-2003 13:30:00
In OS4: Wind velocity= 15.00 m/s Wind direction= 308degN Water level= NAP2.70m
SCHB(Hm0 = 3.94m)
BG2(Hm0 = 3.96m)
DORA(Hm0 = 3.36m)
OS4(Hm0 = 1.92m)
E [m²/Hz]
freq [Hz]

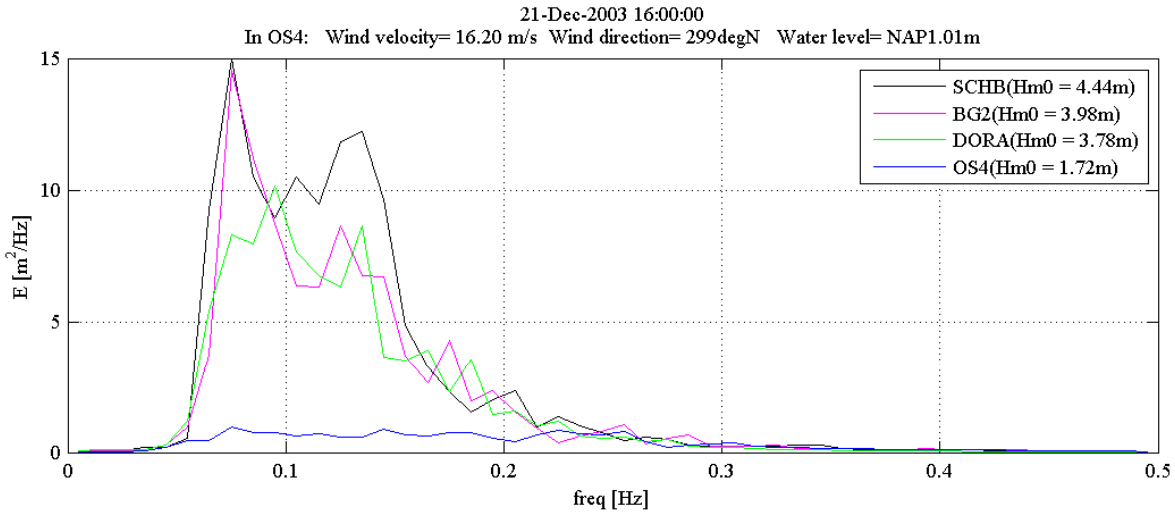
21-Dec-2003 16:00:00
In OS4: Wind velocity= 16.20 m/s Wind direction= 299degN Water level= NAP1.01m
SCHB(Hm0 = 4.44m)
BG2(Hm0 = 3.98m)
DORA(Hm0 = 3.78m)
OS4(Hm0 = 1.72m)
E [m²/Hz]
freq [Hz]

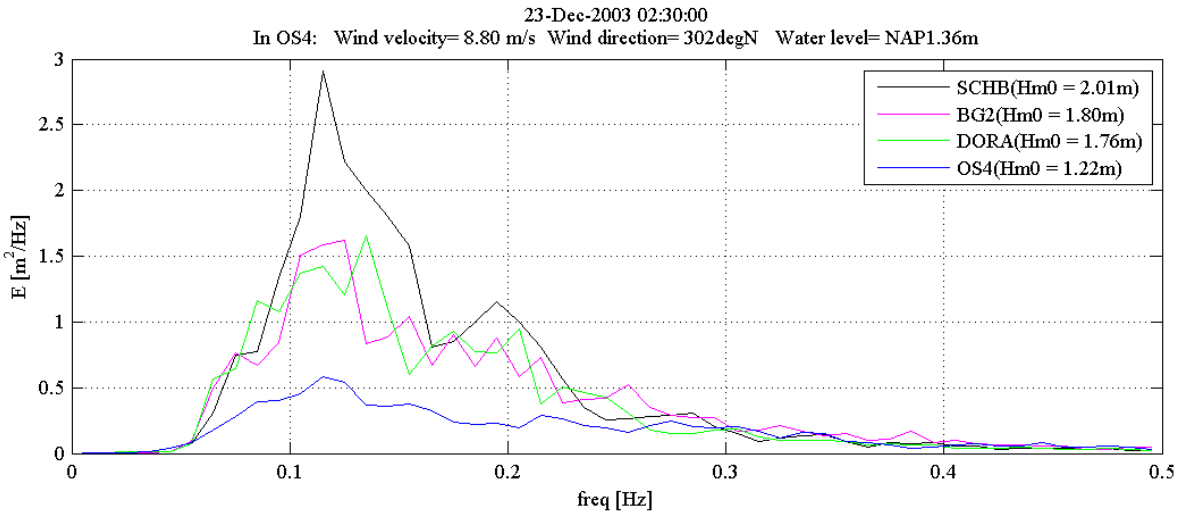
23-Dec-2003 02:30:00
In OS4: Wind velocity= 8.80 m/s Wind direction= 302degN Water level= NAP1.36m
SCHB(Hm0 = 2.01m)
BG2(Hm0 = 1.80m)
DORA(Hm0 = 1.76m)
OS4(Hm0 = 1.22m)
E [m²/Hz]
freq [Hz]

MEASURED 2d spectrum EUR storm A t1

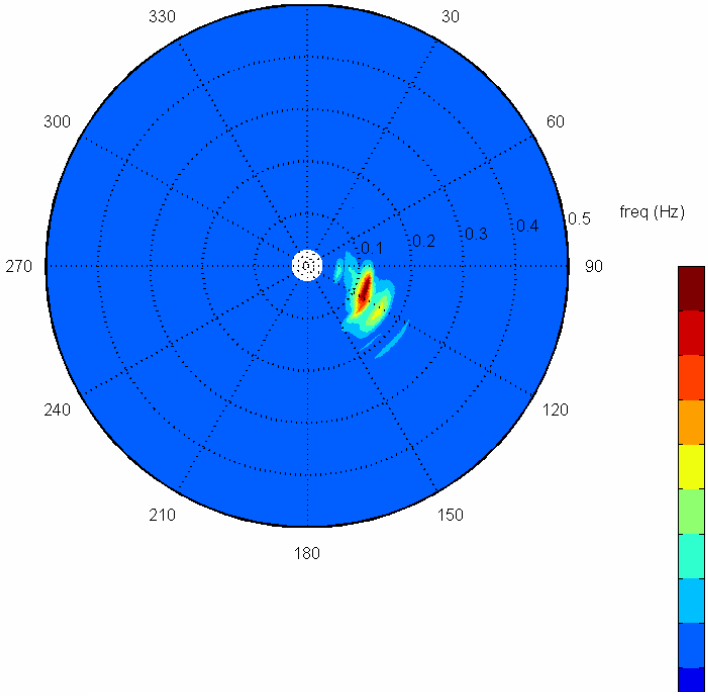

INPUT N-grid storm A t1

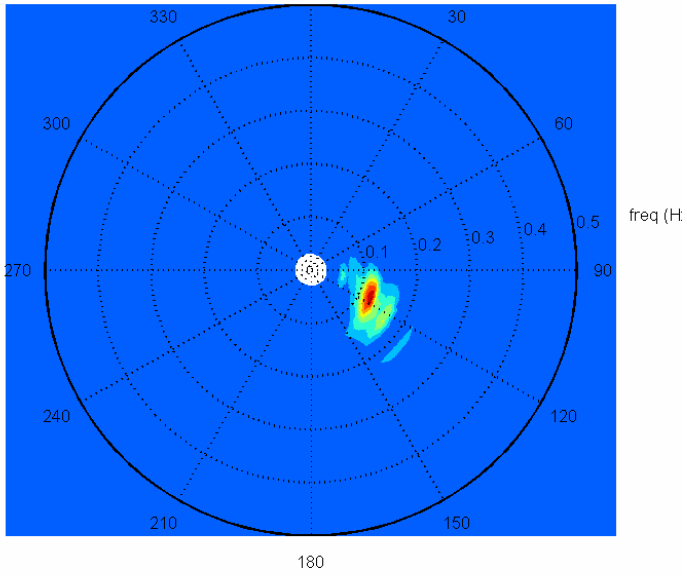

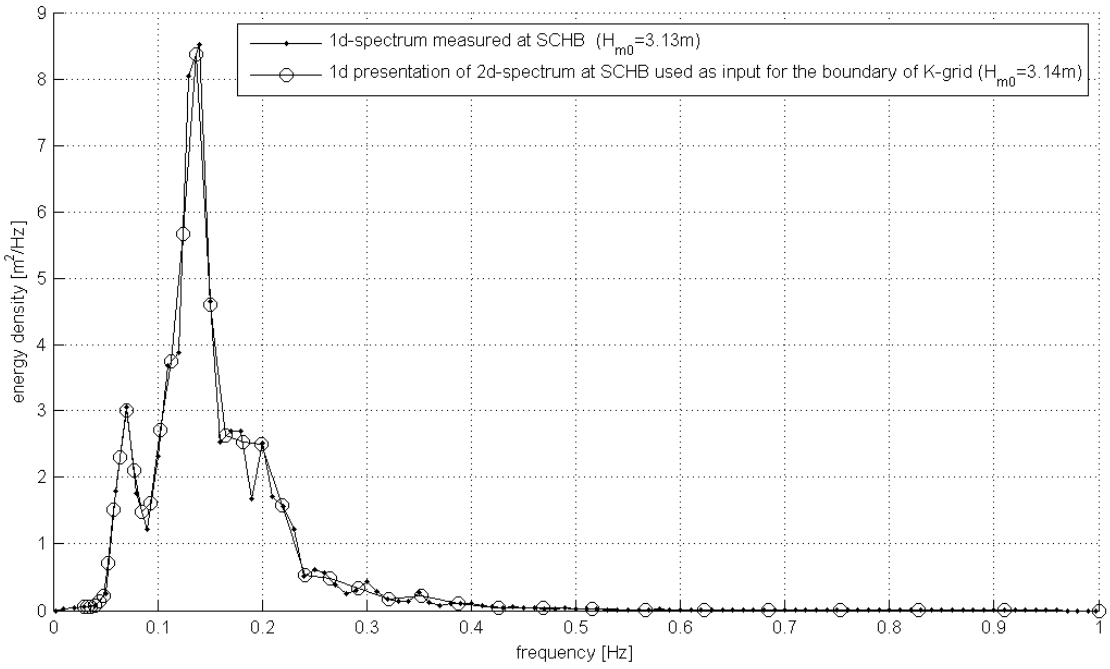

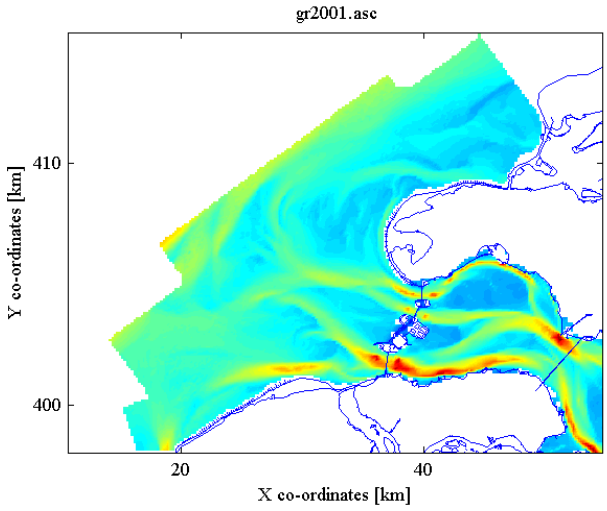

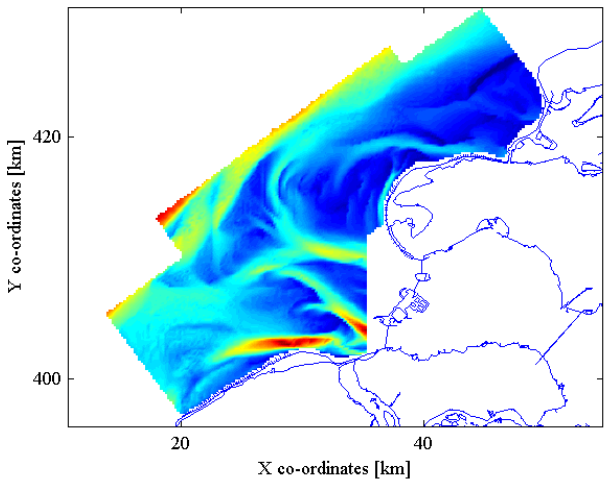

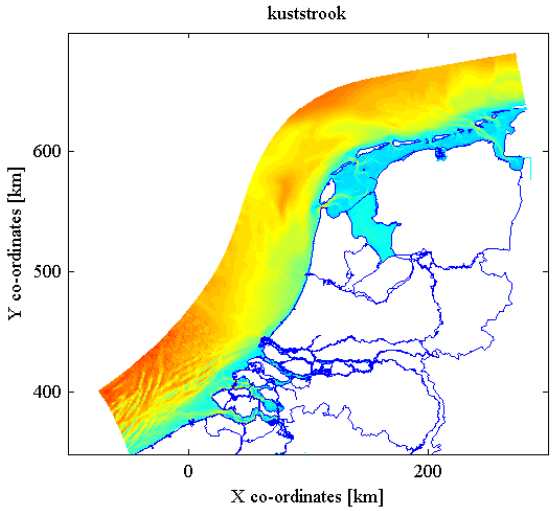

SVASEK HYDRAULICS

Depth files used for the bathymetry

2001: gr2001.asc + kustrook
2003: gr2004.asc + gr2001.asc + kustrook

APPENDIX 4.2
1461
07-Dec-2007

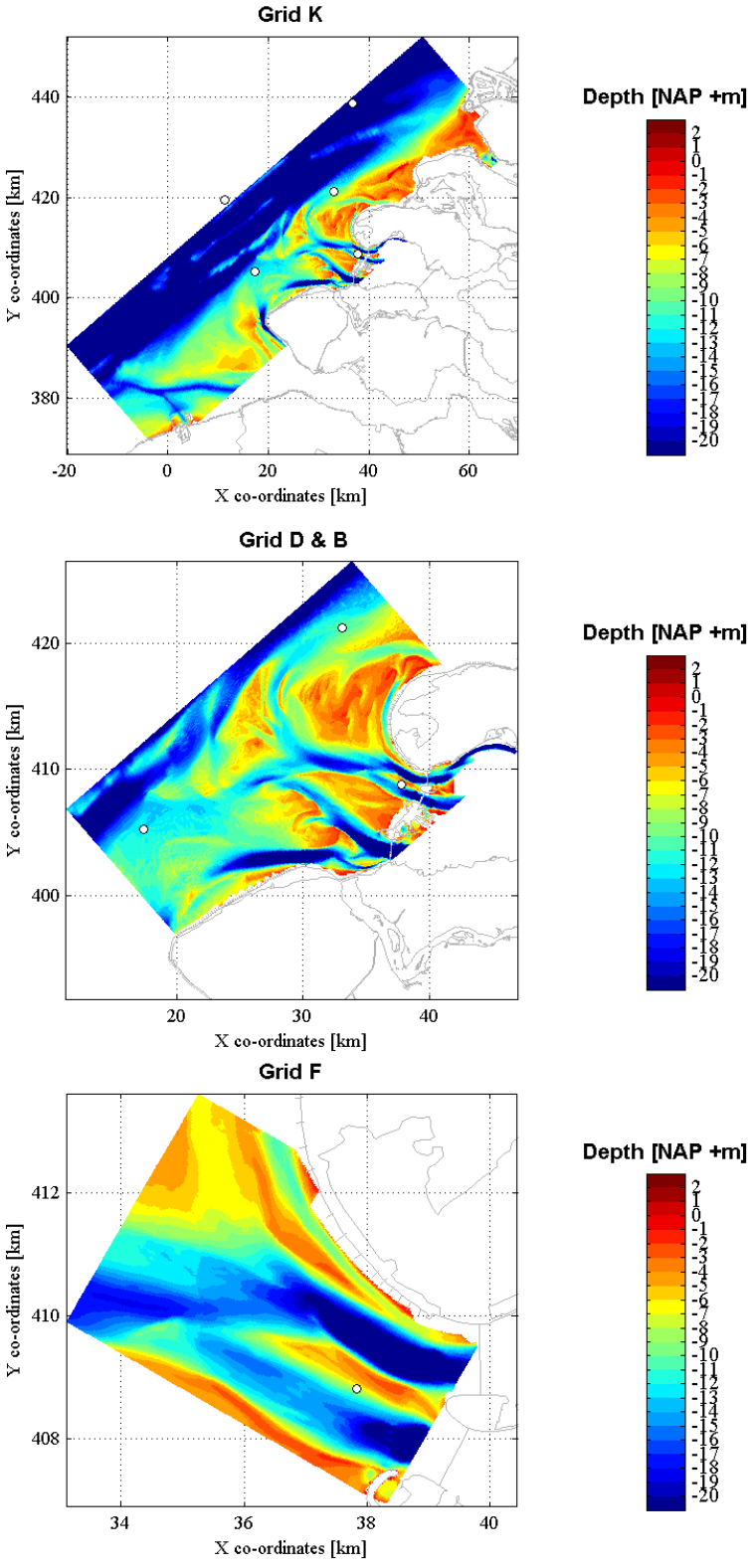

Bathymetry of the computational grids
Storm A

APPENDIX 4.3.A
1461
18-Dec-2007

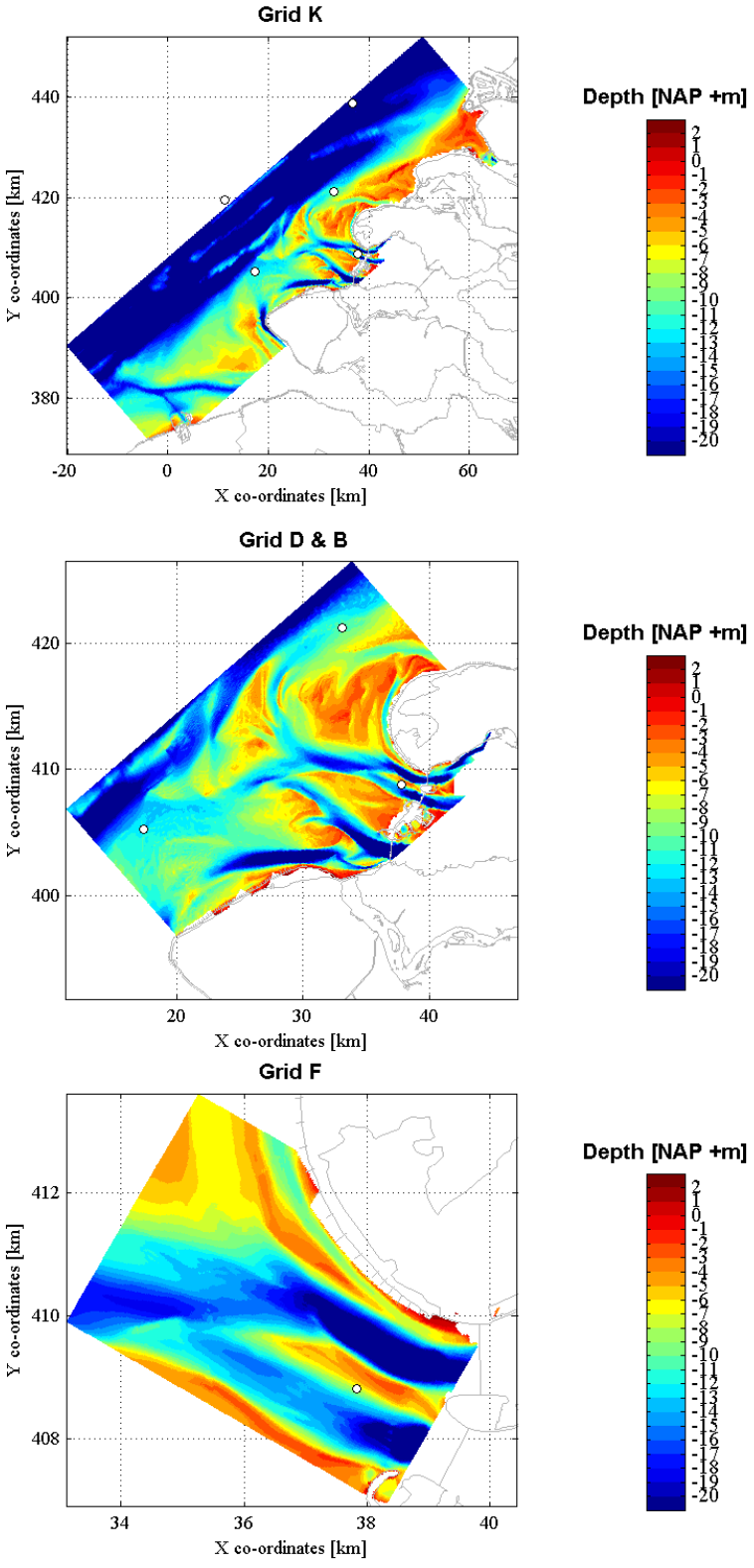

Bathymetry of the computational grids
Storm B

APPENDIX 4.3.B
1461
18-Dec-2007

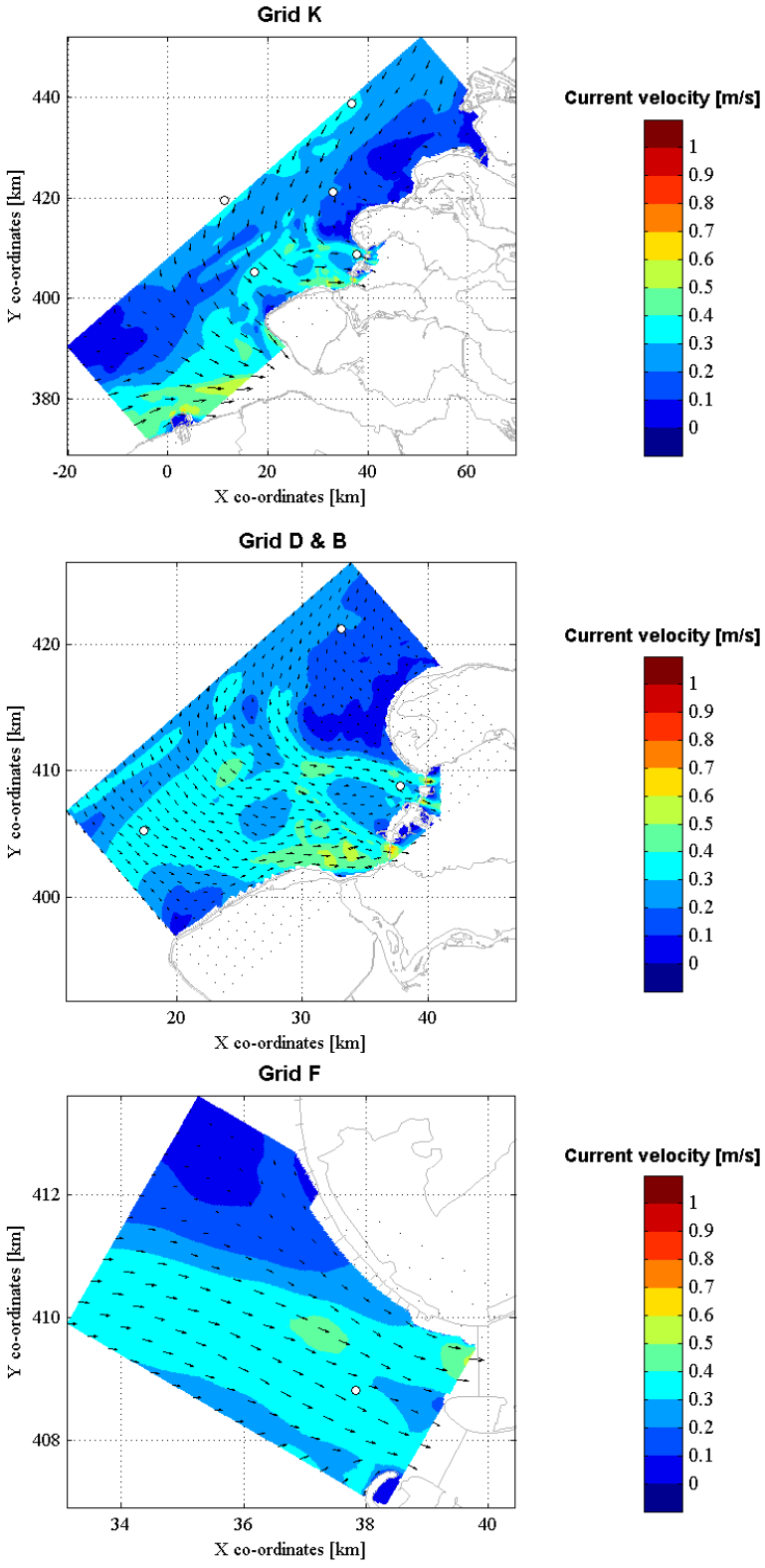

SVASEK HYDRAULICS

SWAN results: The current velocity [m/s]

Storm A t1 (26-Dec-2001 09:00:00)

APPENDIX 4.4.A1
1461
18-Dec-2007

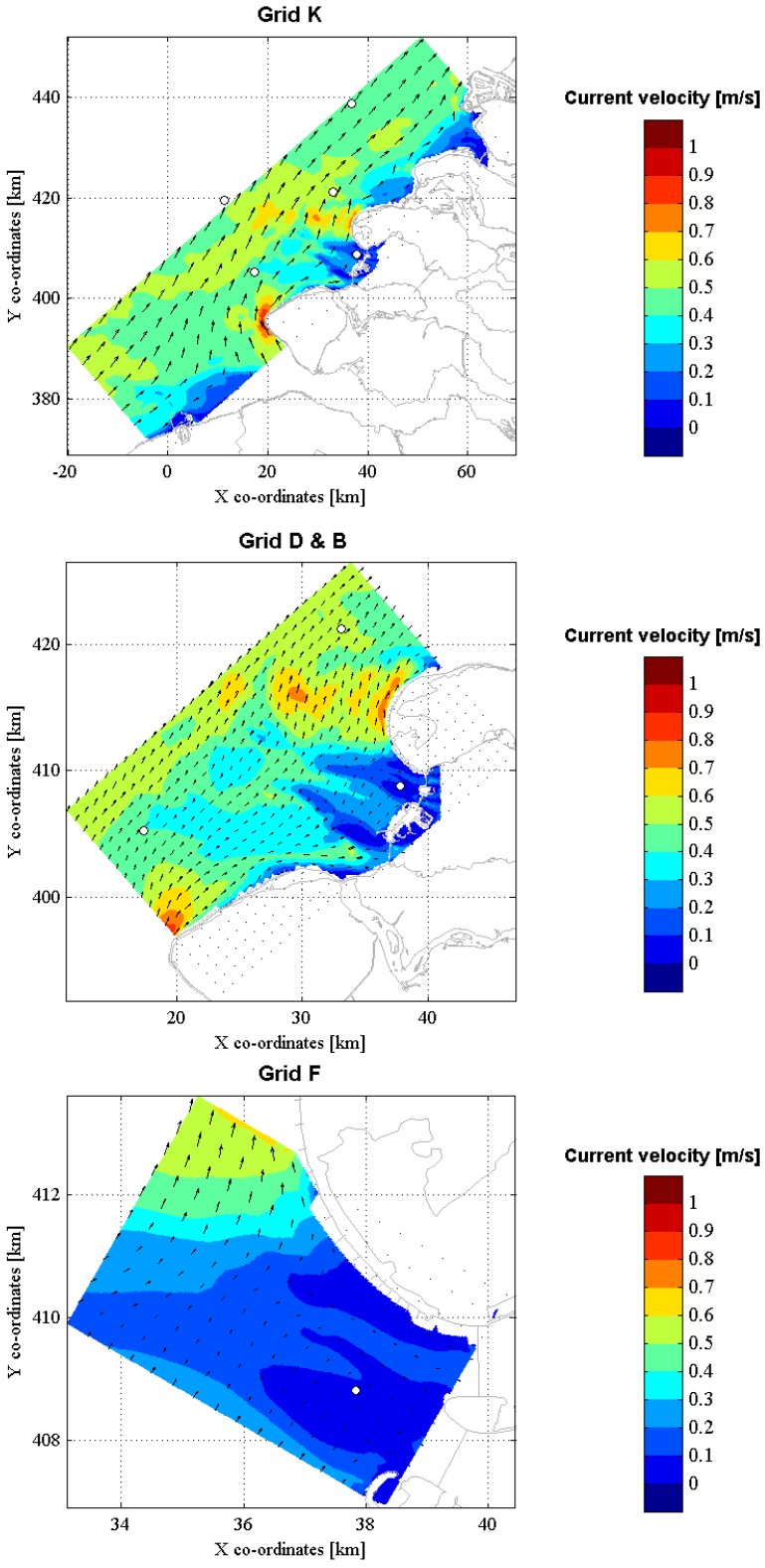

SVASEK HYDRAULICS

SWAN results: The current velocity [m/s]

Storm A t2 (26-Dec-2001 12:00:00)

APPENDIX 4.4.A2
1461
18-Dec-2007

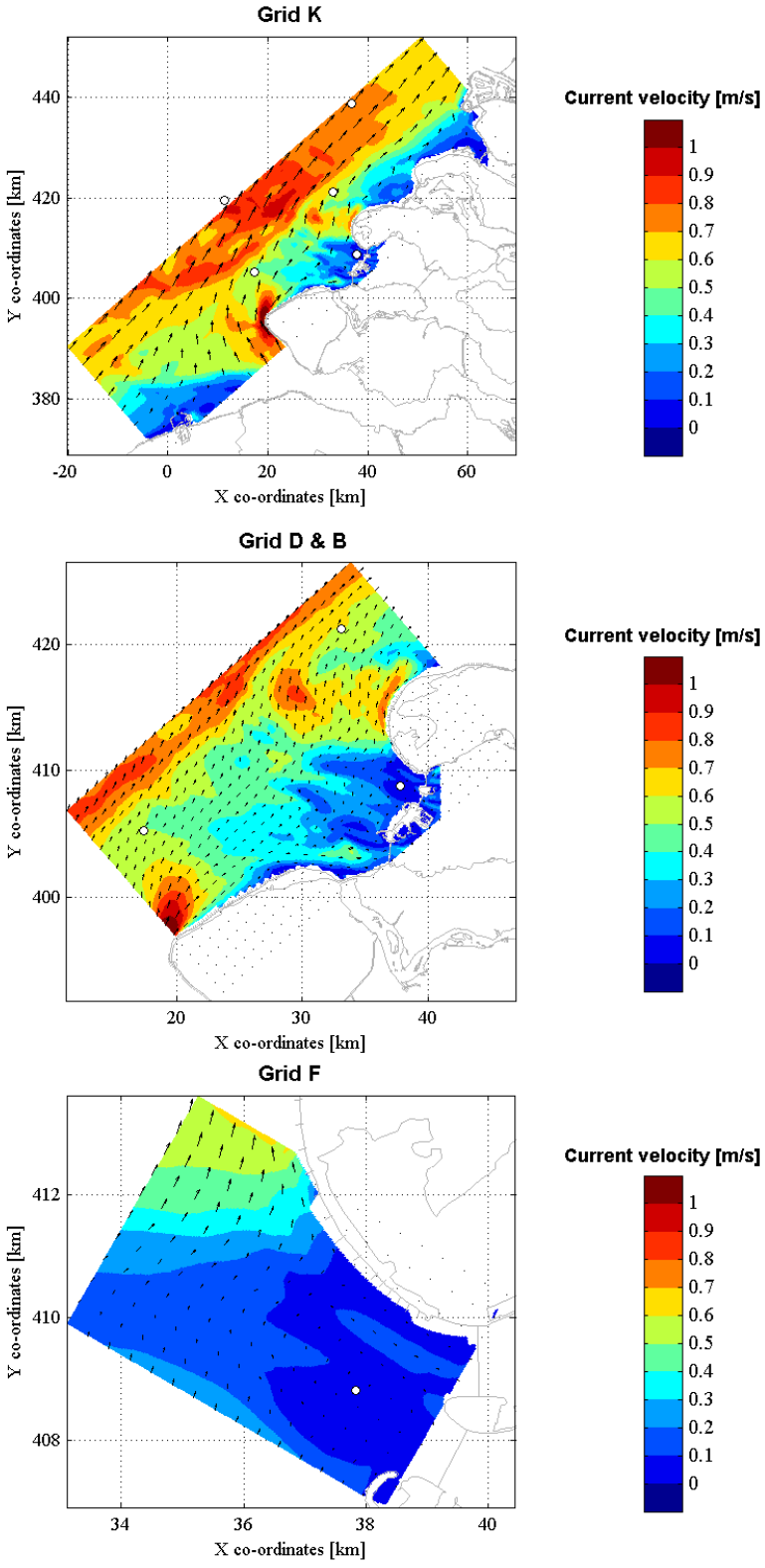

SVASEK HYDRAULICS

SWAN results: The current velocity [m/s]

Storm A t3 (29-Dec-2001 15:00:00)

APPENDIX 4.4.A3
1461
18-Dec-2007

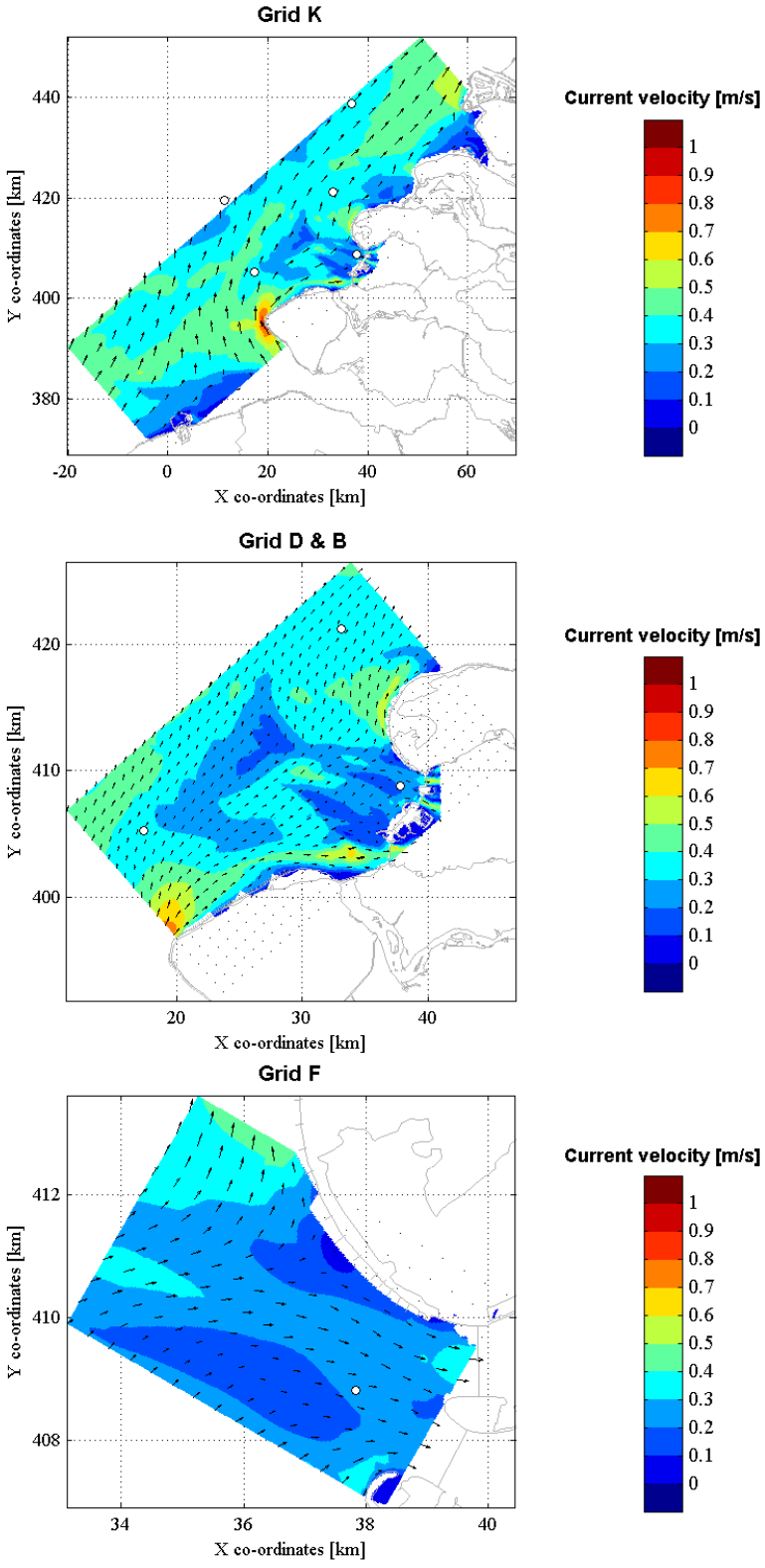

SVASEK HYDRAULICS

SWAN results: The current velocity [m/s]

Storm B t1 (21-Dec-2003 13:30:00)

APPENDIX 4.4.B1
1461
18-Dec-2007

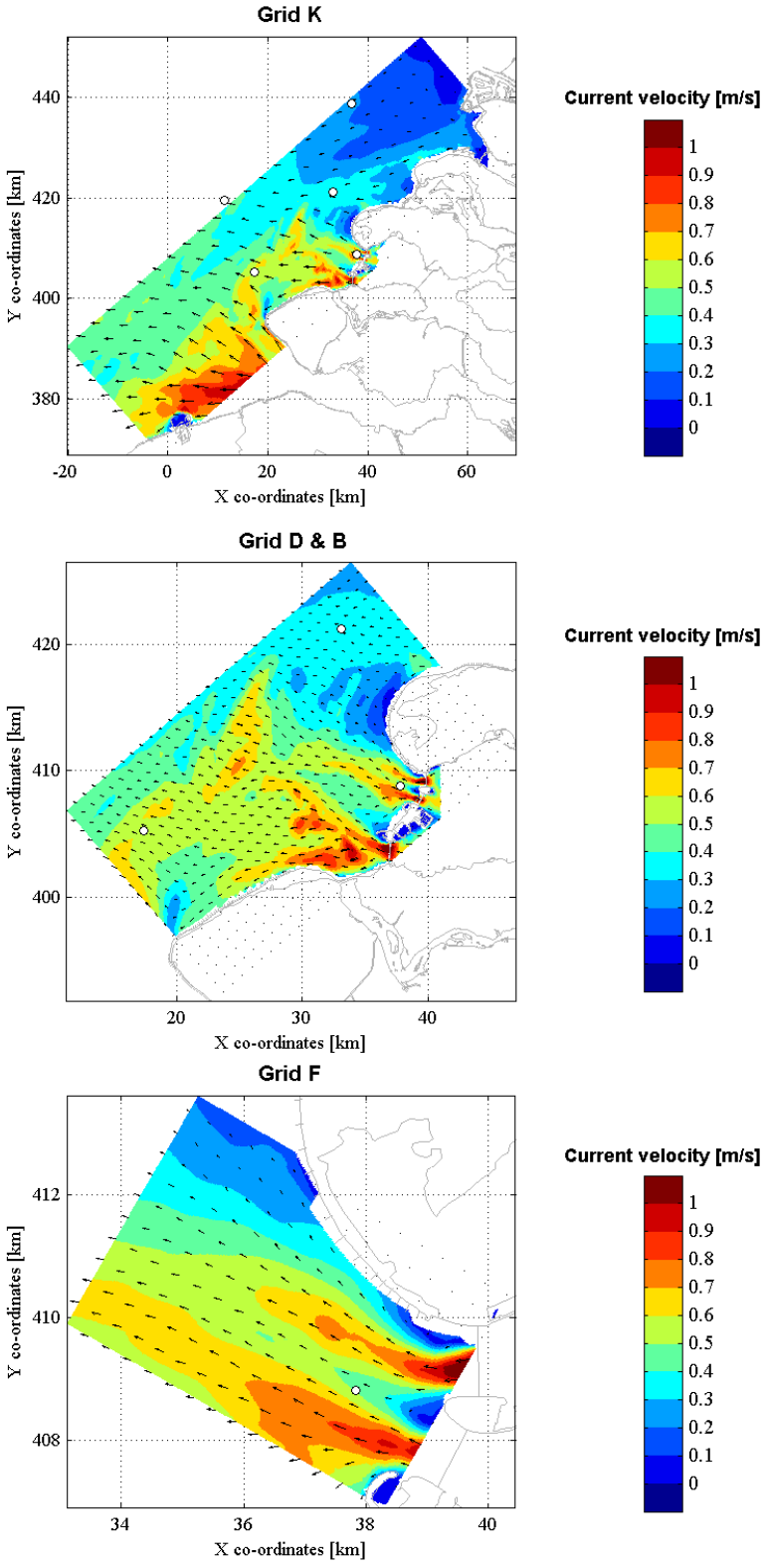

SVASEK HYDRAULICS

SWAN results: The current velocity [m/s]

Storm B t2 (21-Dec-2003 16:00:00)

APPENDIX 4.4.B2
1461
18-Dec-2007

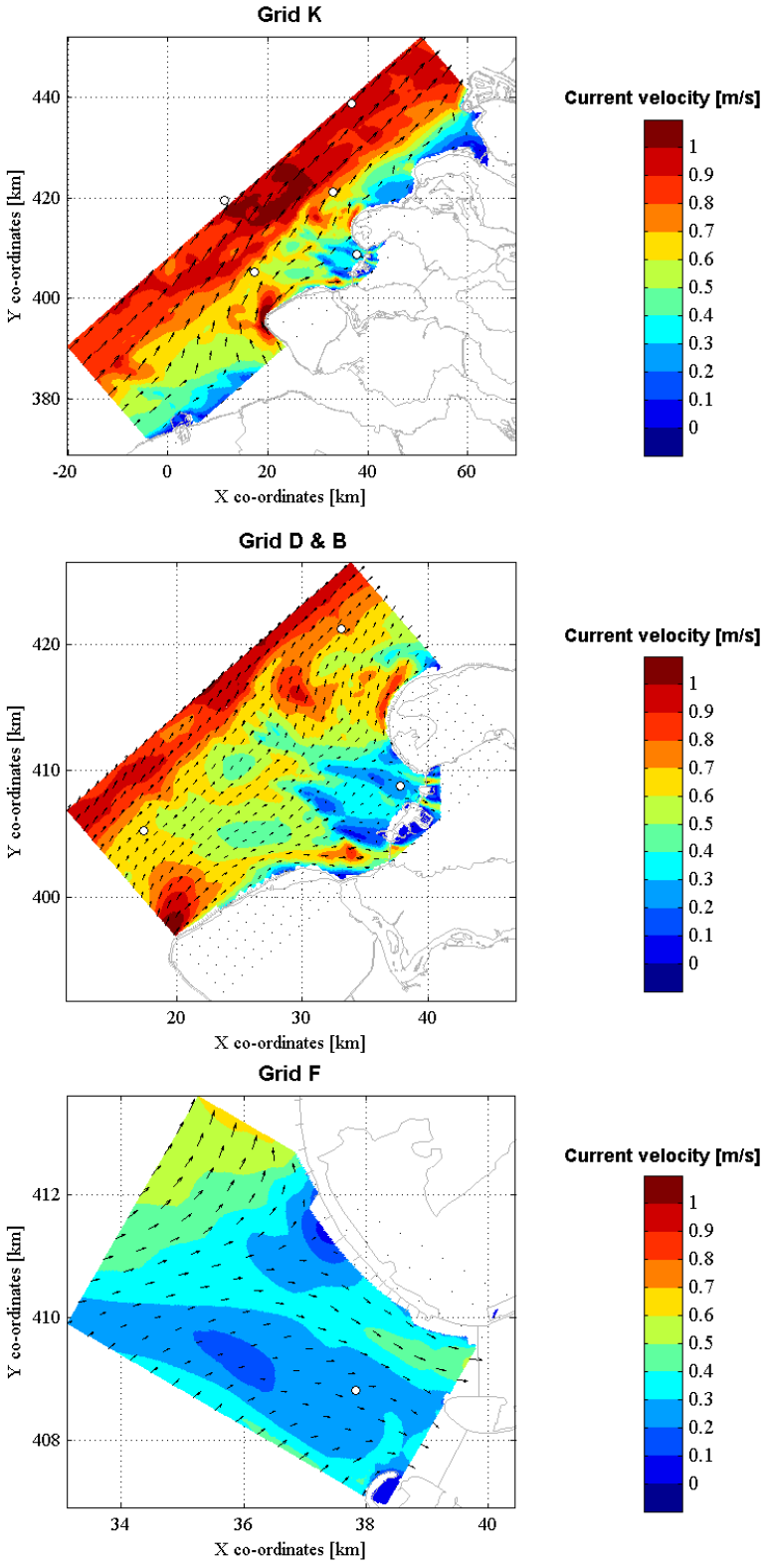

SVASEK HYDRAULICS

SWAN results: The current velocity [m/s]

Storm B t3 (23-Dec-2003 02:30:00)

APPENDIX 4.4.B3
1461
18-Dec-2007

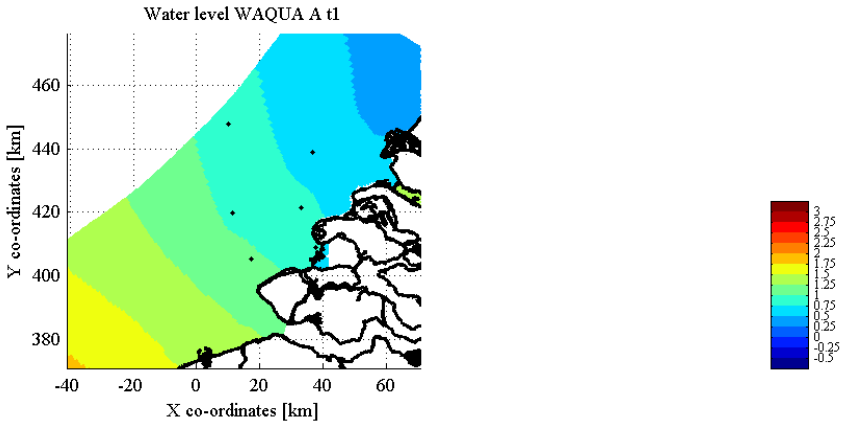

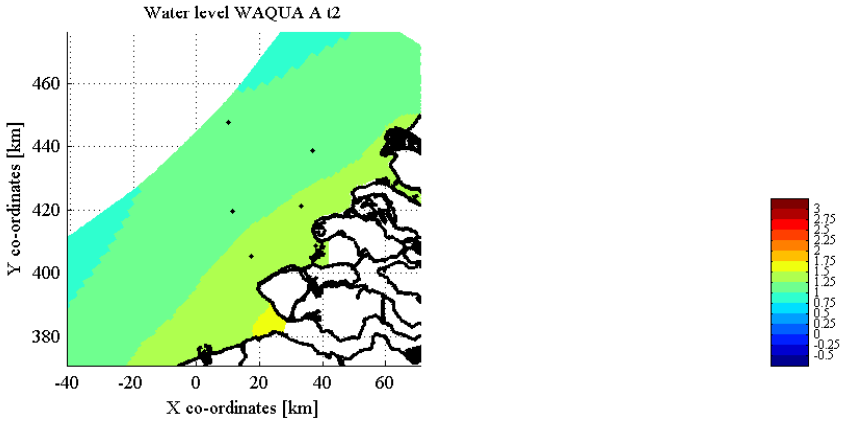

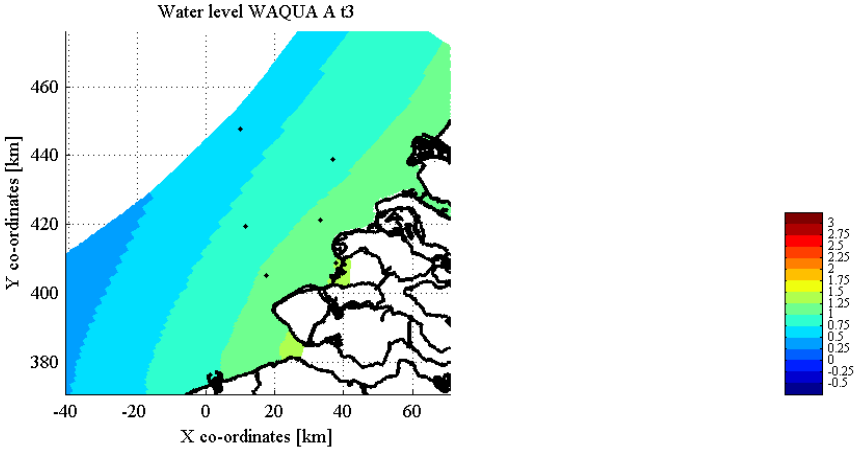

SVASEK HYDRAULICS

WAQUA waterlevel fields

storm A

APPENDIX 4.5A
1461
18-Dec-2007

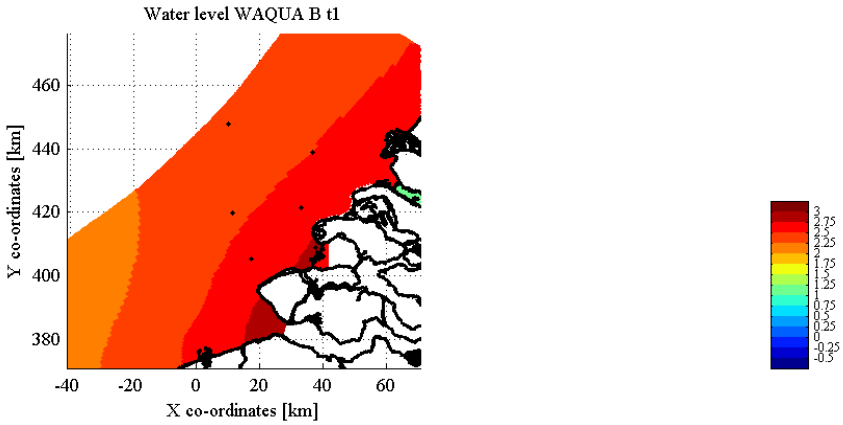

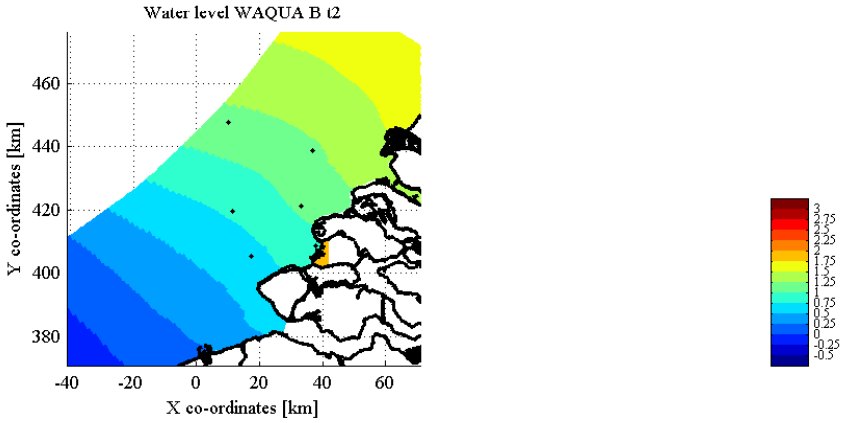

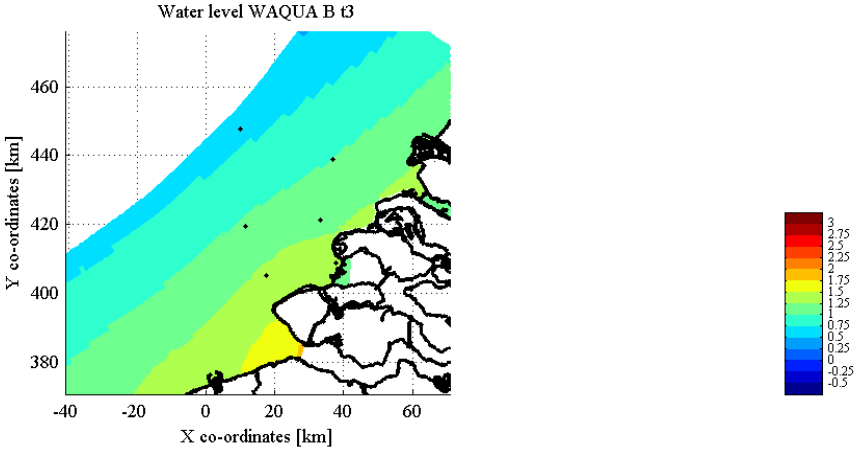

SVASEK HYDRAULICS

WAQUA waterlevel fields

storm B

APPENDIX 4.5B
1461
18-Dec-2007

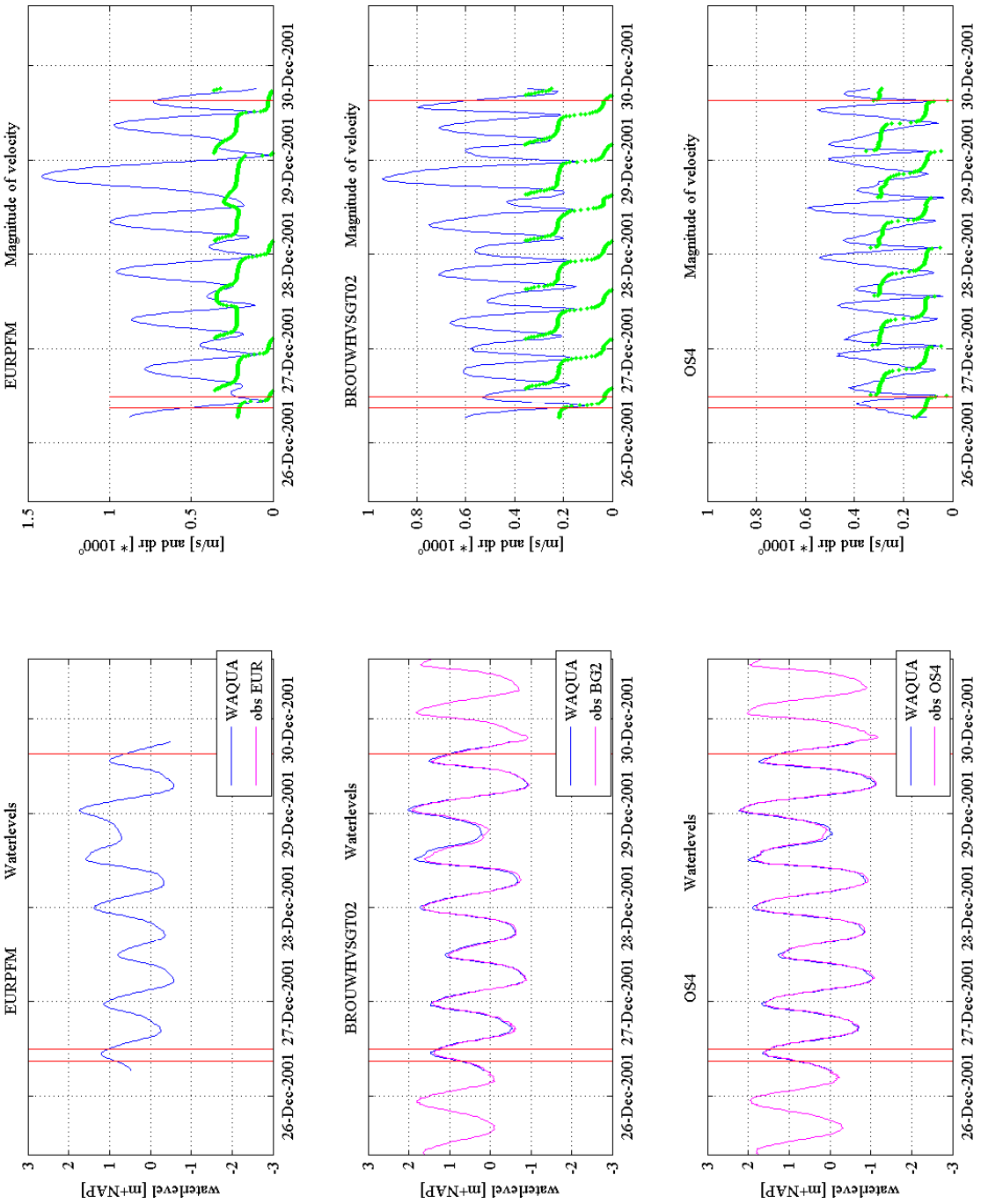

Check waterlevel timeseries storm A (obs and WAQUA)

and presentation WAQUA flow

APPENDIX 4.6
1461
18-Dec-2007

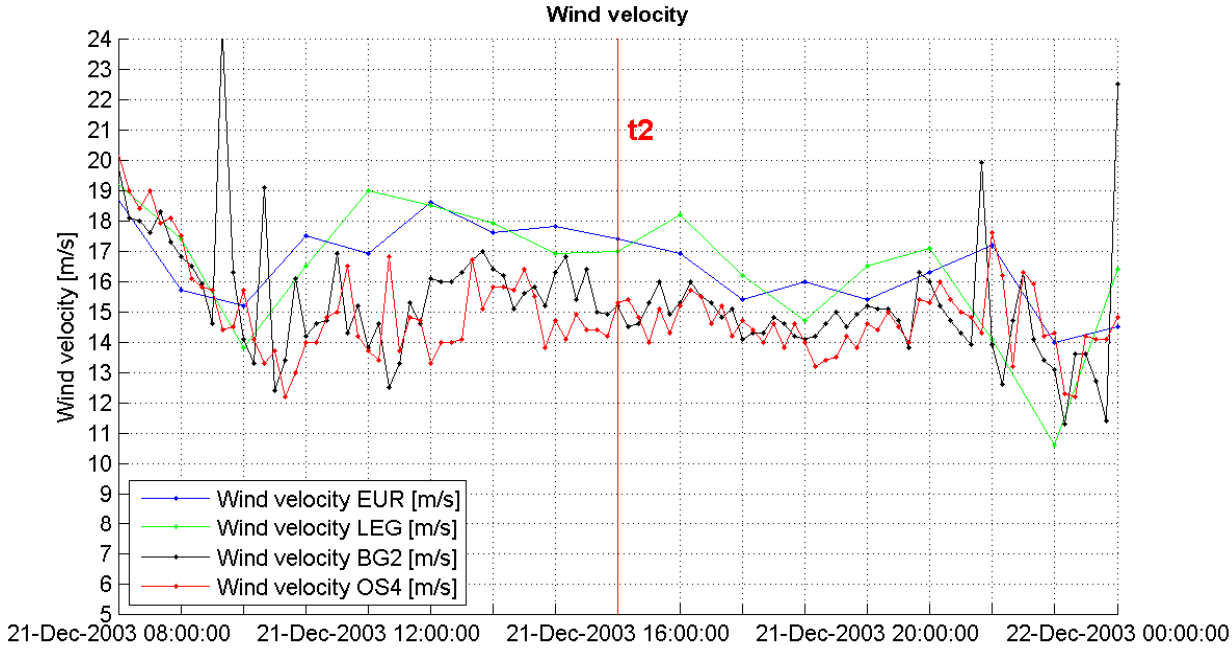
Wind velocity
Wind velocity [m/s]
t2
Wind velocity EUR [m/s]
Wind velocity LEG [m/s]
Wind velocity BG2 [m/s]
Wind velocity OS4 [m/s]
21-Dec-2003 08:00:00
21-Dec-2003 12:00:00
21-Dec-2003 16:00:00
21-Dec-2003 20:00:00
22-Dec-2003 00:00:00

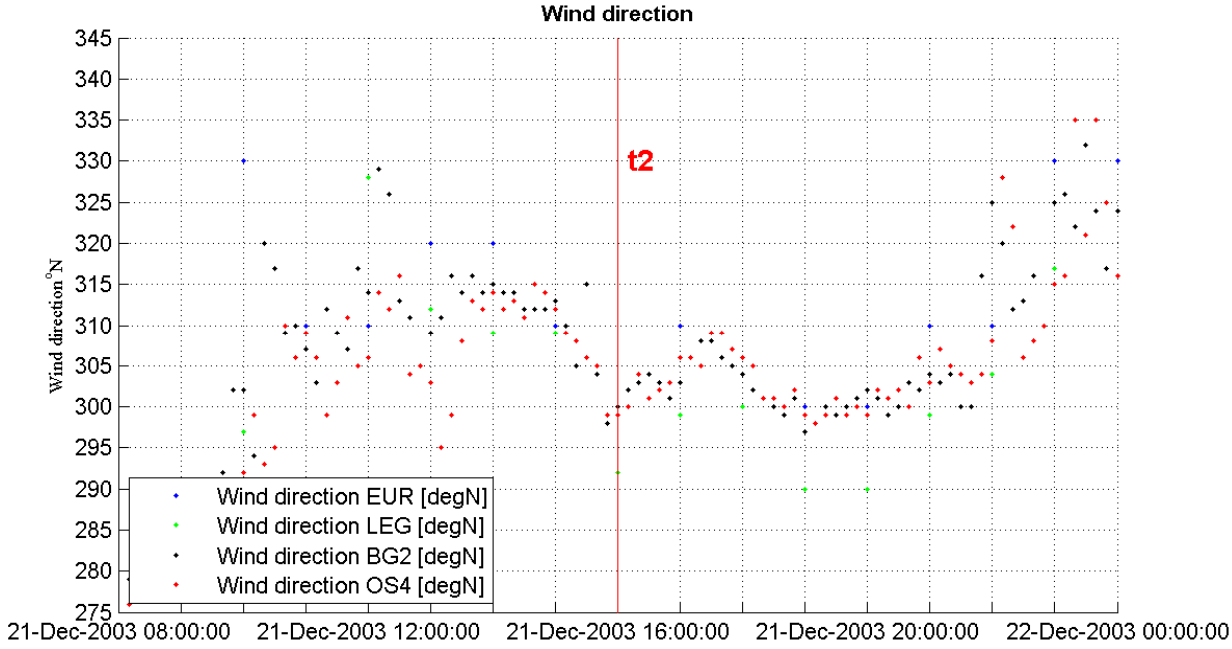
Wind direction
Wind direction °N
t2
Wind direction EUR [degN]
Wind direction LEG [degN]
Wind direction BG2 [degN]
Wind direction OS4 [degN]
21-Dec-2003 08:00:00
21-Dec-2003 12:00:00
21-Dec-2003 16:00:00
21-Dec-2003 20:00:00
22-Dec-2003 00:00:00

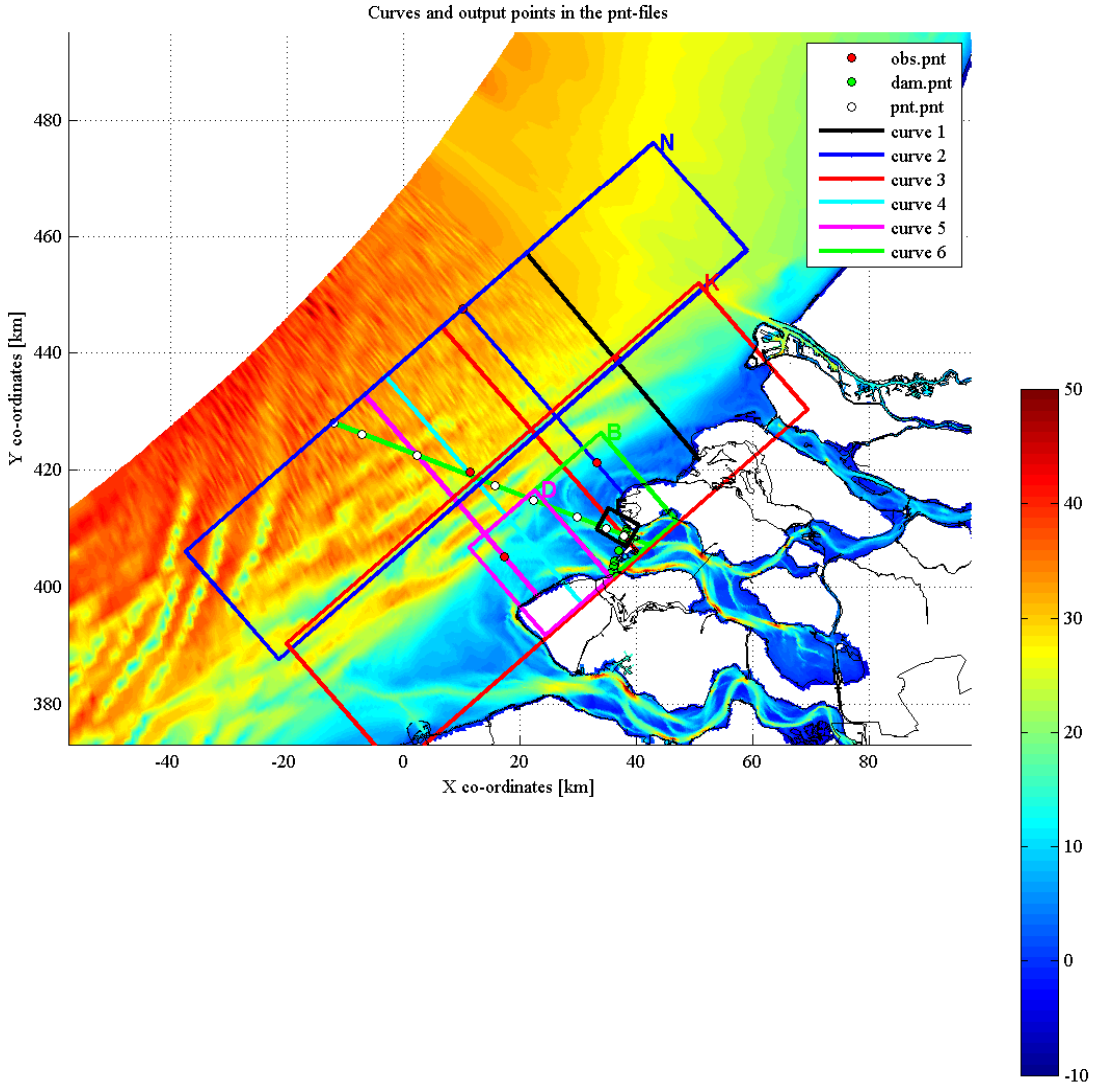

Overview of the output locations
Curves and output points in the pnt-files

APPENDIX 4.8
1461
18-Dec-2007

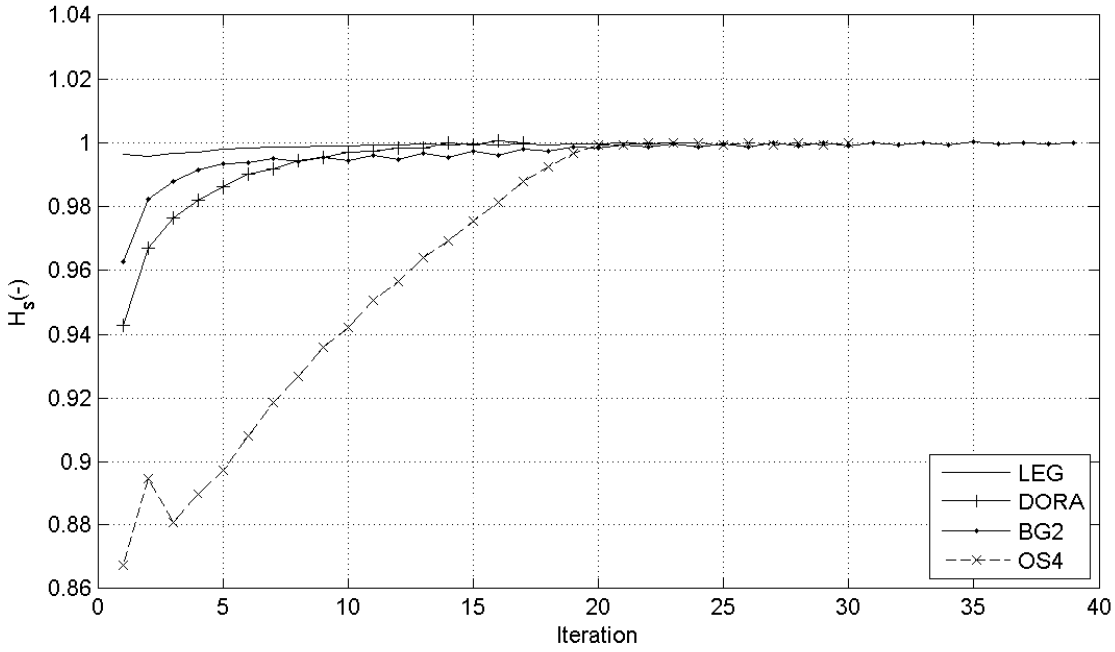

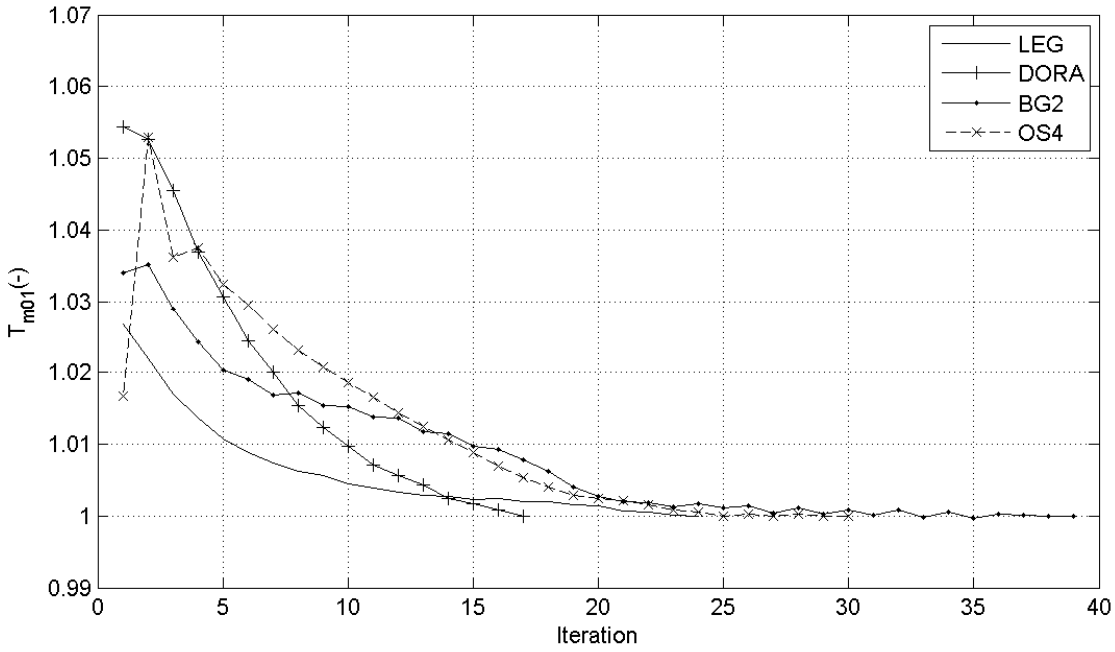

SVASEK HYDRAULICS

Convergence behaviour of the wave parameters H_{m0} and T_{m01} (normalized with the last value per location)

Storm A t1 (26-Dec-2001 09:00:00)

APPENDIX 5.1.A1

1461

18-Dec-2007

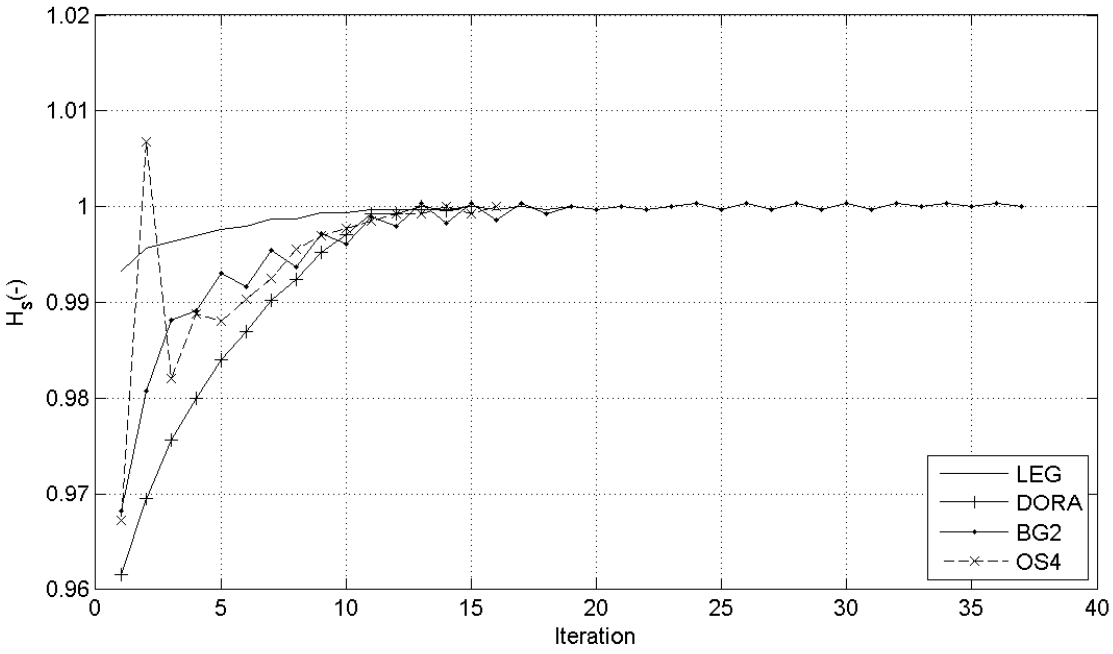

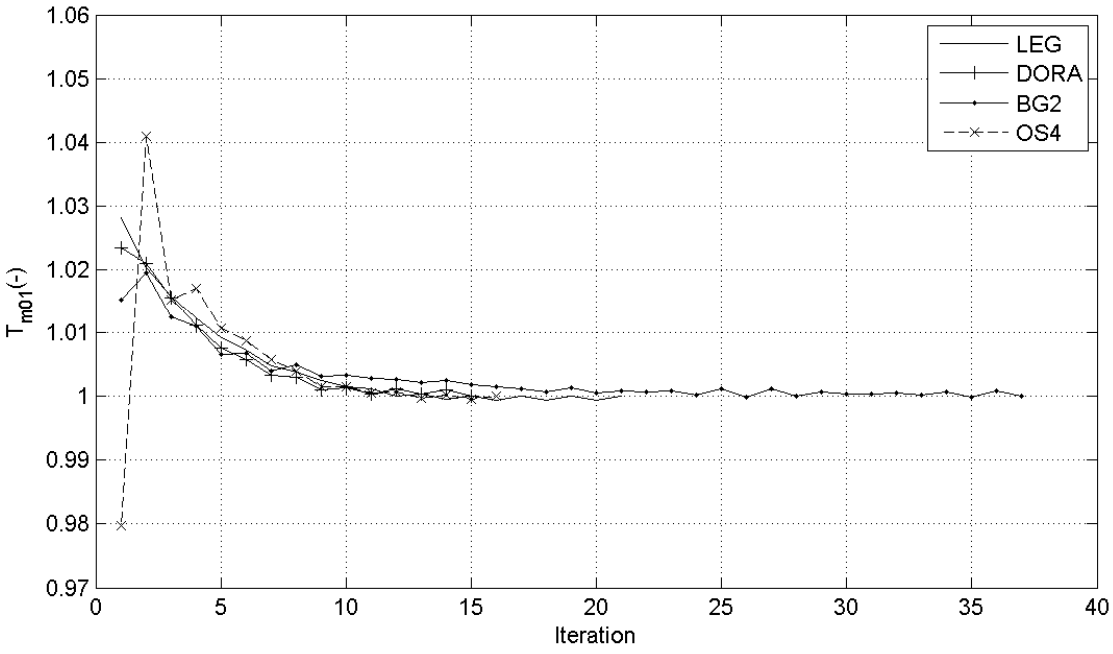

SVASEK HYDRAULICS

Convergence behaviour of the wave parameters H_{m0} and T_{m01} APPENDIX 5.1.A2
(normalized with the last value per location)
1461
Storm A t2 (26-Dec-2001 12:00:00)
18-Dec-2007

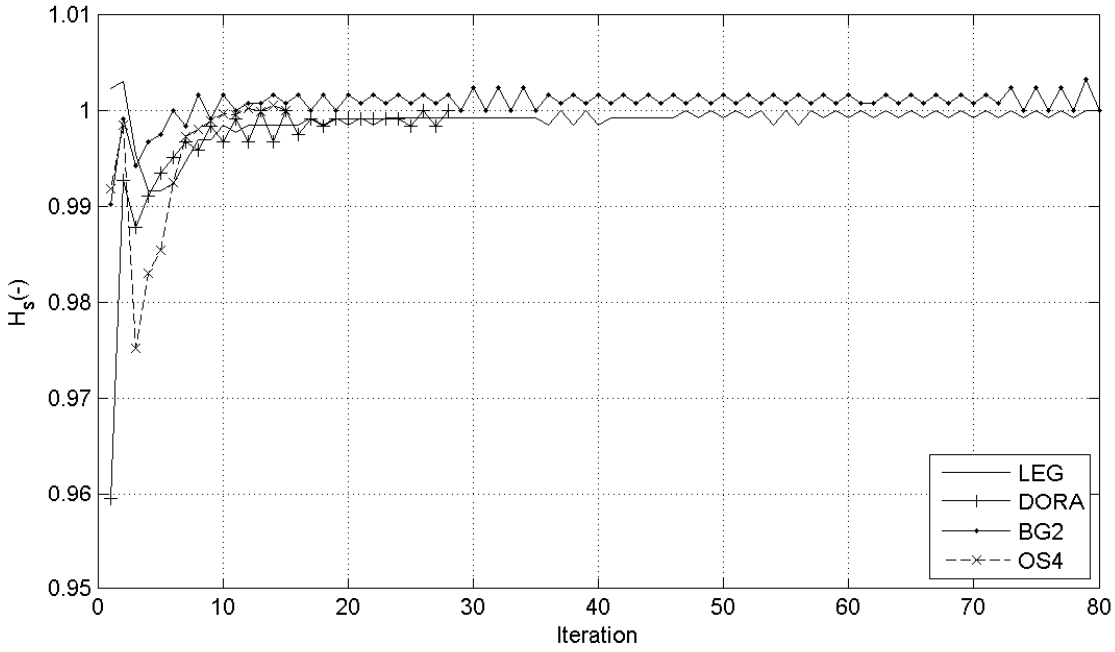

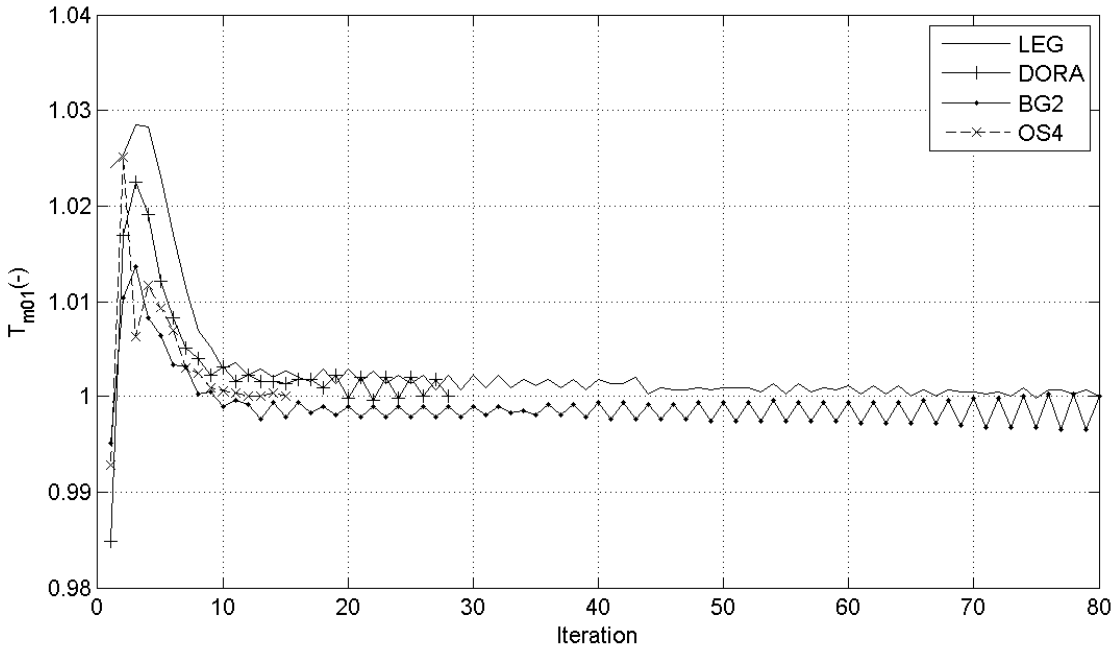

SVASEK HYDRAULICS

Convergence behaviour of the wave parameters H_{m0} and T_{m01} (normalized with the last value per location)

Storm A t3 (29-Dec-2001 15:00:00)

APPENDIX 5.1.A3

1461

18-Dec-2007

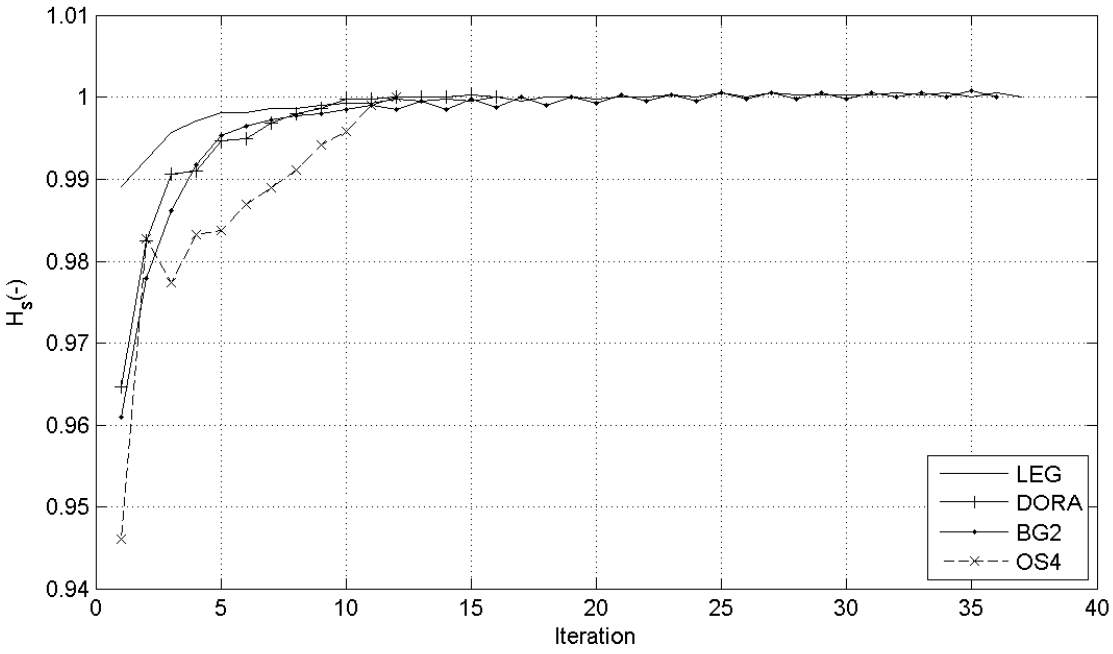

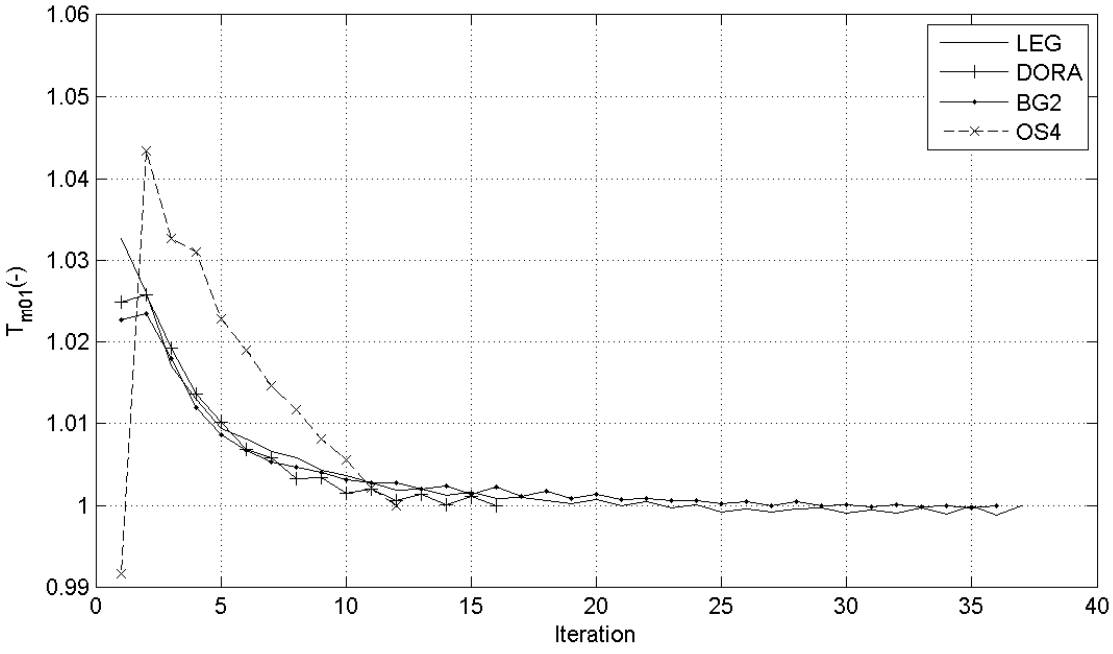

SVASEK HYDRAULICS

Convergence behaviour of the wave parameters H_{m0} and T_{m01} APPENDIX 5.1.B1
(normalized with the last value per location)
1461
Storm B t1 (21-Dec-2003 13:30:00)
18-Dec-2007

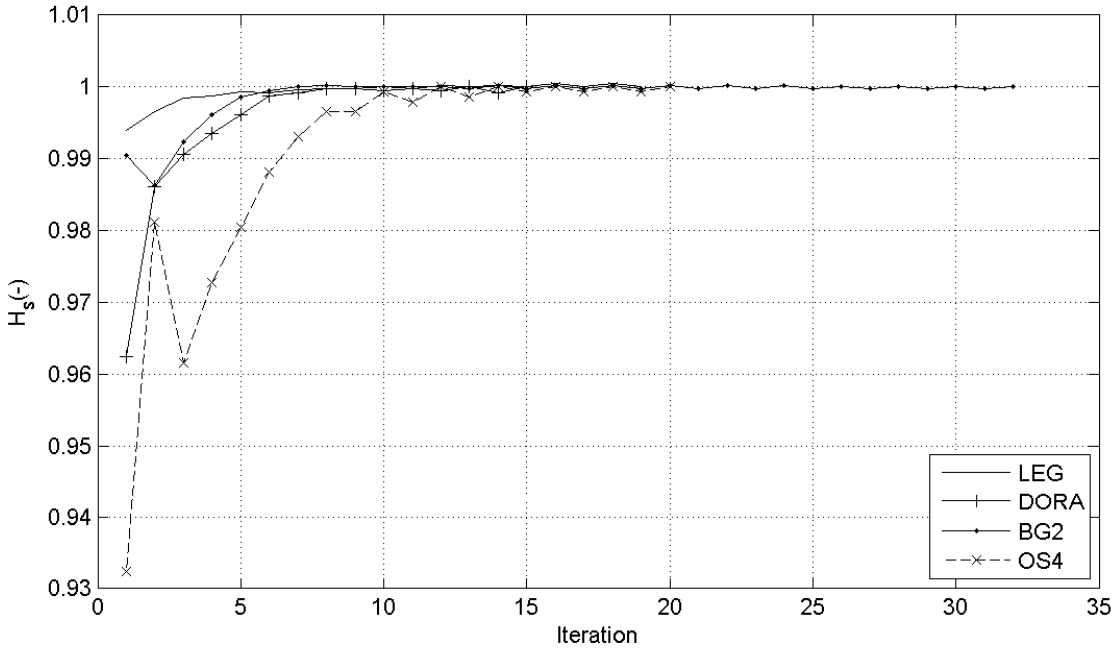

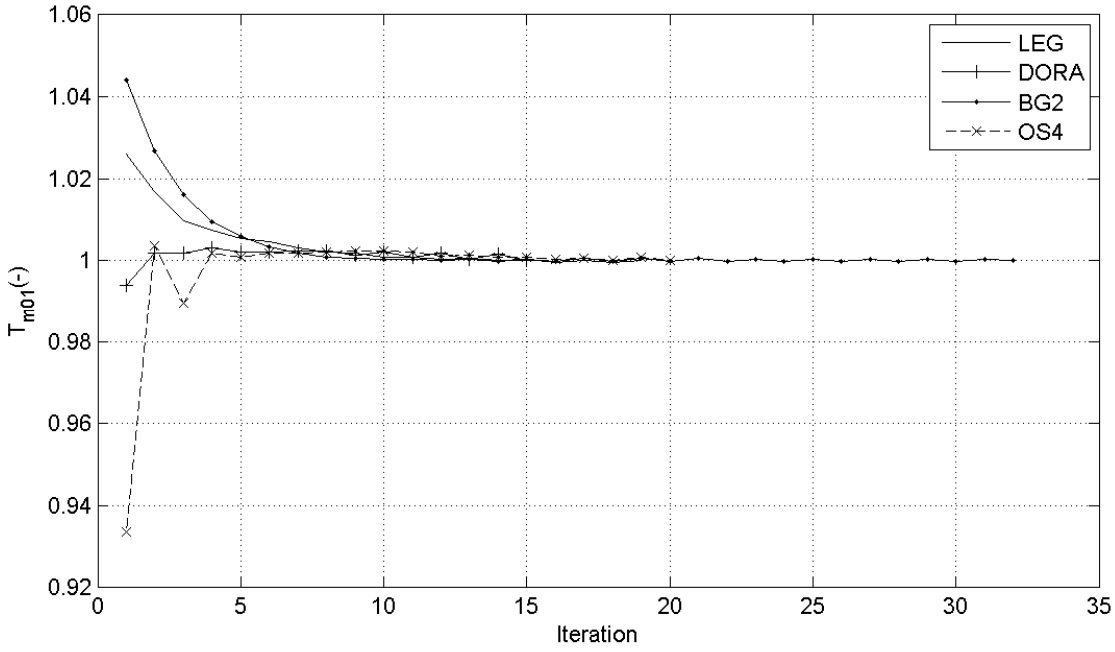

Convergence behaviour of the wave parameters H_{m0} and T_{m01} (normalized with the last value per location)

Storm B t2 (21-Dec-2003 16:00:00)

APPENDIX 5.1.B2

1461

18-Dec-2007

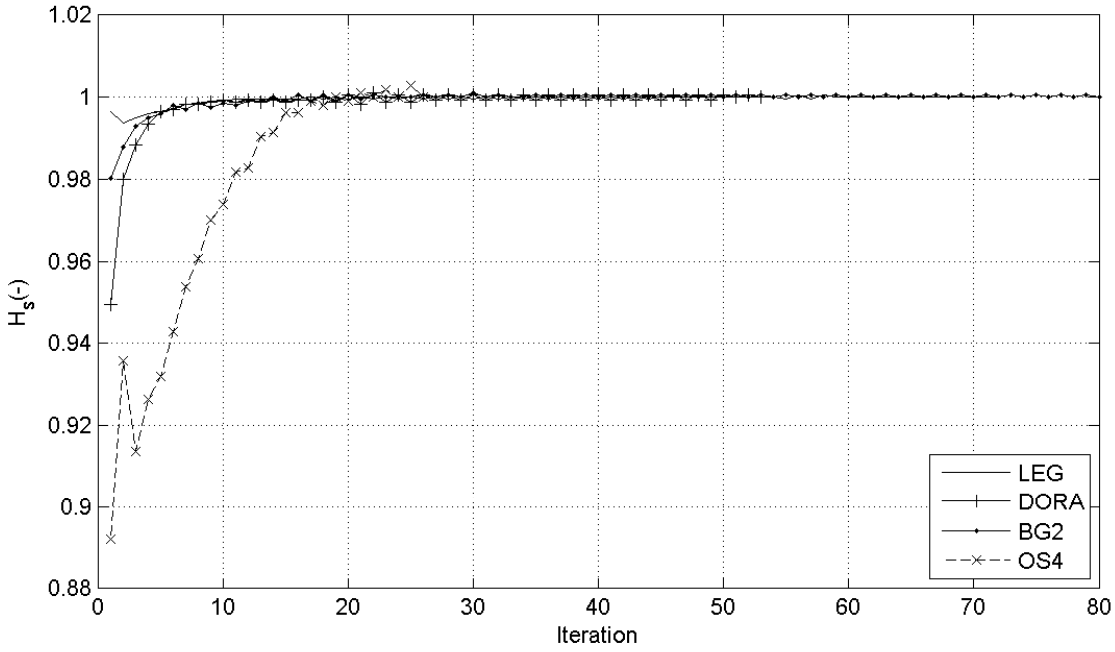

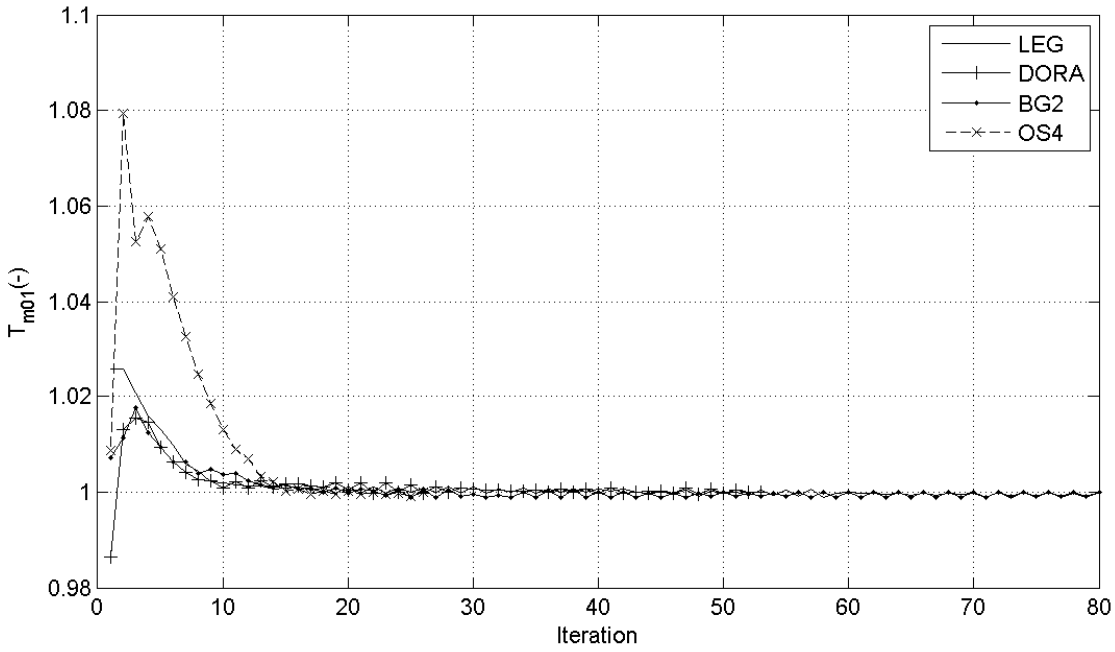

SVASEK HYDRAULICS

Convergence behaviour of the wave parameters H_{m0} and T_{m01} (normalized with the last value per location)

Storm B t3 (23-Dec-2003 02:30:00)

APPENDIX 5.1.B3

1461

18-Dec-2007

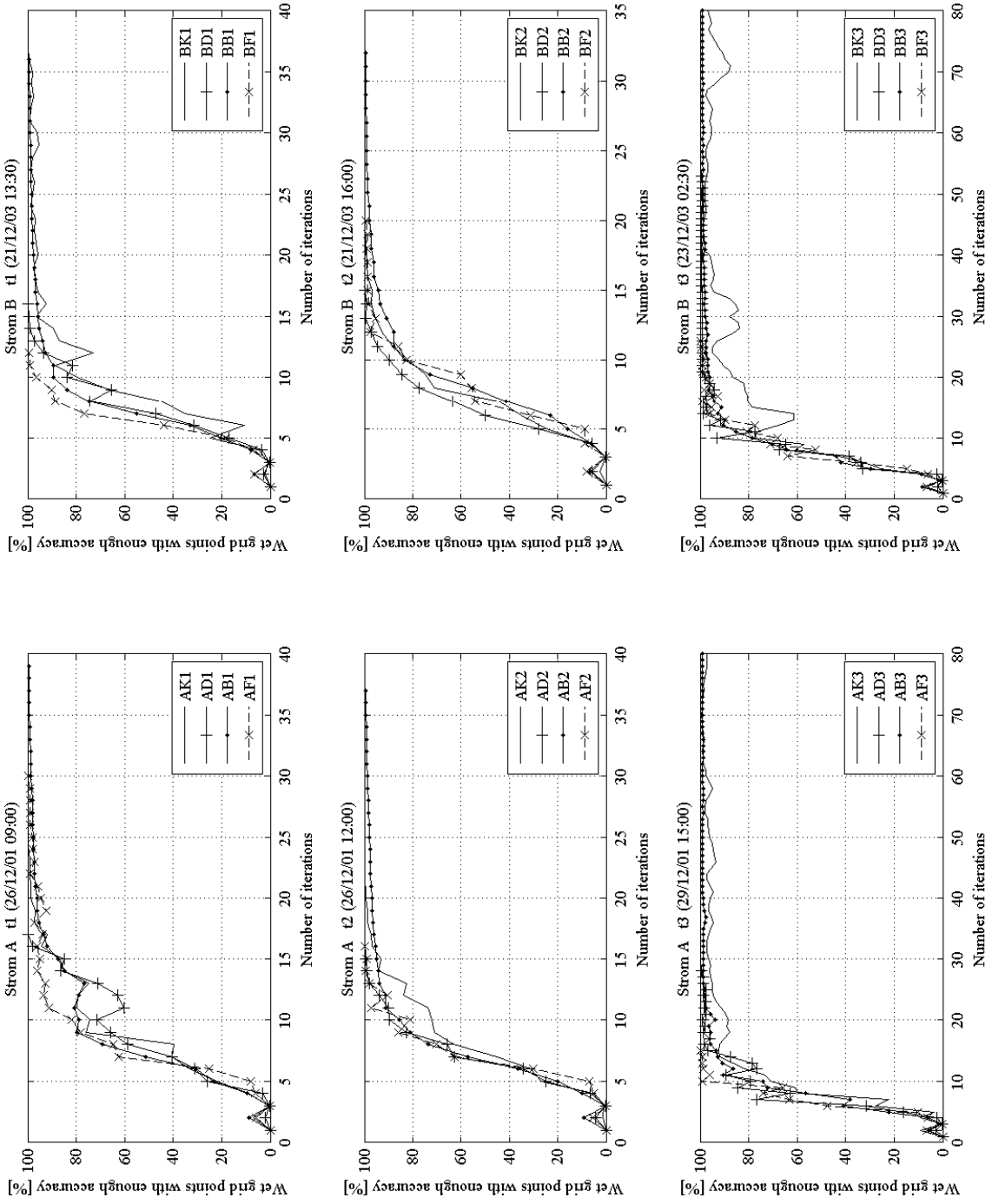

SVASEK HYDRAULICS

Iteration process on wet gridpoints
Storm A & B

APPENDIX 5.2
1461
18-Dec-2007

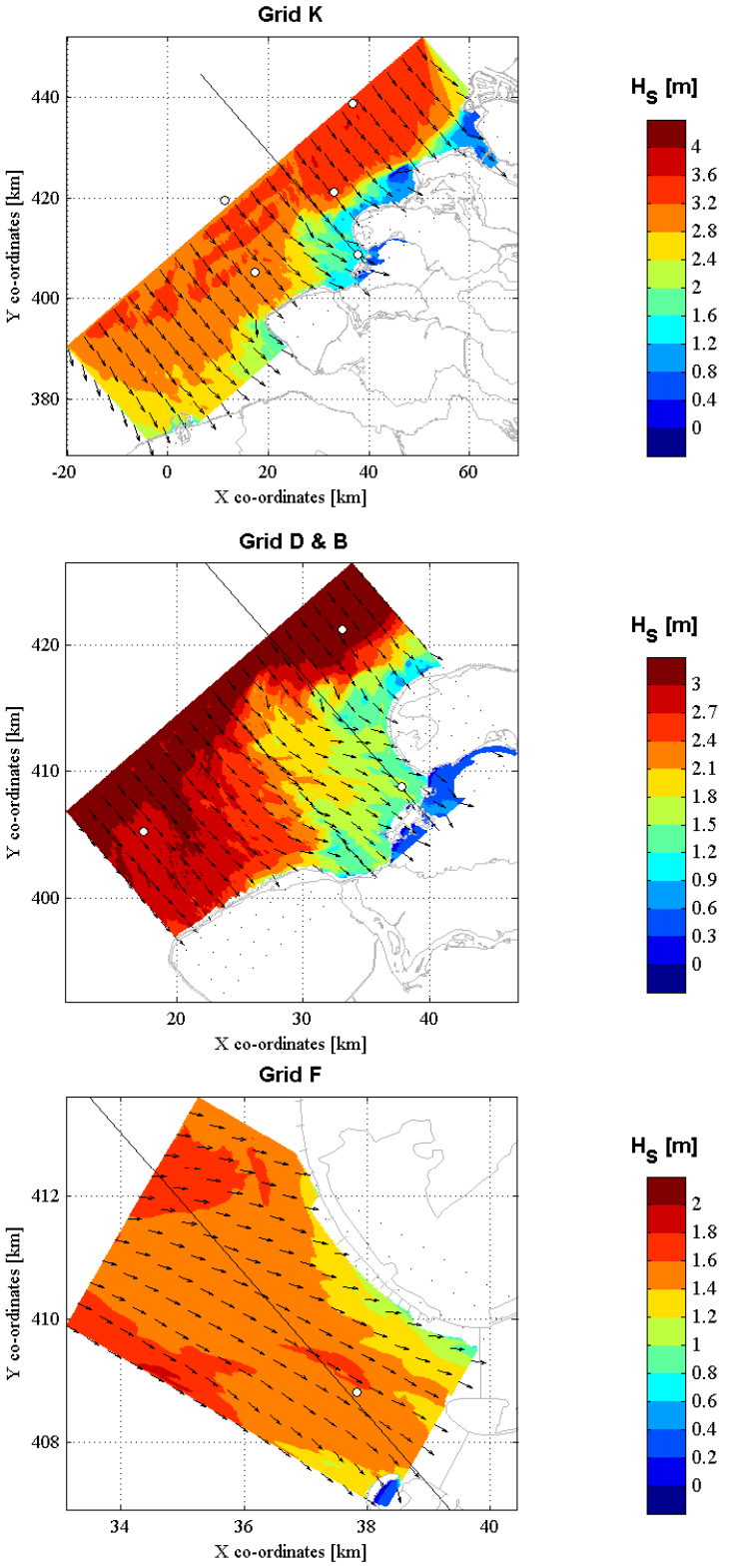

SVASEK HYDRAULICS

SWAN results: The wave height H_{m0} [m]

Storm A t1 (26-Dec-2001 09:00:00)

APPENDIX 5.3.A1
1461
18-Dec-2007

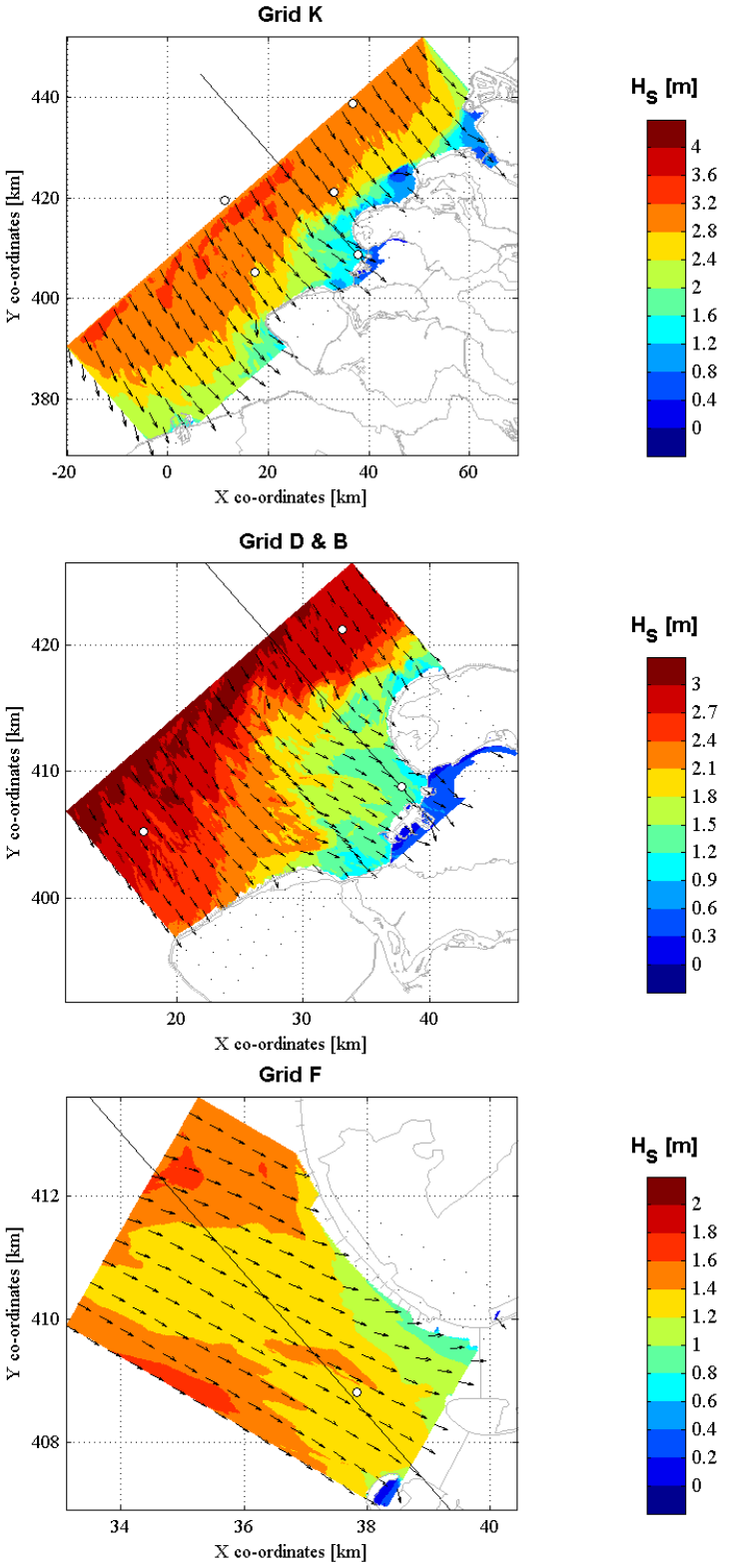

SVASEK HYDRAULICS

SWAN results: The wave height H_{m0} [m]

Storm A t2 (26-Dec-2001 12:00:00)

APPENDIX 5.3.A2
1461
18-Dec-2007

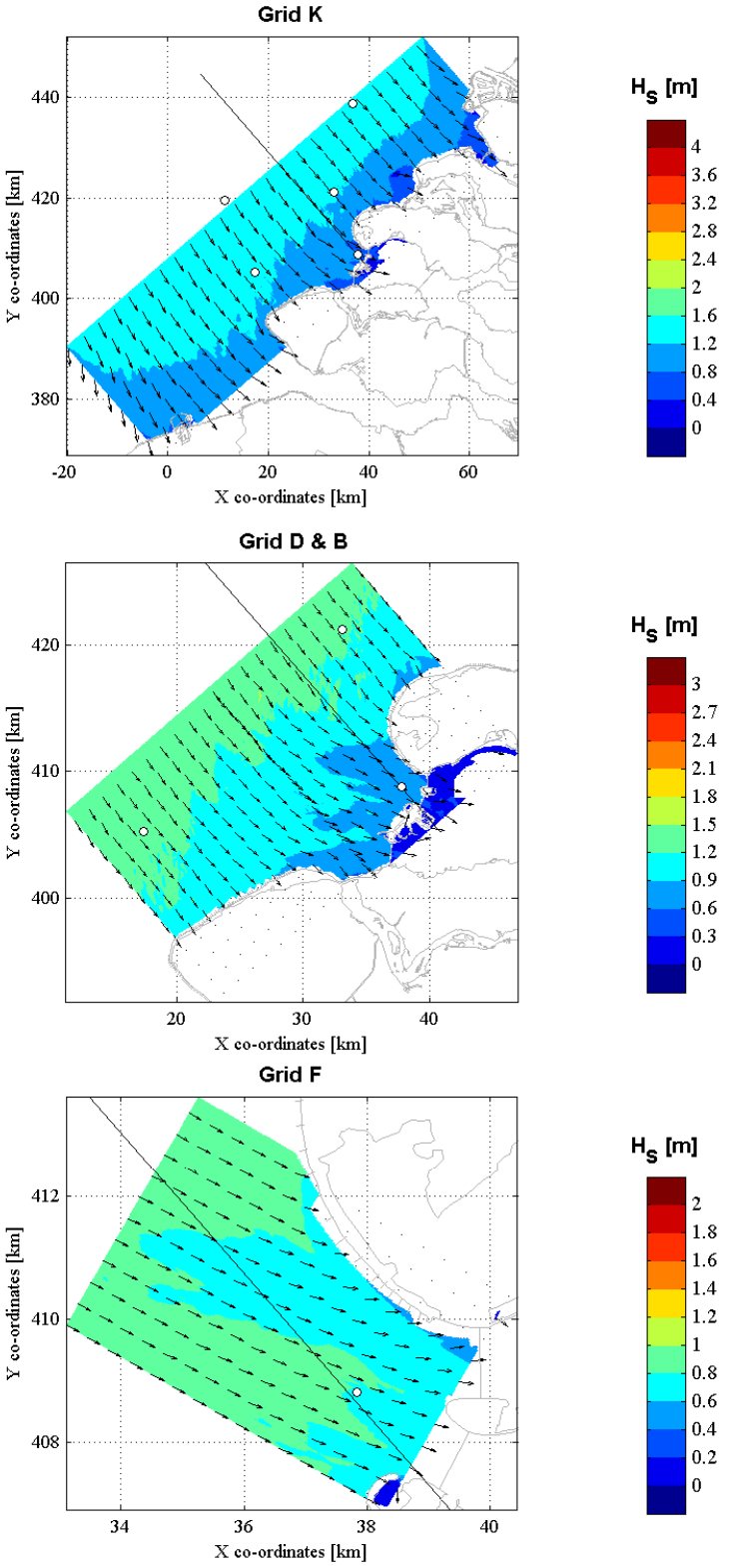

SVASEK HYDRAULICS

SWAN results: The wave height H_{m0} [m]

Storm A t3 (29-Dec-2001 15:00:00)

APPENDIX 5.3.A3
1461
18-Dec-2007

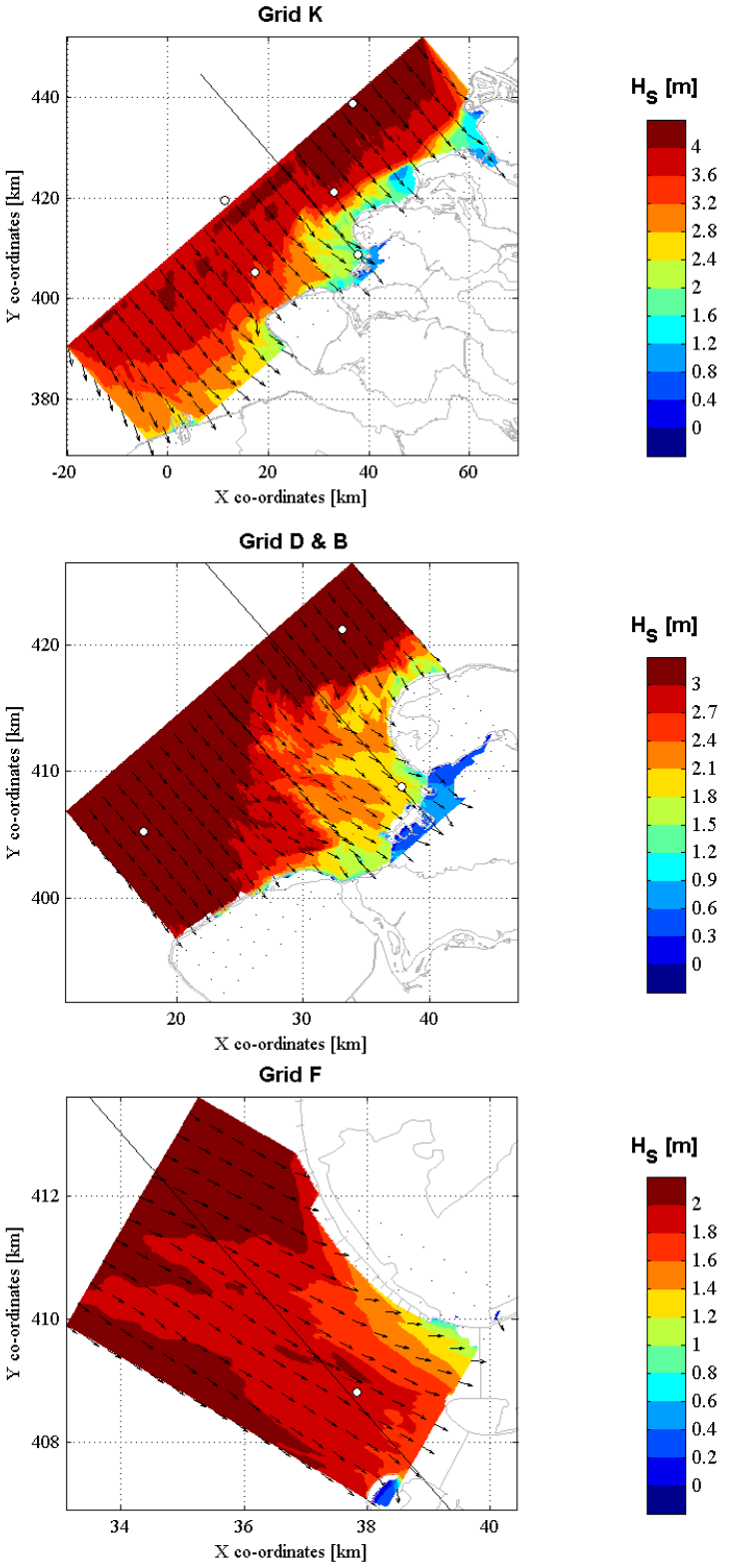

SVASEK HYDRAULICS

SWAN results: The wave height H_{m0} [m]

Storm B t1 (21-Dec-2003 13:30:00)

APPENDIX 5.3.B1
1461
18-Dec-2007

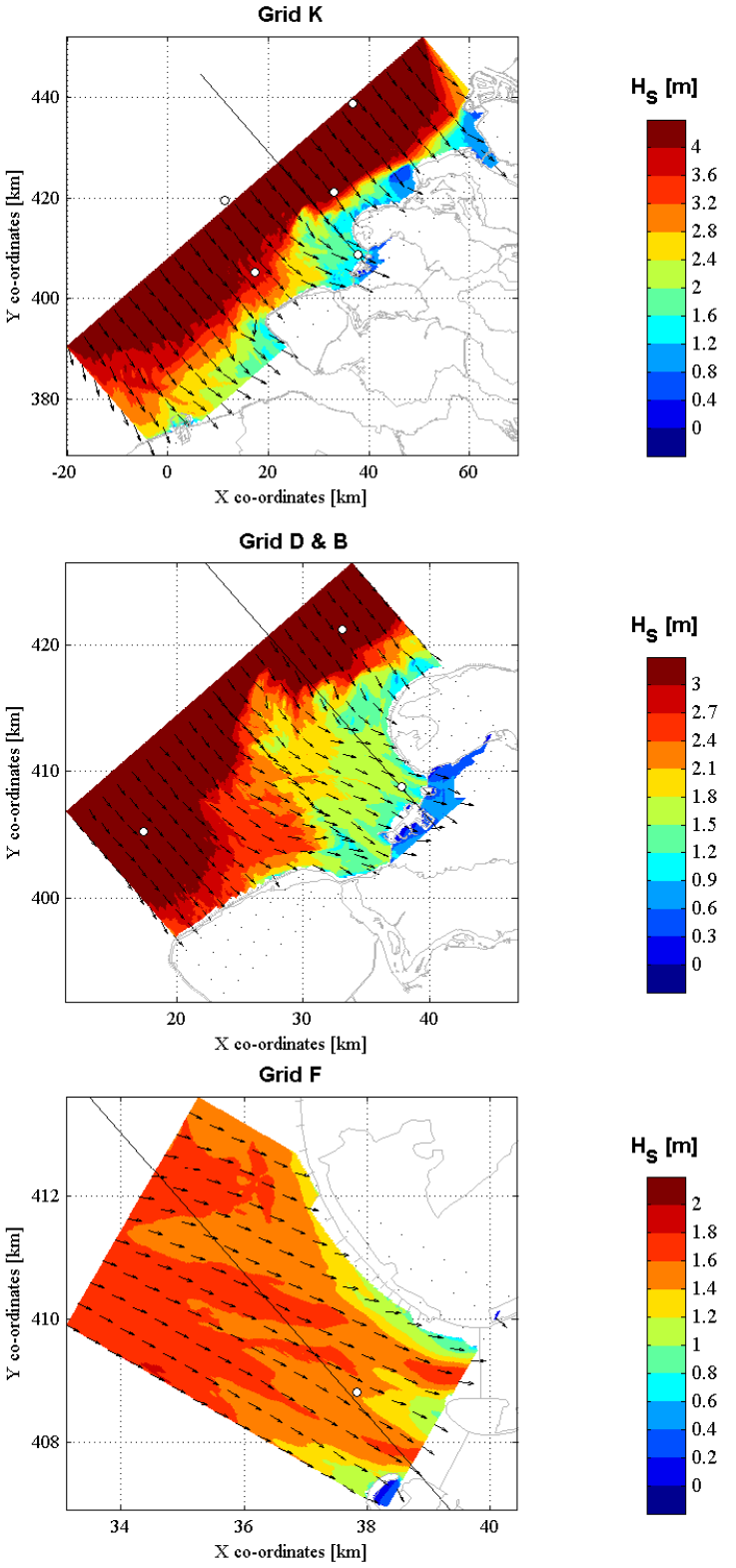

SVASEK HYDRAULICS

SWAN results: The wave height H_{m0} [m]

Storm B t2 (21-Dec-2003 16:00:00)

APPENDIX 5.3.B2
1461
18-Dec-2007

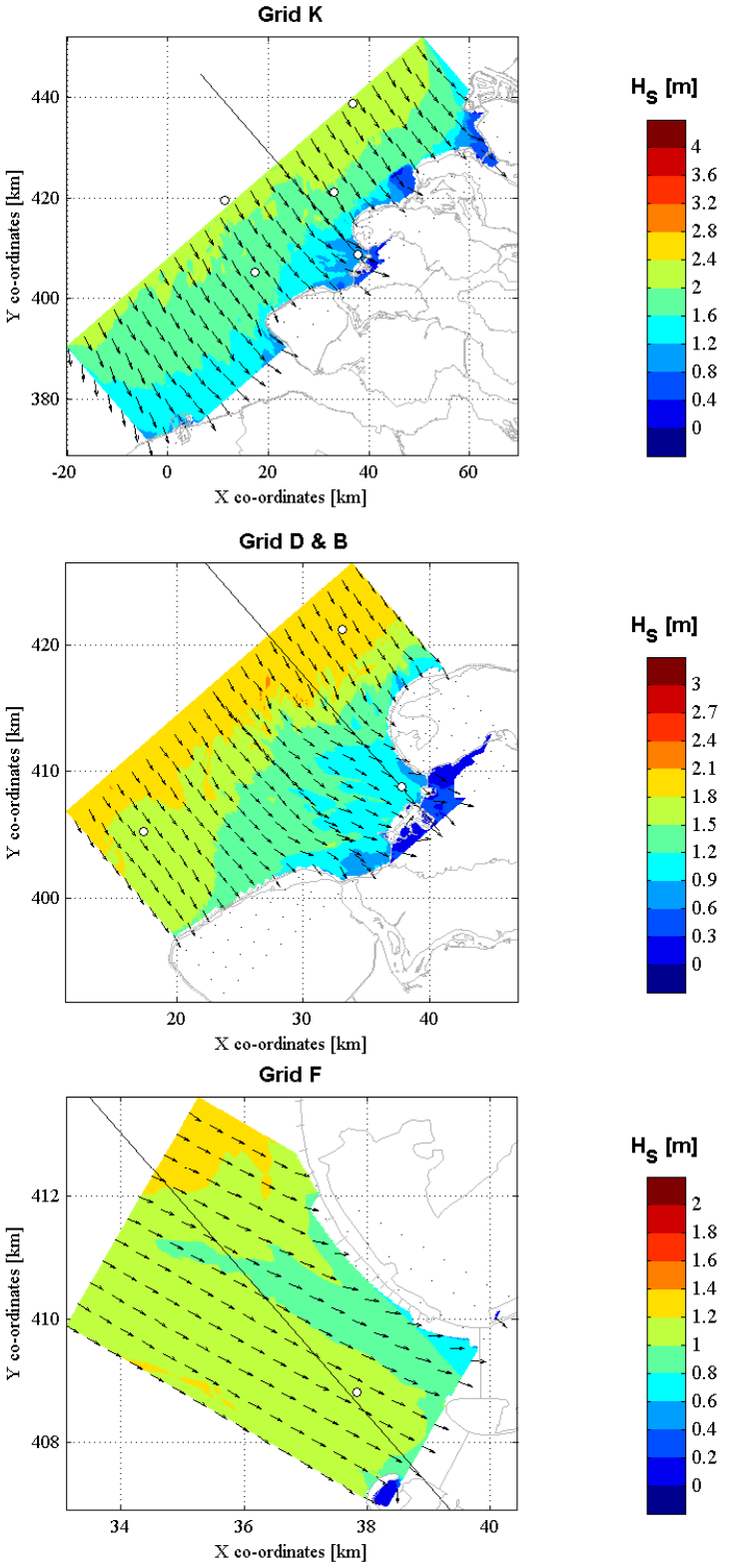

SVASEK HYDRAULICS

SWAN results: The wave height H_{m0} [m]

Storm B t3 (23-Dec-2003 02:30:00)

APPENDIX 5.3.B3
1461
18-Dec-2007

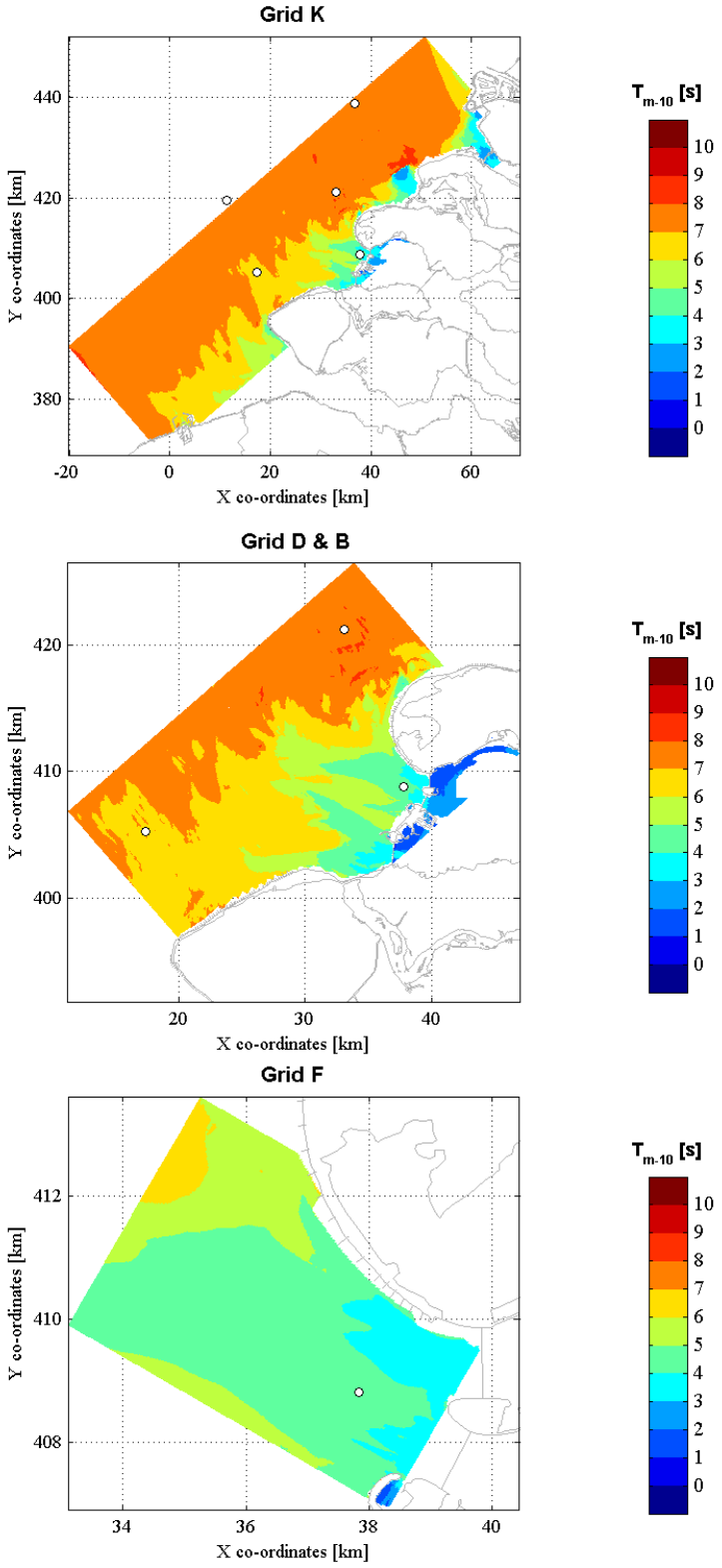

SVASEK HYDRAULICS

SWAN results: The wave period T_{m-10}

Storm A t1 (26-Dec-2001 09:00:00)

APPENDIX 5.4.A1
1461
18-Dec-2007

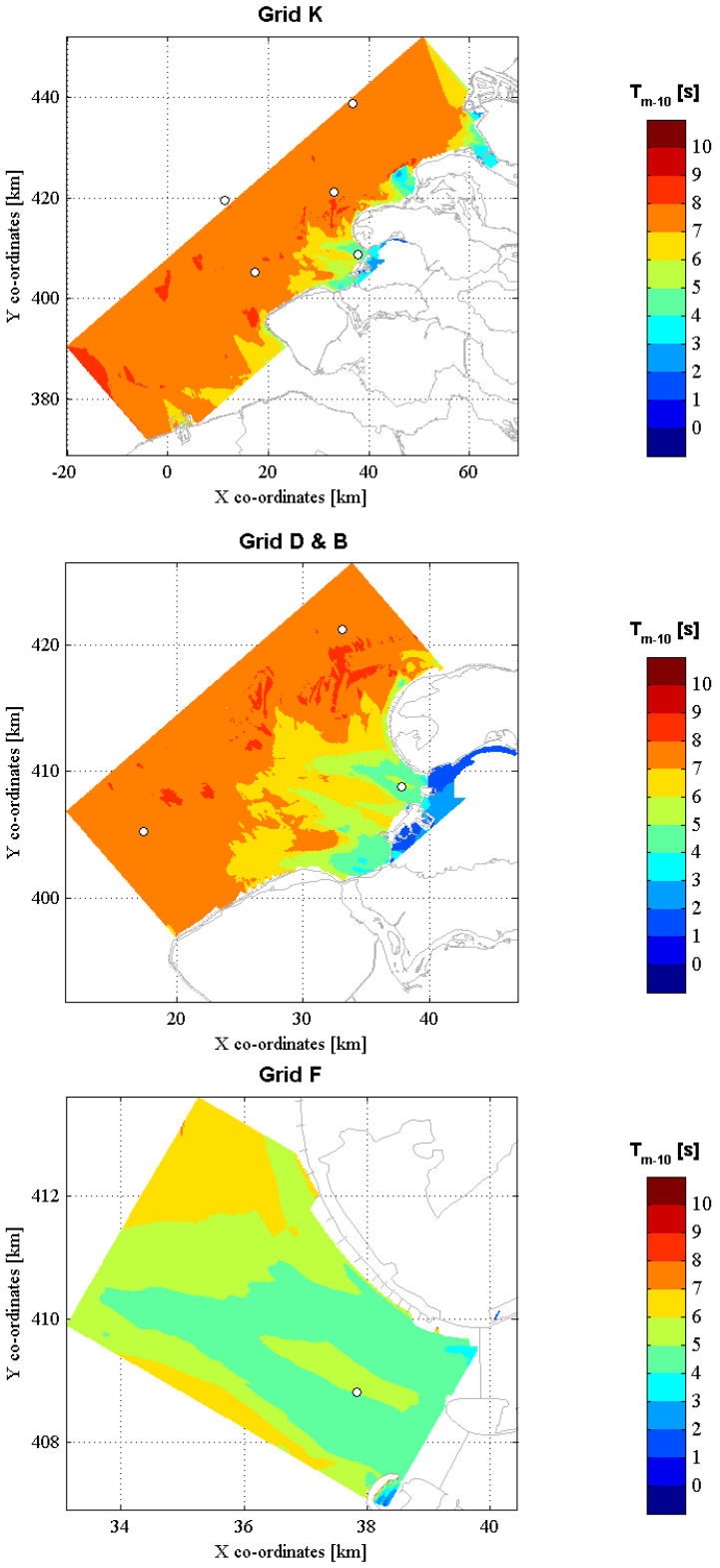

SVASEK HYDRAULICS

SWAN results: The wave period T_{m-10}

Storm A t2 (26-Dec-2001 12:00:00)

APPENDIX 5.4.A2
1461
18-Dec-2007

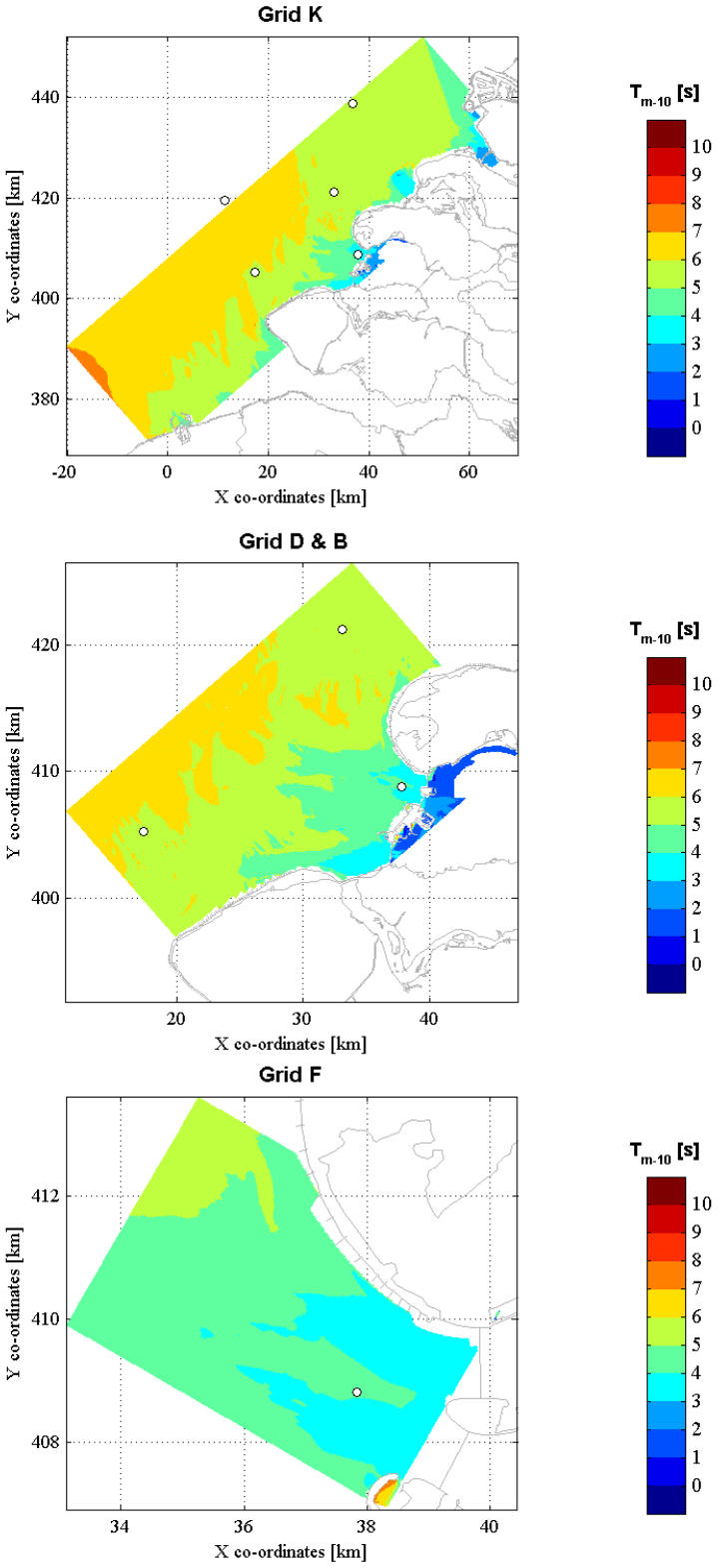

SVASEK HYDRAULICS

SWAN results: The wave period T_{m-10}

Storm A t3 (29-Dec-2001 15:00:00)

APPENDIX 5.4.A3
1461
18-Dec-2007

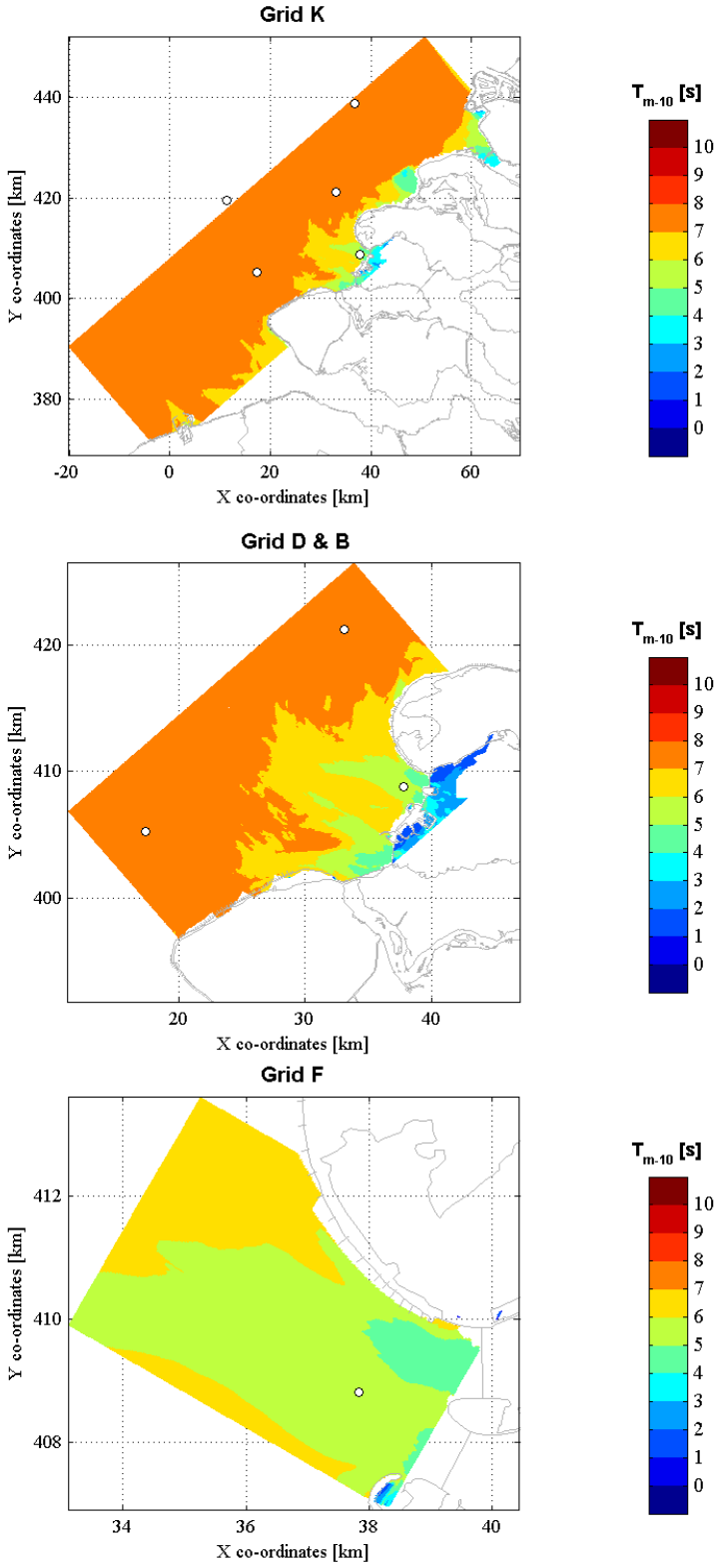

SVASEK HYDRAULICS

SWAN results: The wave period T_{m-10}

Storm B t1 (21-Dec-2003 13:30:00)

APPENDIX 5.4.B1
1461
18-Dec-2007

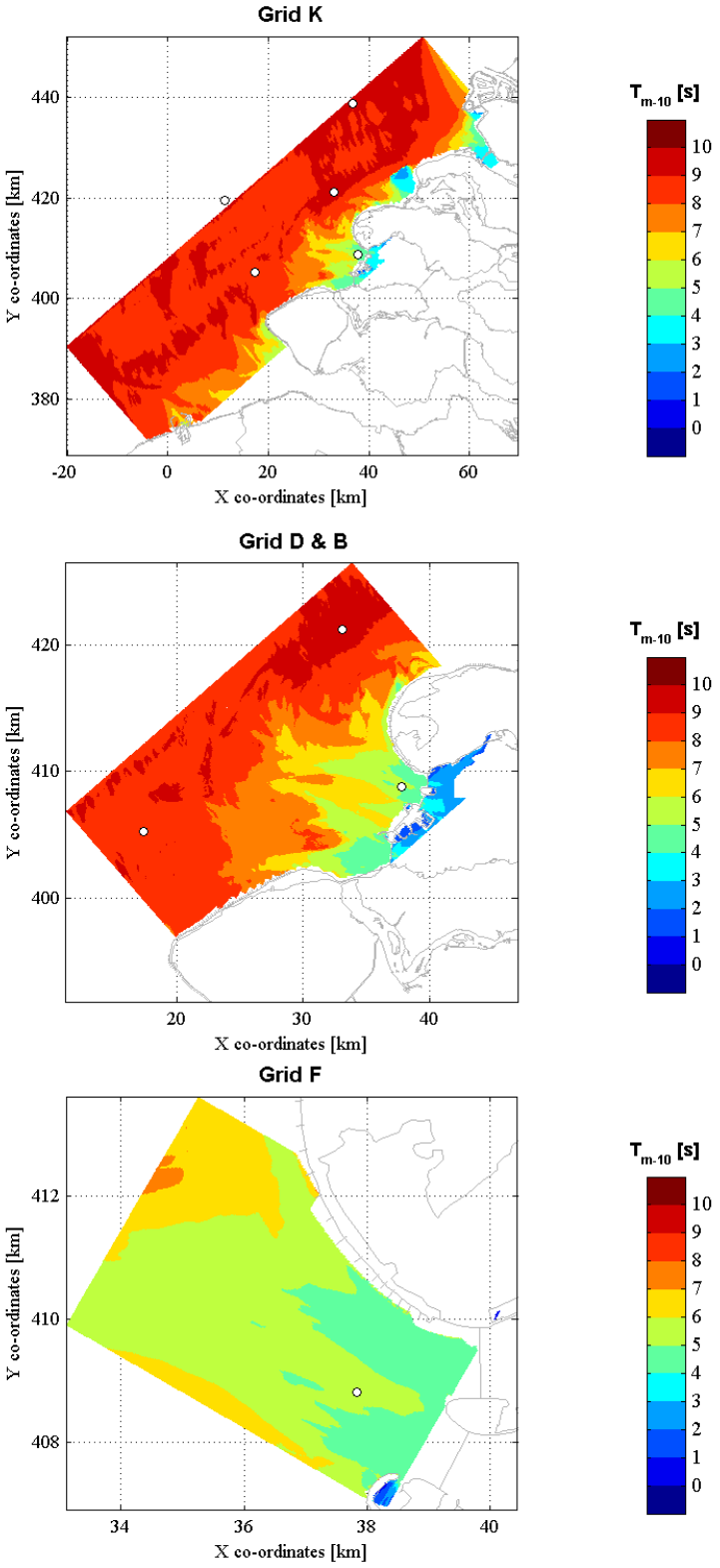

SVASEK HYDRAULICS

SWAN results: The wave period T_{m-10}

Storm B t2 (21-Dec-2003 16:00:00)

APPENDIX 5.4.B2
1461
18-Dec-2007

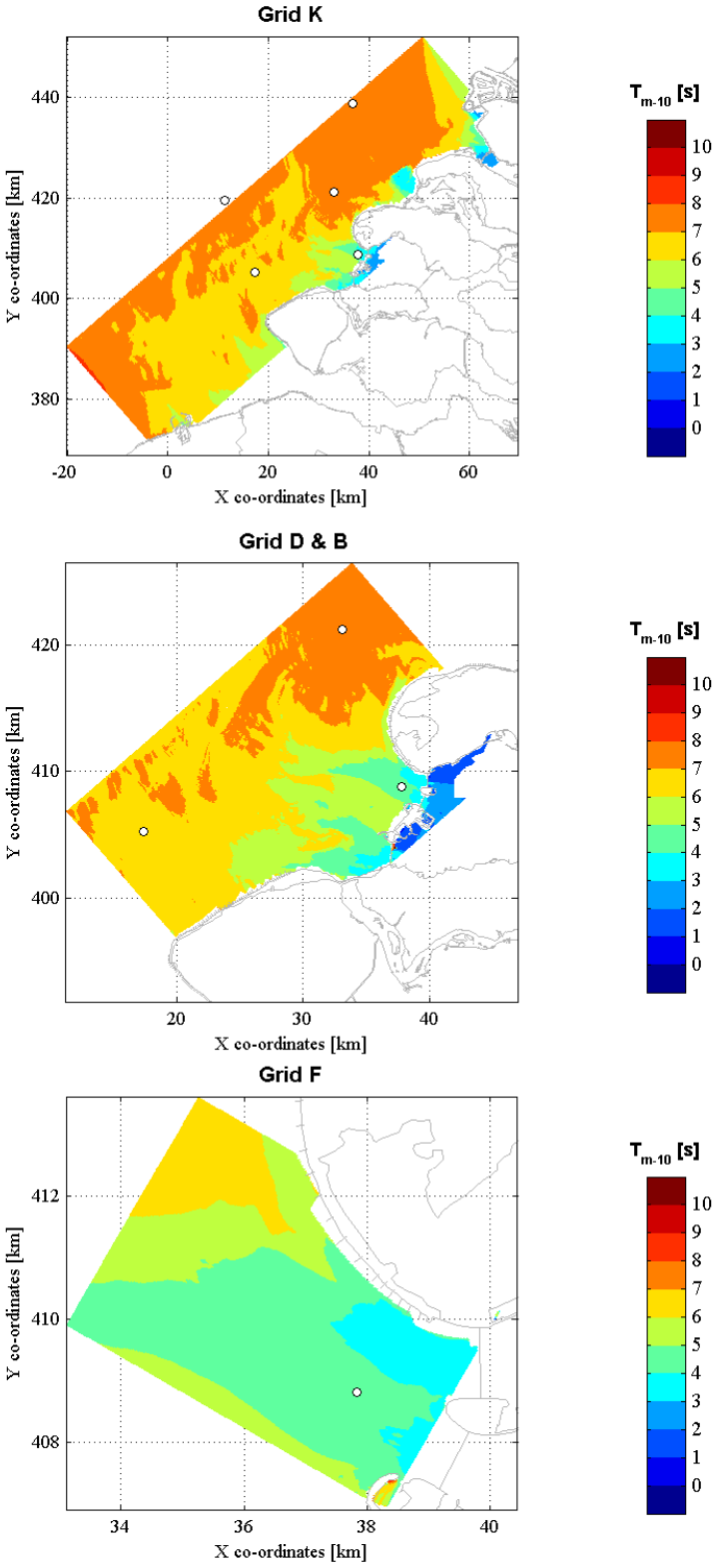

SVASEK HYDRAULICS

SWAN results: The wave period T_{m-10}

Storm B t3 (23-Dec-2003 02:30:00)

APPENDIX 5.4.B3
1461
18-Dec-2007

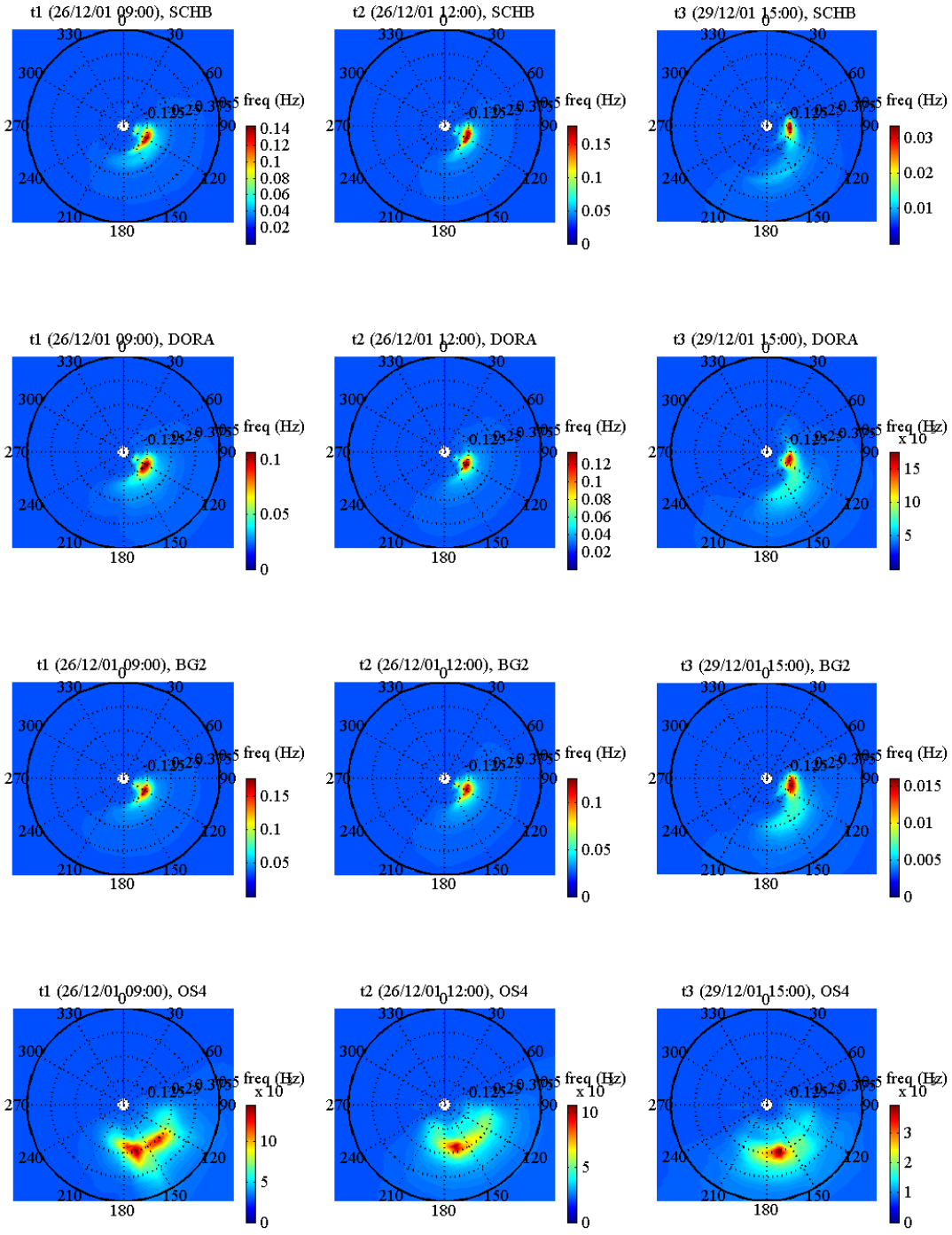

SWAN results: 2D Energy Density Spectrum
Storm A

radial gridlines: 0.125 0.2 0.375 0.5Hz
direction: going to

APPENDIX 5.5.A
1461
18-Dec-2007

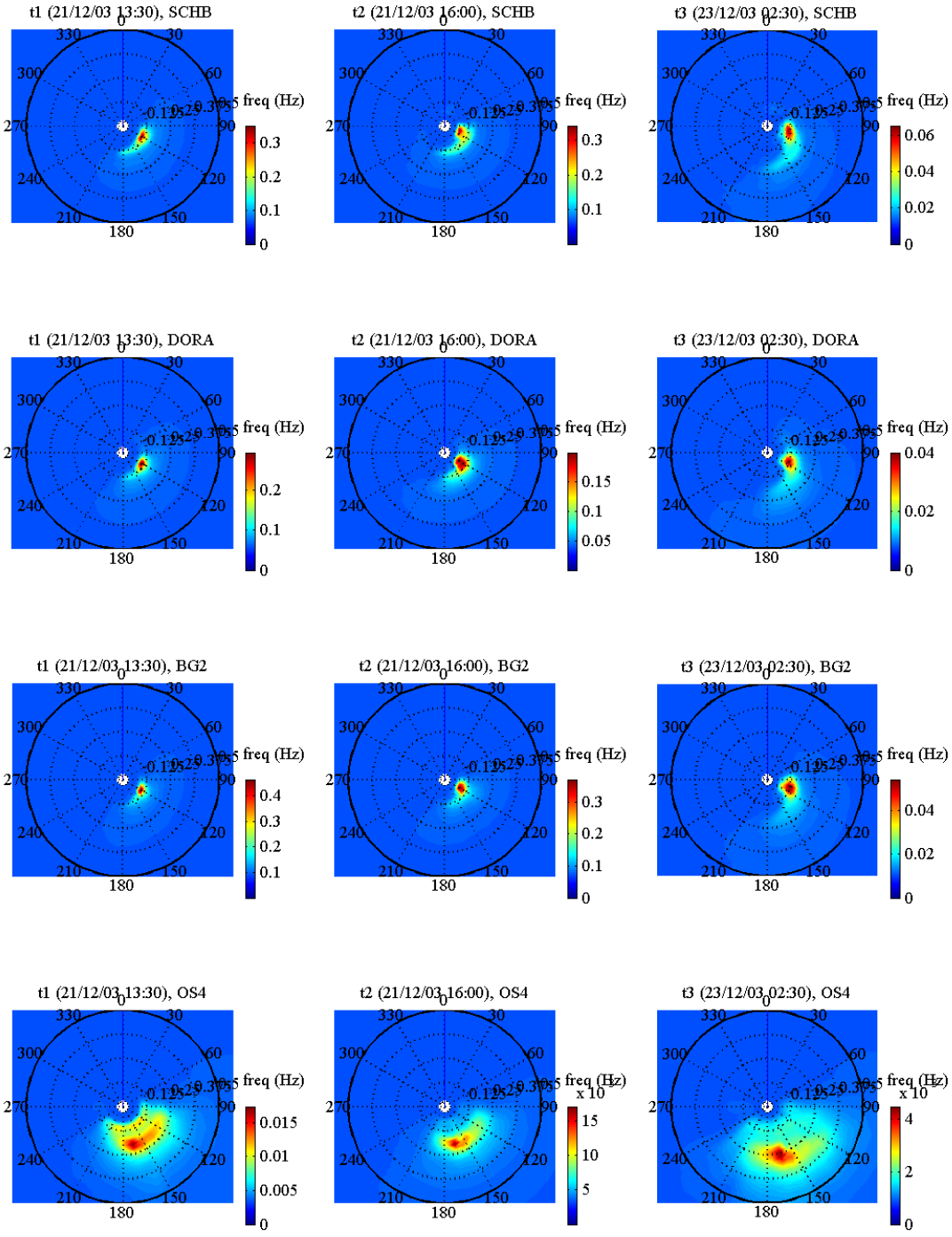

SWAN results: 2D Energy Density Spectrum
Storm B

radial gridlines: 0.125 0.2 0.375 0.5Hz
direction: going to

APPENDIX 5.5.B
1461
18-Dec-2007

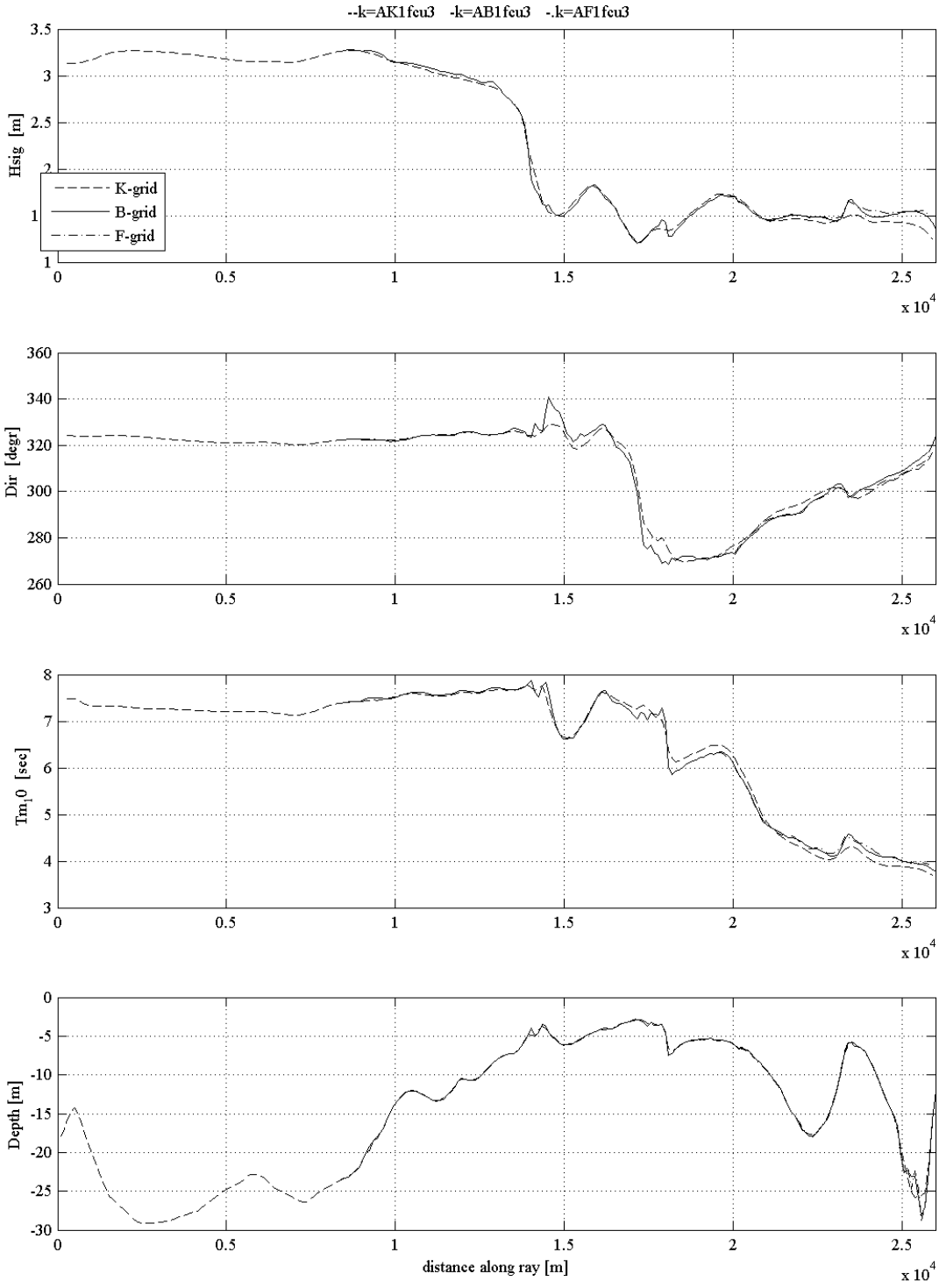

SWAN paramters on curve 3

Storm A t1

APPENDIX 5.6.A1
1461
18-Dec-2007

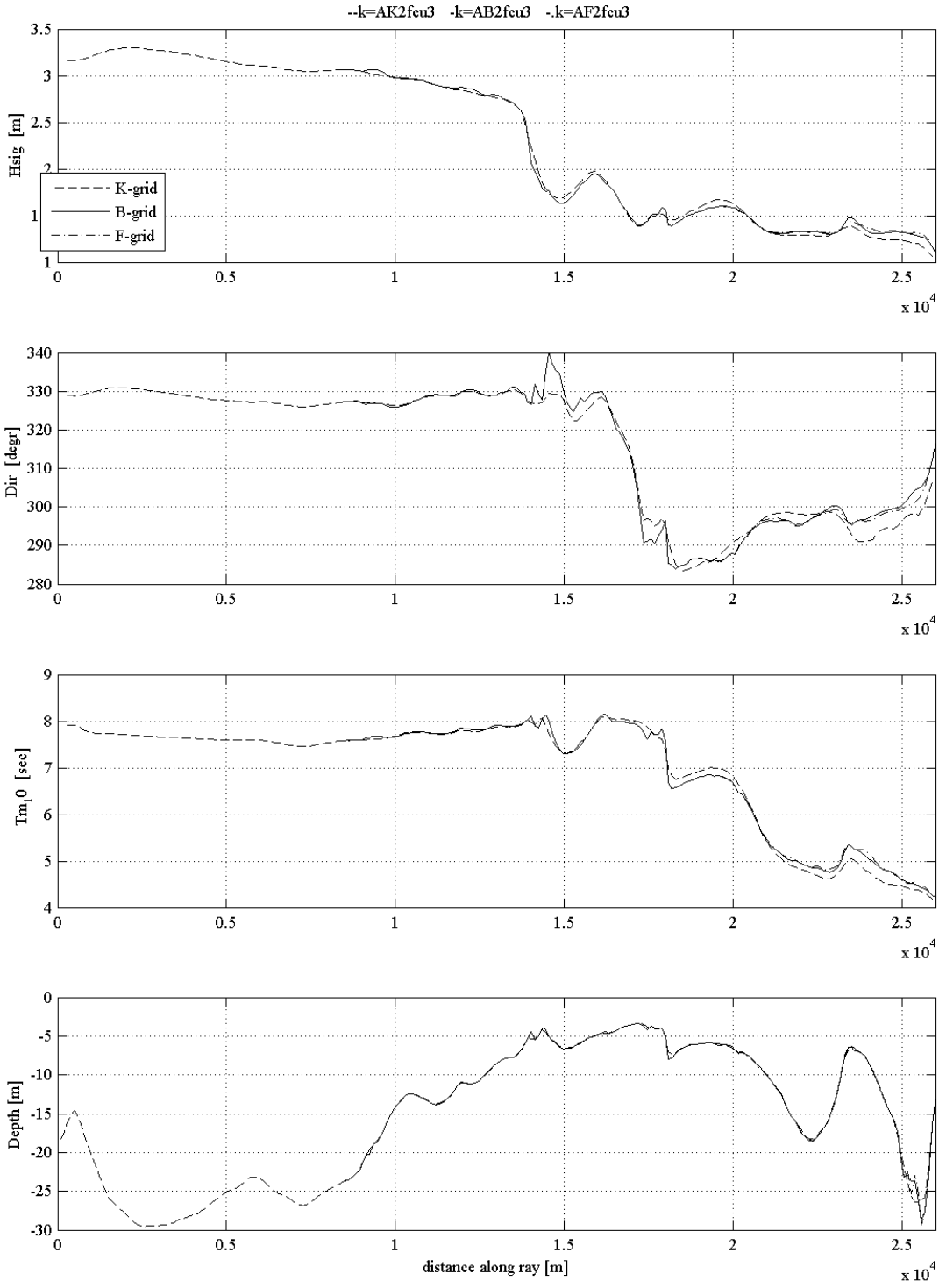

SWAN paramters on curve 3

Storm A t2

APPENDIX 5.6.A2
1461
18-Dec-2007

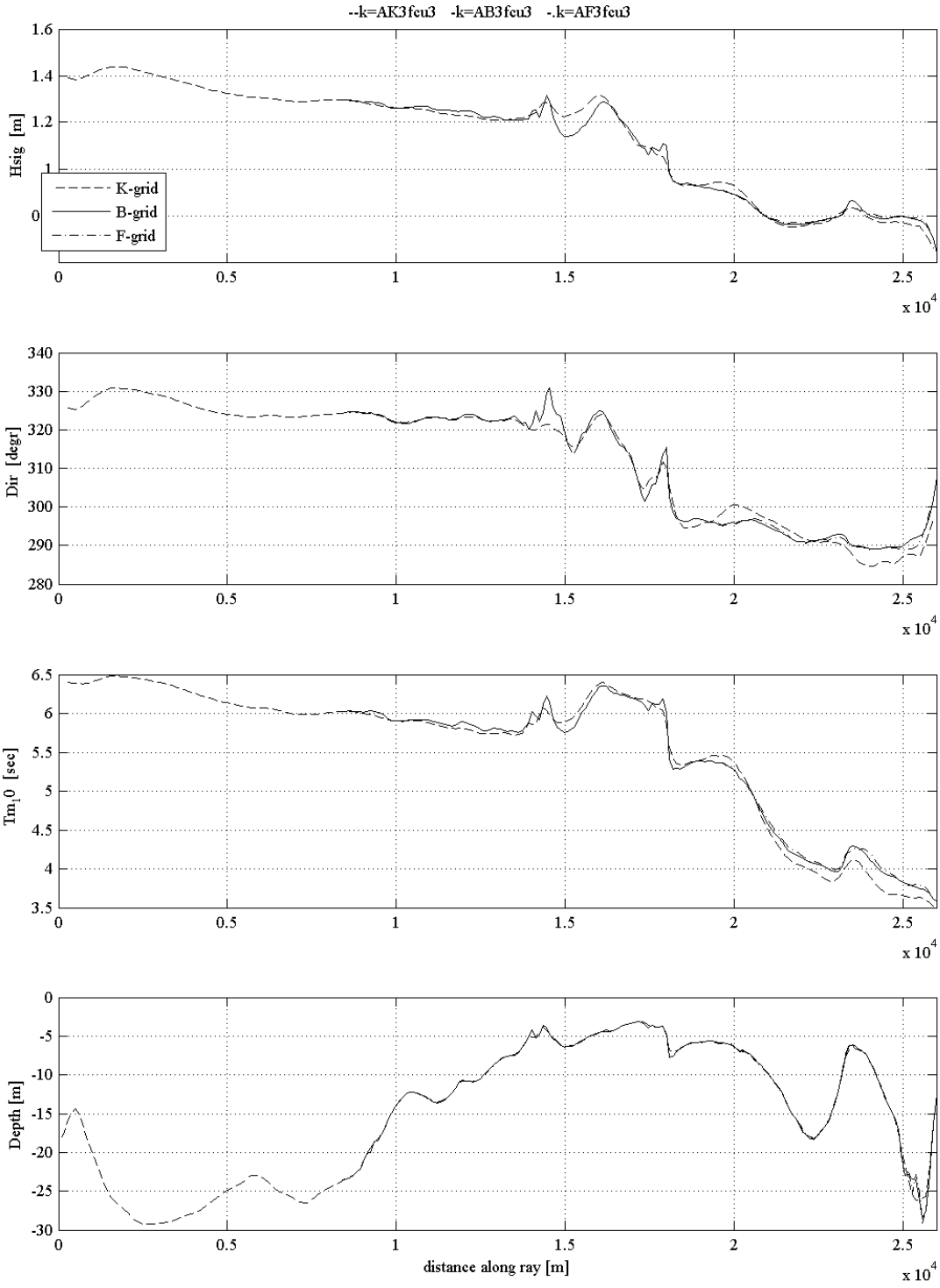

SVASEK HYDRAULICS

SWAN paramters on curve 3

Storm A t3

APPENDIX 5.6.A3
1461
18-Dec-2007

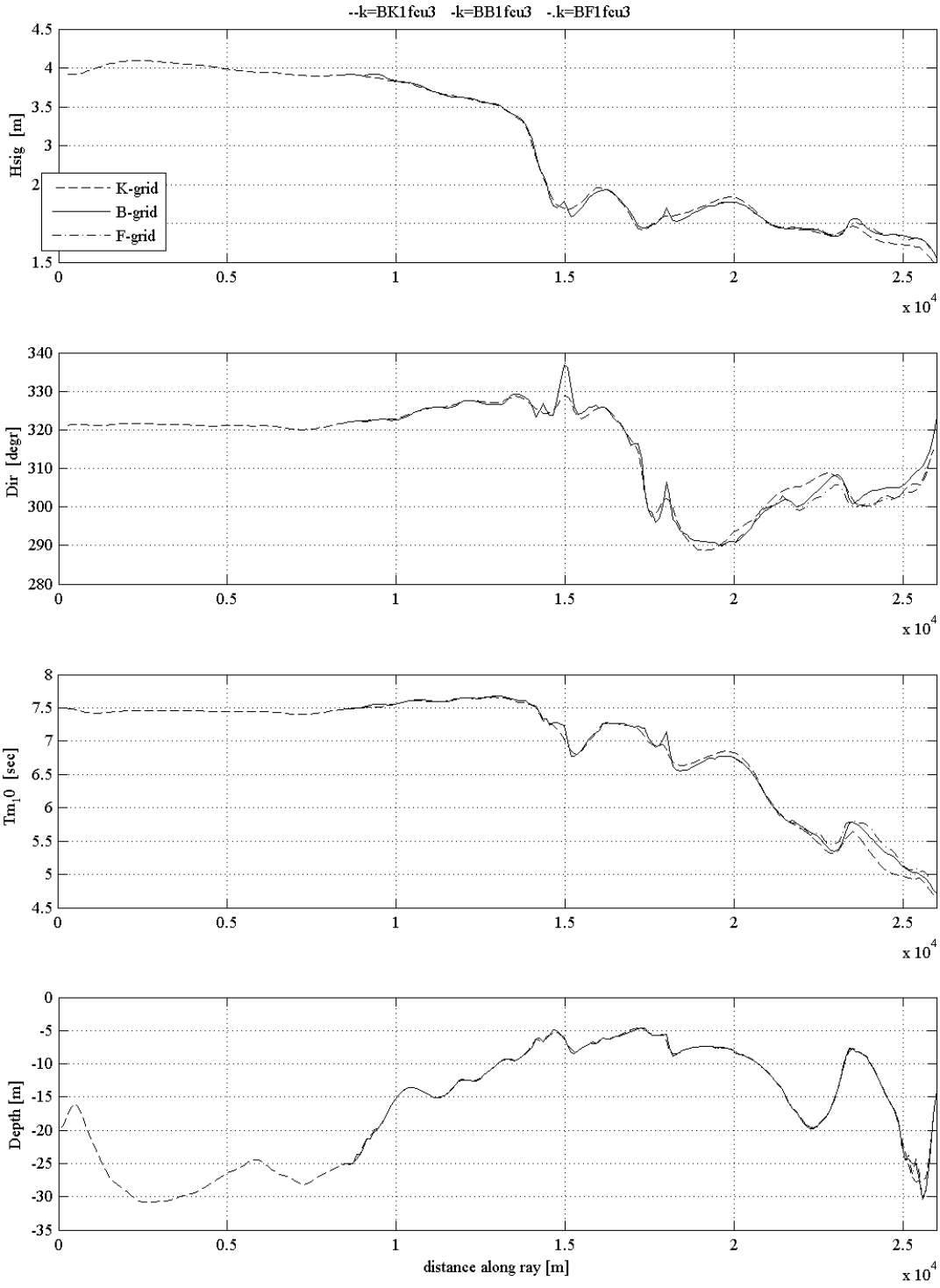

SVASEK HYDRAULICS

SWAN paramters on curve 3

Storm B t1

APPENDIX 5.6.B1
1461
18-Dec-2007

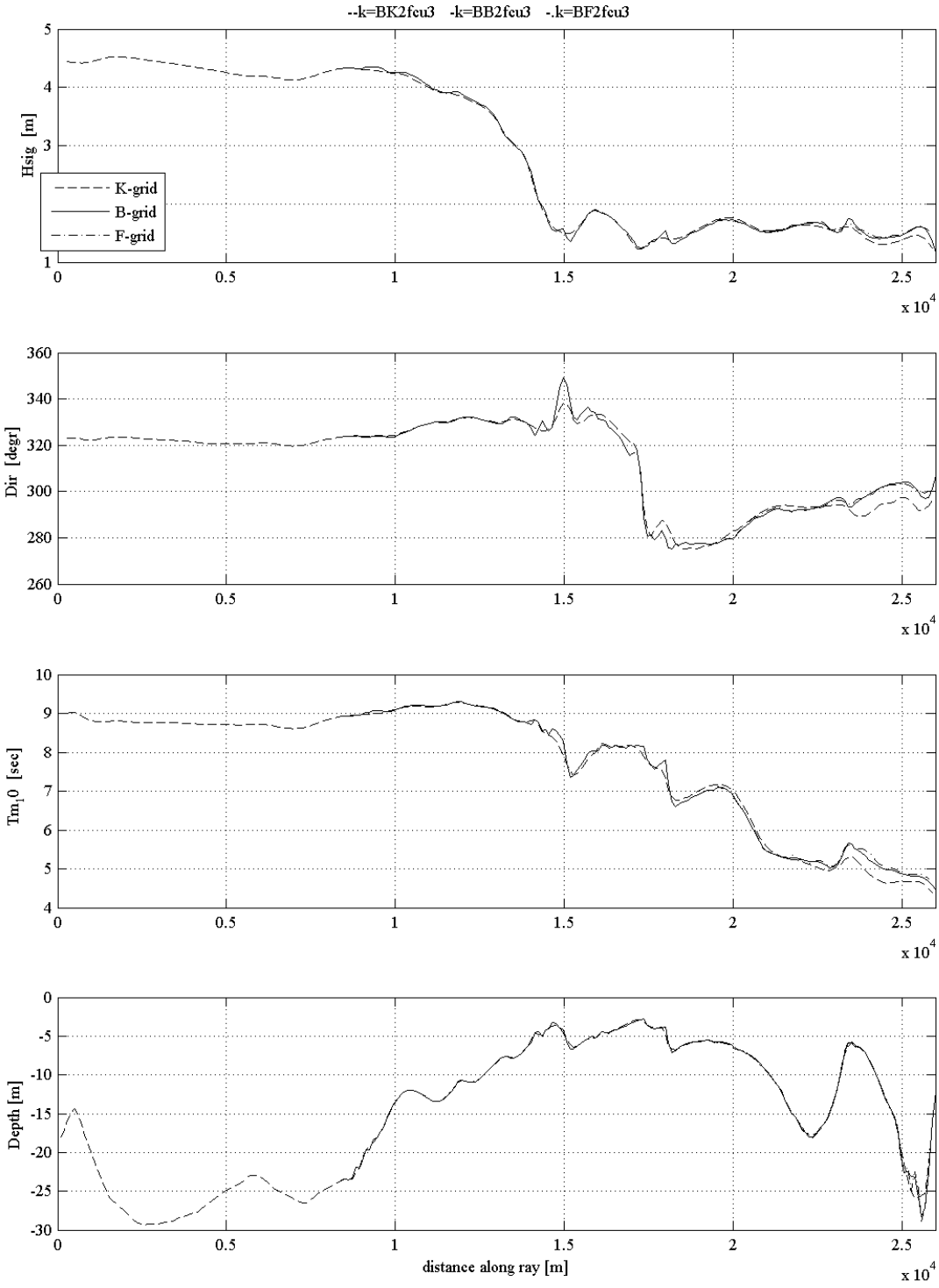

SVASEK HYDRAULICS

SWAN paramters on curve 3

Storm B t2

APPENDIX 5.6.B2
1461
18-Dec-2007

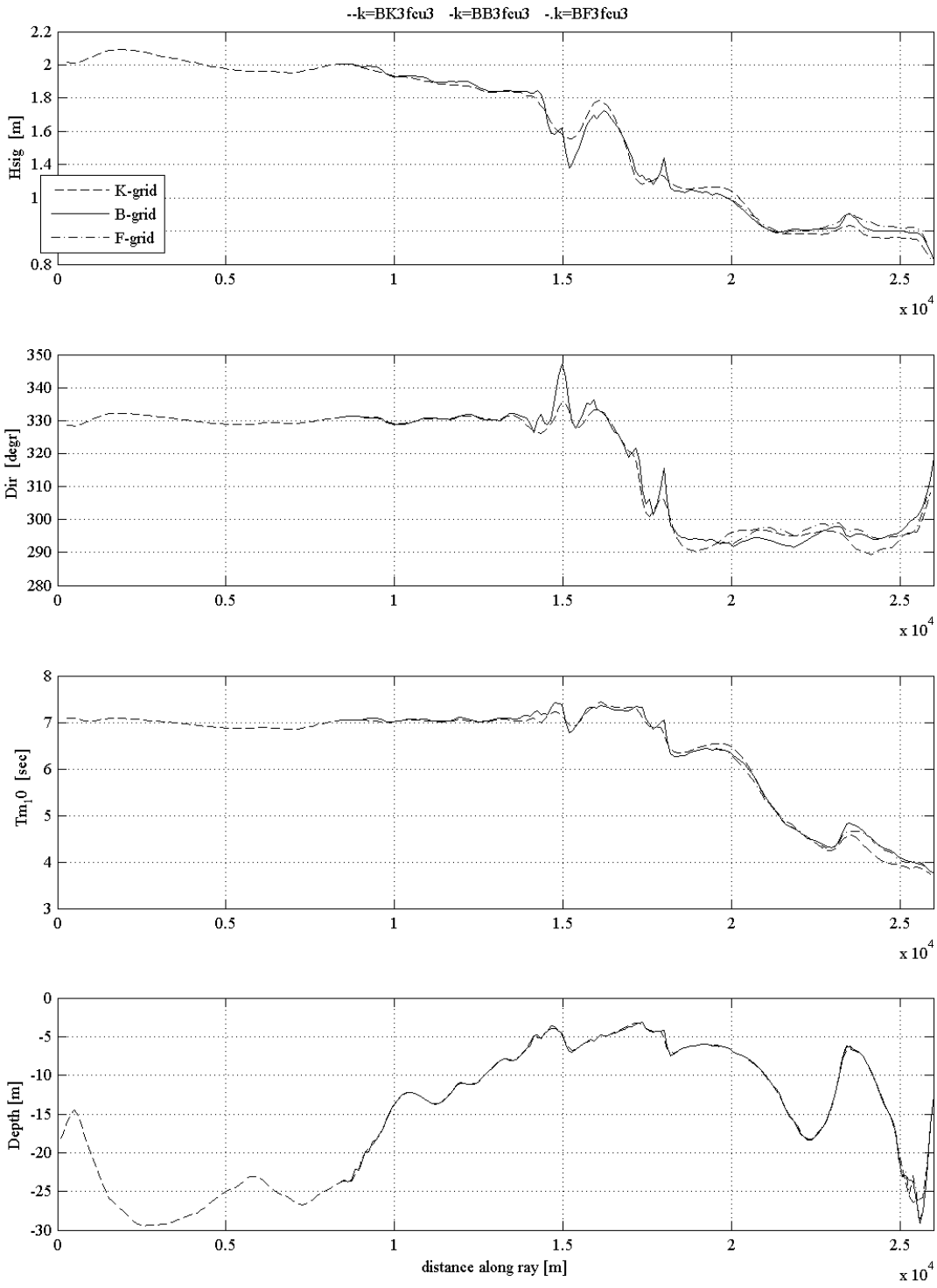

SVASEK HYDRAULICS

SWAN paramters on curve 3

Storm B t3

APPENDIX 5.6.B3
1461
18-Dec-2007

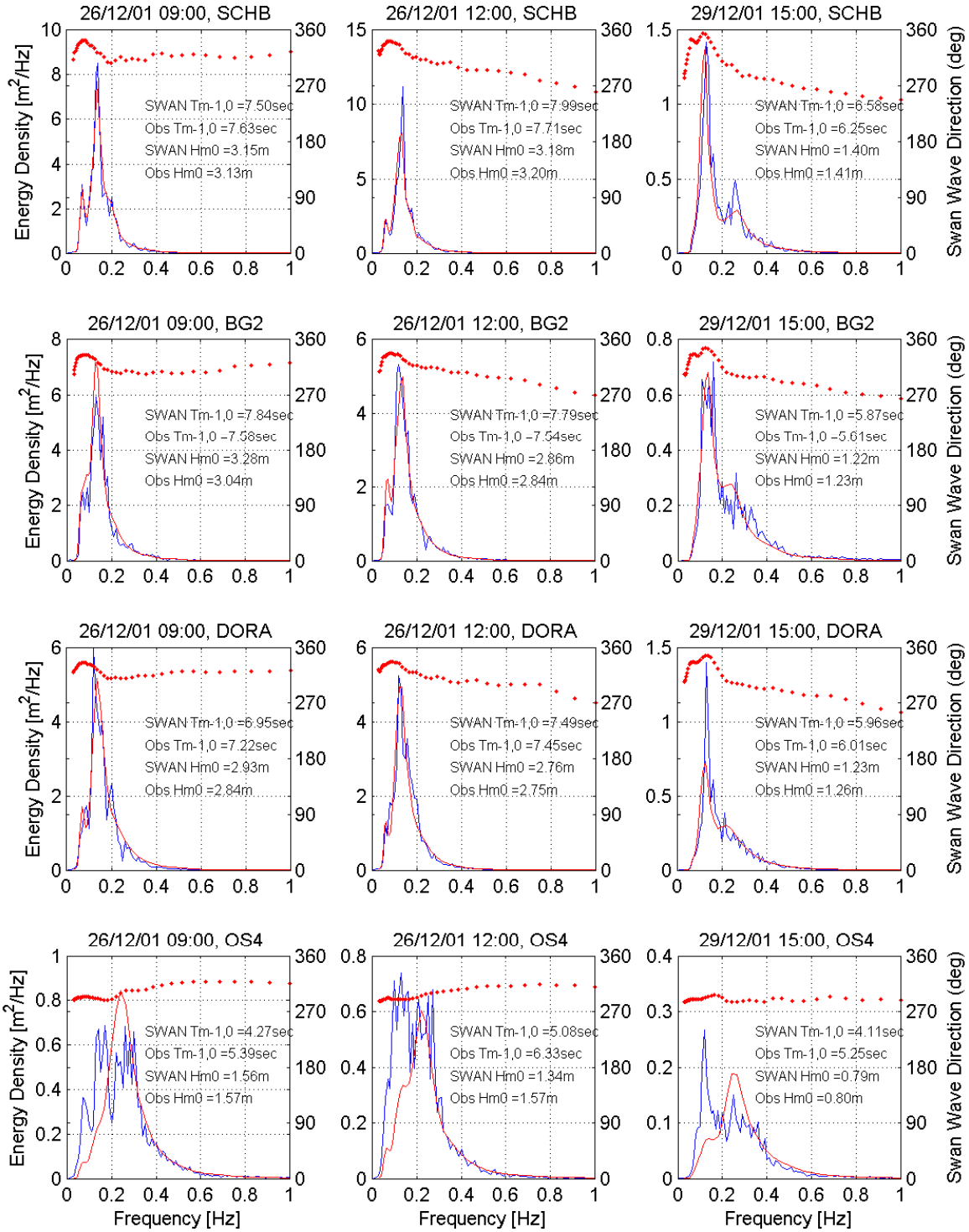

SVASEK HYDRAULICS

Energy Density Spectrum Storm A, layout versie f **APPENDIX 6.1.a**

1461

blue line = observation; red line = SWAN calc.; circle = SWAN dir. 14-Dec-2007

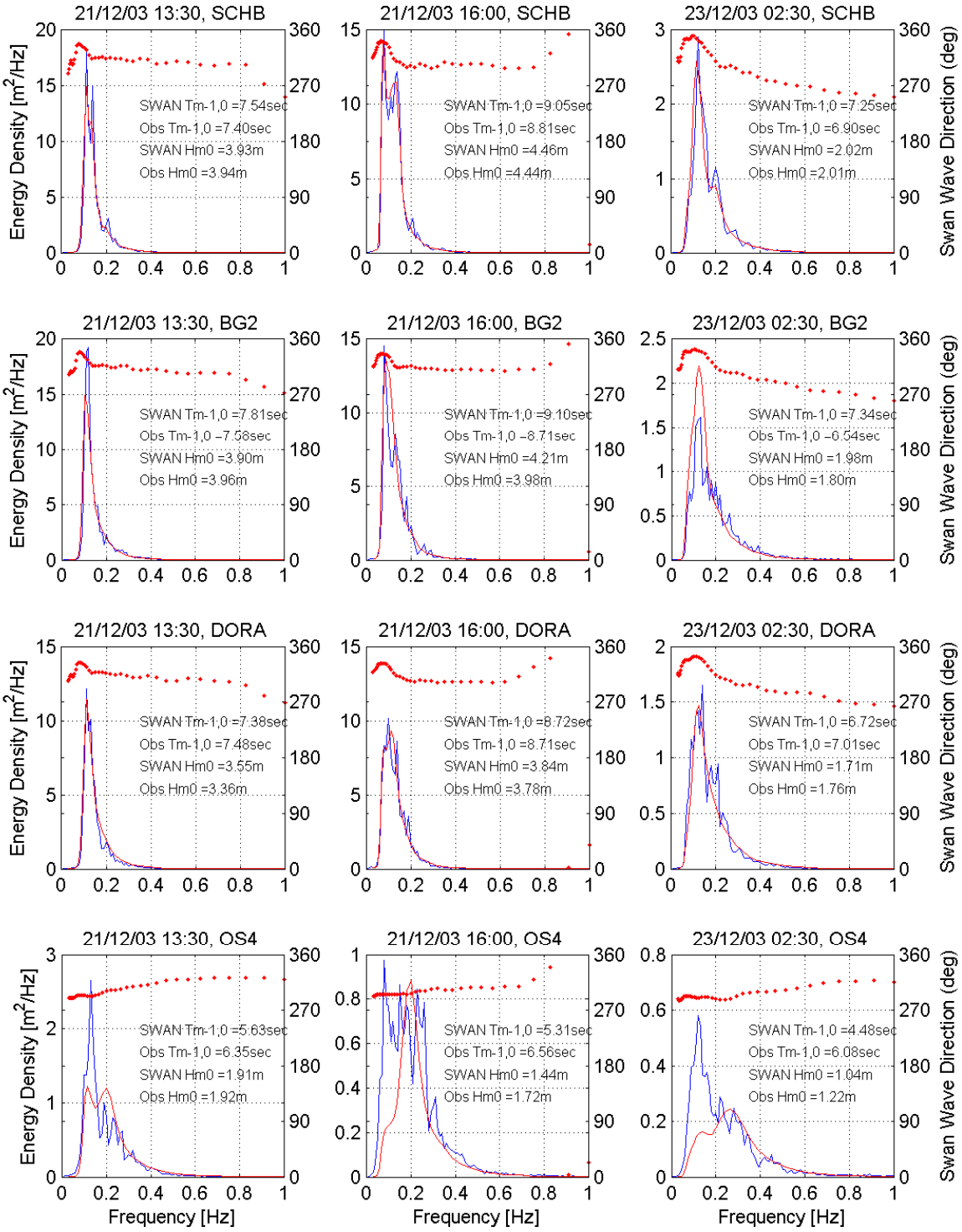

SVASEK HYDRAULICS

Energy Density Spectrum Storm B, layout versie f **APPENDIX 6.1.b**

1461

blue line = observation; red line = SWAN calc.; circle = SWAN dir. 14-Dec-2007

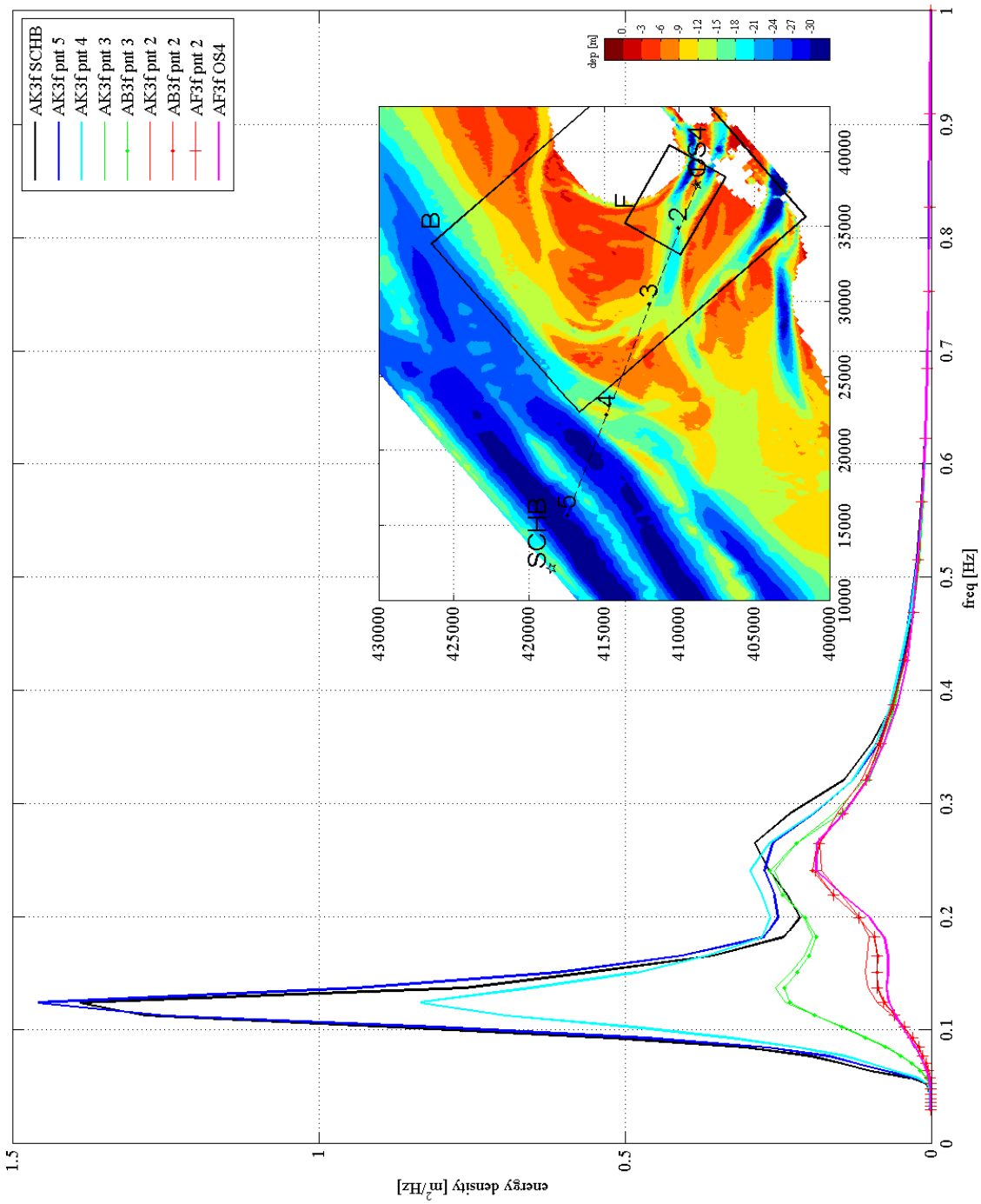

1D spectra on curve 6

Storm A , time 3 , version f

FIGUUR 6.2.A
1461
19-Dec-2007

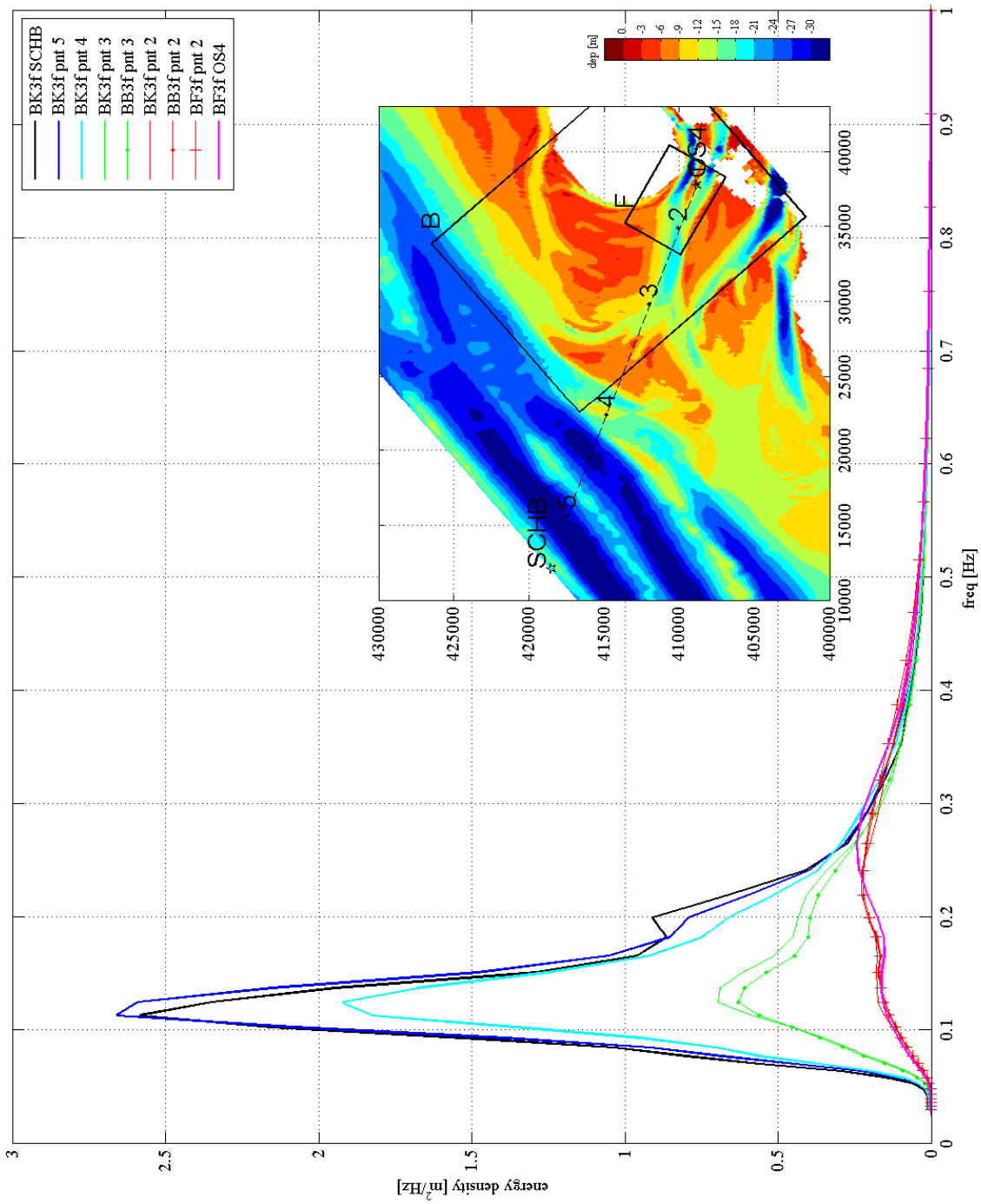

SVASEK HYDRAULICS

1D spectra on curve 6

Storm B , time 3 , version f

FIGUUR 6.2.B
1461
19-Dec-2007

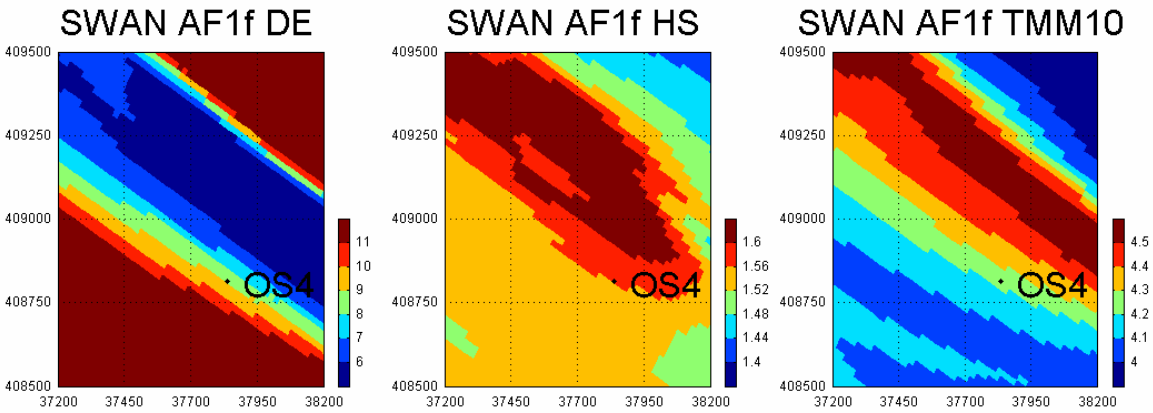
SWAN AF1f DE
SWAN AF1f HS
SWAN AF1f TMM10
OS4
409500
409250
409000
408750
408500
37200
37450
37700
37950
38200
11
10
9
8
7
6
1.6
1.56
1.52
1.48
1.44
1.4
4.5
4.4
4.3
4.2
4.1
4

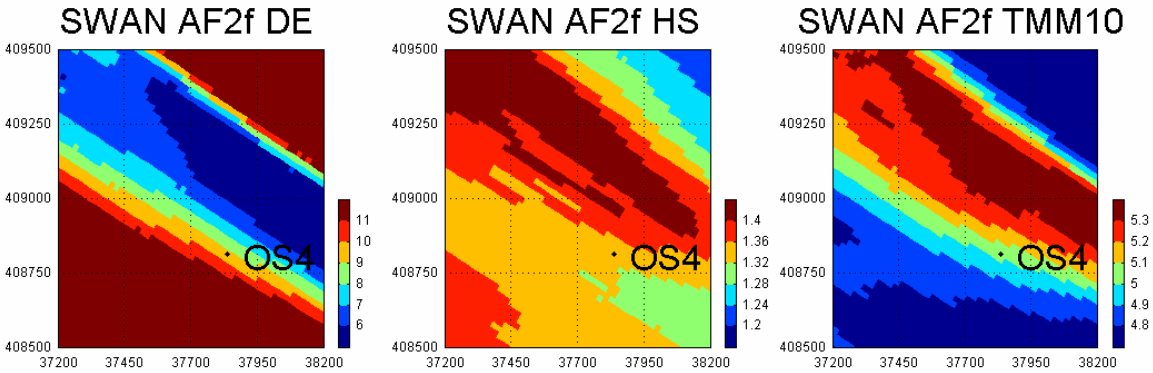
SWAN AF2f DE
SWAN AF2f HS
SWAN AF2f TMM10
OS4
409500
409250
409000
408750
408500
37200
37450
37700
37950
38200
11
10
9
8
7
6
1.4
1.36
1.32
1.28
1.24
1.2
5.3
5.2
5.1
5
4.9
4.8

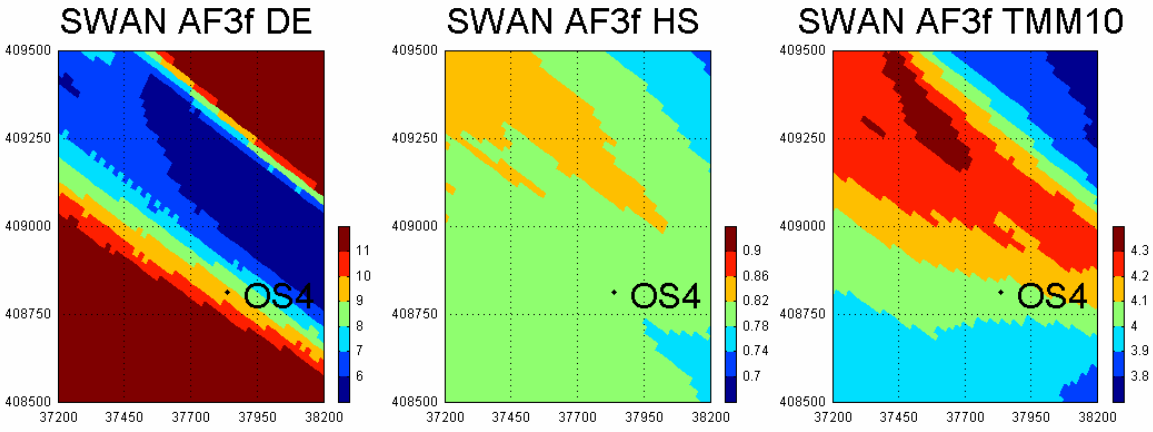
SWAN AF3f DE
SWAN AF3f HS
SWAN AF3f TMM10
OS4
409500
409250
409000
408750
408500
37200
37450
37700
37950
38200
11
10
9
8
7
6
0.9
0.86
0.82
0.78
0.74
0.7
4.3
4.2
4.1
4
3.9
3.8

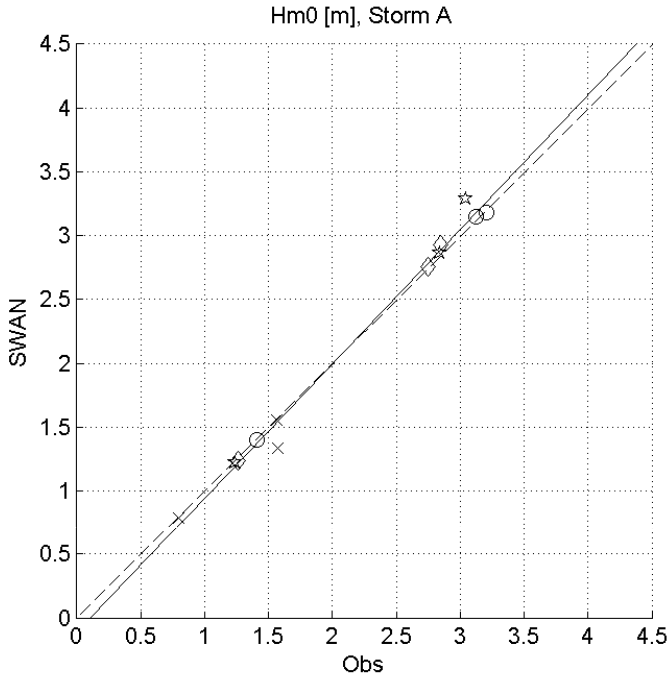

SWAN =1.05* Obs -0.11
r = 1.00

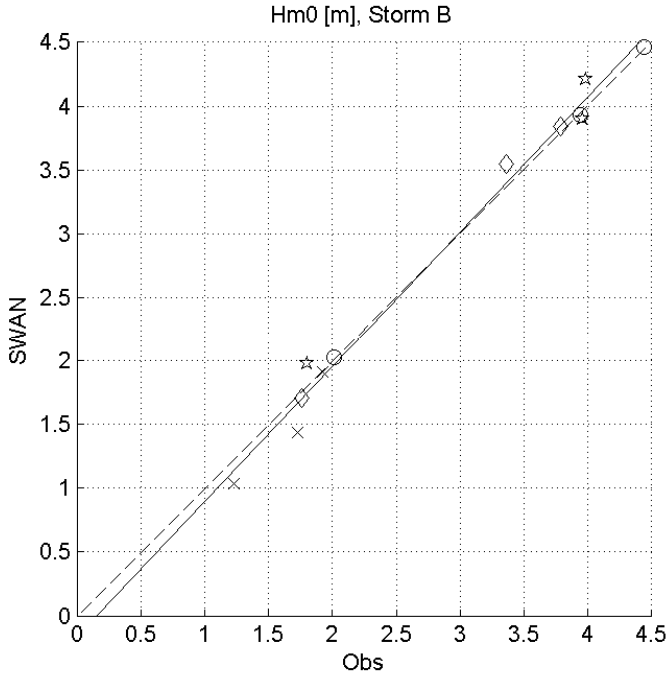

SWAN =1.06* Obs -0.16
r = 0.99

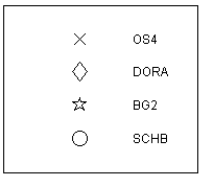

Scatterplots Storm A en Storm B

parameter Hm0, layout versie f

APPENDIX 6.4.a
1461
14-Dec-2007

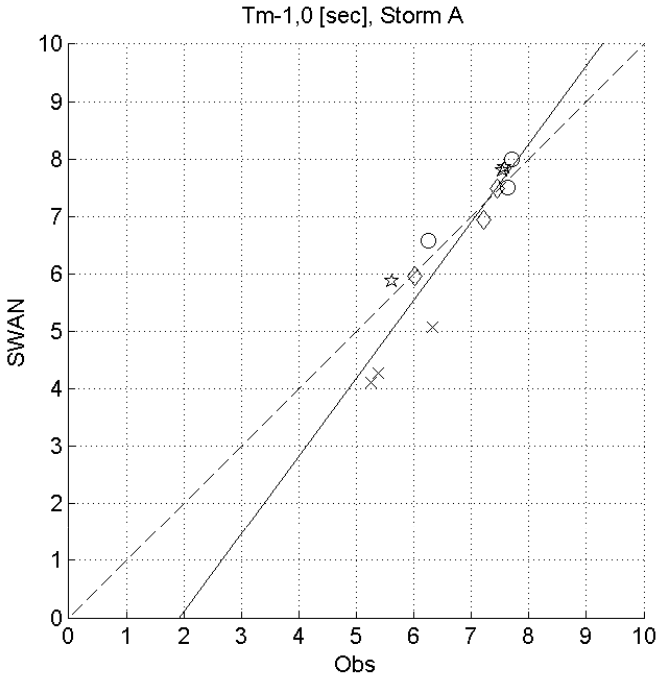

SWAN =1.36* Obs -2.61
r = 0.93

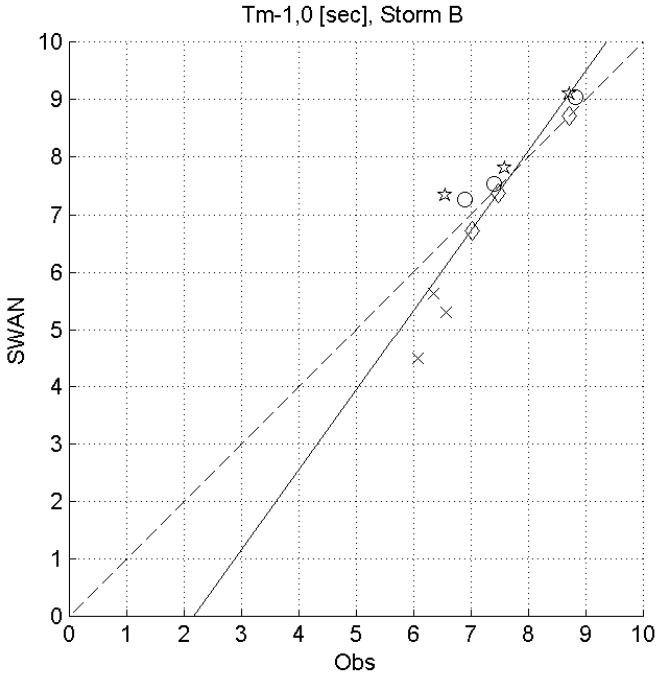

SWAN =1.39* Obs -3.03
r = 0.91

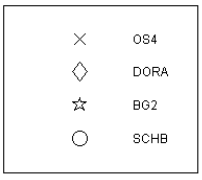

Scatterplots Storm A en Storm B

parameter Tm-1,0, layout versie f

APPENDIX 6.4.b
1461
14-Dec-2007

Storm A

Parameter	Hm0	Tp	Tm-1,0	Tm02
n	12	12	12	12
BIAS %	0.2	-10.7	-3.2	-4.1
St dev %	5.2	20.5	10.5	7
MAE %	2.8	16.1	7.4	7.1
r	1	0.2	0.93	0.96
a	1.05	0.36	1.36	1.01
b	-0.11	3.99	-2.61	-0.24

Storm B

Parameter	Hm0	Tp	Tm-1,0	Tm02
n	12	12	12	12
BIAS %	0.2	-8.6	-2	-1.9
St dev %	7.8	25.2	11	8.6
MAE %	5.1	16.3	7.7	6.6
r	0.99	0.32	0.91	0.95
a	1.06	0.4	1.39	1.06
b	-0.16	4.85	-3.03	-0.44

Storm A & B

Parameter	Hm0	Tp	Tm-1,0	Tm02
n	24	24	24	24
BIAS %	0.2	-9.5	-2.6	-2.9
St dev %	6.5	22.6	10.5	7.7
MAE %	3.9	16.2	7.6	6.8
r	1	0.46	0.93	0.96
a	1.05	0.57	1.34	1.05
b	-0.12	2.82	-2.57	-0.4

The following statistical parameters have been determined:

N = number of observations (or calculations) in population (N=12 per storm)

$$BIAS = \left(\frac{\bar{y} - \bar{x}}{\bar{x}} \right) \times 100(\%)$$

With , $\bar{y}$ = mean calculated $\frac{1}{N}\sum_{i=1}^{N} y_i$ $\bar{x}$ = mean observed $\frac{1}{N}\sum_{i=1}^{N} x_i$

y_i = value calculation x_i = value observation

The standard deviation is calculated on the normalized difference between calculation and observation

$$STDEV = STD(a) \times 100(\%)$$

$$a = \left(\frac{(y_i - x_i)}{x_i} \right), \quad \text{i = 1 to N}$$

$$STD(a) = \sqrt{\frac{n\sum a^2 - (\sum a)^2}{n \times (n-1)}}$$

MAE =relative Mean Absolute Error

$$\text{MAE} = \frac{1}{N}\sum_{i=1}^{N} \left| \frac{y_i - x_i}{x_i} \right| \times 100(\%)$$

A lineair relationship has been fitted between calculation and the observation.
The lineair relationship is presented by:

$$y = a \times x + b$$

The coefficient of lineair correlation, r, is calculated by:

$$r = \frac{\sum_{i=1}^{N} (x_i - \bar{x}) \times (y_i - \bar{y})}{\sqrt{\sum_{i=1}^{N} (x_i - \bar{x})^2} \times \sqrt{\sum_{i=1}^{N} (y_i - \bar{y})^2}}$$

STORM A

loc	Hm0 (measurement) [m] t1	t2	t3	Hm0 (swan) [m] t1	t2	t3	Hm0 (measurement) - Hm0 (swan) [m] t1	t2	t3
SCHB	3.13	3.2	1.41	3.15	3.18	1.4	-0.02	0.03	0.01
BG2	3.04	2.85	1.24	3.29	2.86	1.22	-0.24	-0.02	0.02
DORA	2.84	2.75	1.26	2.93	2.76	1.24	-0.09	-0.01	0.03
OS4	1.57	1.57	0.8	1.57	1.34	0.79	0.01	0.23	0.01

loc	Tm-10 (measurement) [s] t1	t2	t3	Tm-10 (measurement) [s] t1	t2	t3	Tm-10 (measurement) - Tm-10 (swan) [s] t1	t2	t3
SCHB	7.6	7.7	6.3	7.5	8.0	6.6	0.1	-0.3	-0.3
BG2	7.6	7.5	5.5	7.8	7.8	5.9	-0.3	-0.3	-0.3
DORA	7.2	7.5	6.0	6.9	7.5	5.9	0.3	0.0	0.1
OS4	5.3	6.3	5.2	4.3	5.1	4.1	1.1	1.3	1.1

loc	Tm02 (measurement) [s] t1	t2	t3	Tm02 (measurement) [s] t1	t2	t3	Tm02 (measurement) - Tm02 (swan) [s] t1	t2	t3
SCHB	6.0	6.1	4.6	5.4	5.9	4.0	0.6	0.2	0.6
BG2	5.1	4.8	2.9	5.3	5.3	3.7	-0.2	-0.6	-0.7
DORA	5.6	5.8	4.4	4.6	5.3	3.7	1.0	0.5	0.7
OS4	3.0	3.7	3.0	2.9	3.2	2.7	0.1	0.5	0.3

STORM B

loc	Hm0 (measurement) [m] t1	t2	t3	Hm0 (swan) [m] t1	t2	t3	Hm0 (measurement) - Hm0 (swan) [m] t1	t2	t3
SCHB	3.94	4.44	2.01	3.93	4.46	2.03	0.01	-0.02	-0.01
BG2	3.96	3.99	1.81	3.9	4.21	1.98	0.06	-0.22	-0.17
DORA	3.36	3.78	1.76	3.55	3.84	1.71	-0.19	-0.05	0.05
OS4	1.93	1.73	1.23	1.91	1.44	1.04	0.01	0.29	0.19

loc	Tm-10 (measurement) [s] t1	t2	t3	Tm-10 (measurement) [s] t1	t2	t3	Tm-10 (measurement) - Tm-10 (swan) [s] t1	t2	t3
SCHB	7.4	8.8	6.9	7.5	9.1	7.2	-0.1	-0.2	-0.4
BG2	7.6	8.7	6.5	7.8	9.1	7.3	-0.2	-0.4	-0.8
DORA	7.5	8.7	7.0	7.4	8.7	6.7	0.1	0.0	0.3
OS4	6.3	6.5	6.0	5.6	5.3	4.5	0.7	1.2	1.5

loc	Tm02 (measurement) [s] t1	t2	t3	Tm02 (measurement) [s] t1	t2	t3	Tm02 (measurement) - Tm02 (swan) [s] t1	t2	t3
SCHB	6.3	7.0	5.3	6.1	7.0	4.8	0.2	0.0	0.5
BG2	5.7	6.2	3.8	6.0	6.8	4.7	-0.3	-0.6	-1.0
DORA	6.3	6.9	5.2	5.7	6.6	4.3	0.5	0.3	0.8
OS4	4.0	3.7	2.9	3.7	4.0	2.8	0.2	-0.2	0.1

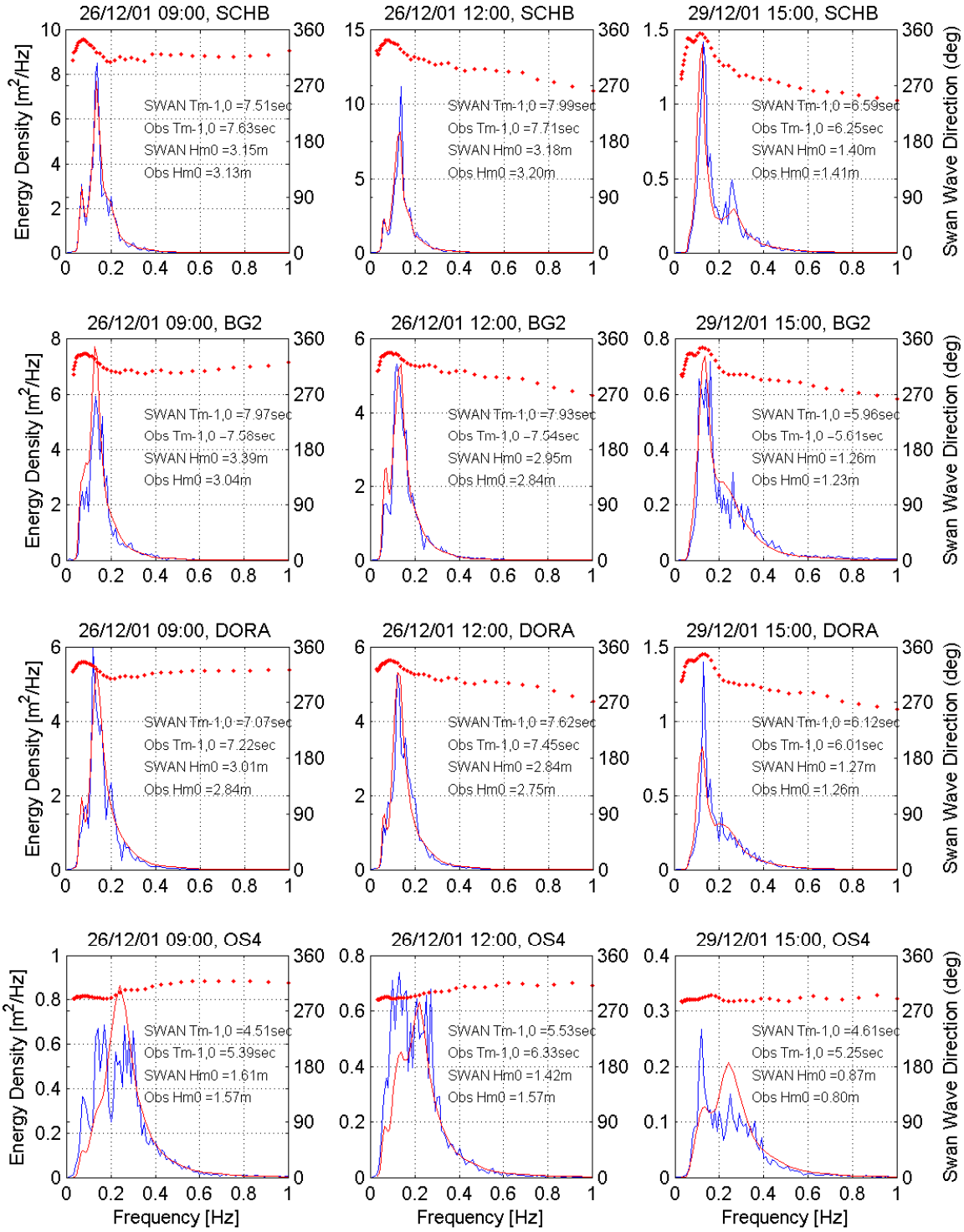

SVASEK HYDRAULICS

Energy Density Spectrum Storm A, layout versie g **APPENDIX 7.1.a**

1461

blue line = observation; red line = SWAN calc.; circle = SWAN dir. 14-Dec-2007

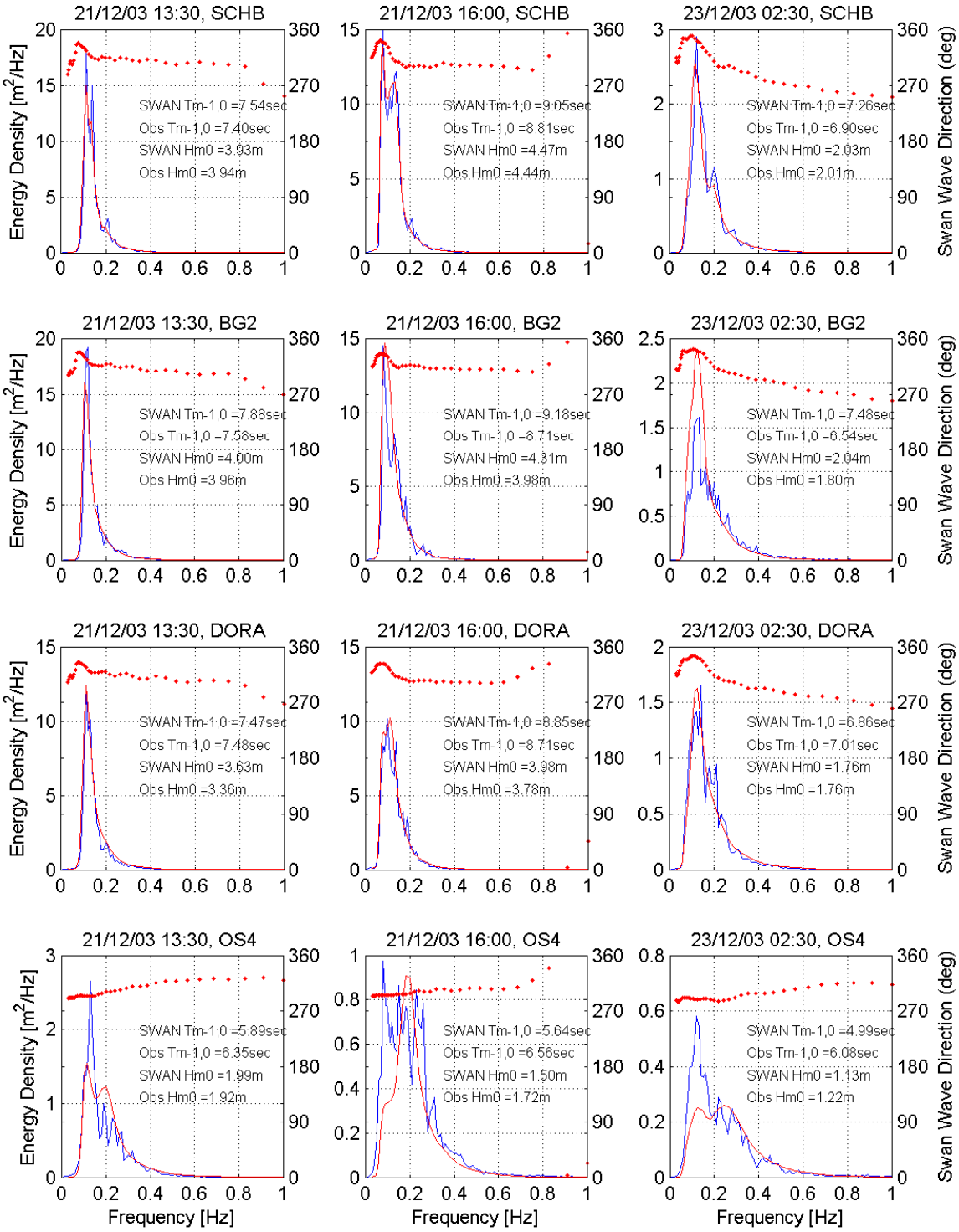

SVASEK HYDRAULICS

Energy Density Spectrum Storm B, layout versie g **APPENDIX 7.1.b**

1461

blue line = observation; red line = SWAN calc.; circle = SWAN dir. 14-Dec-2007

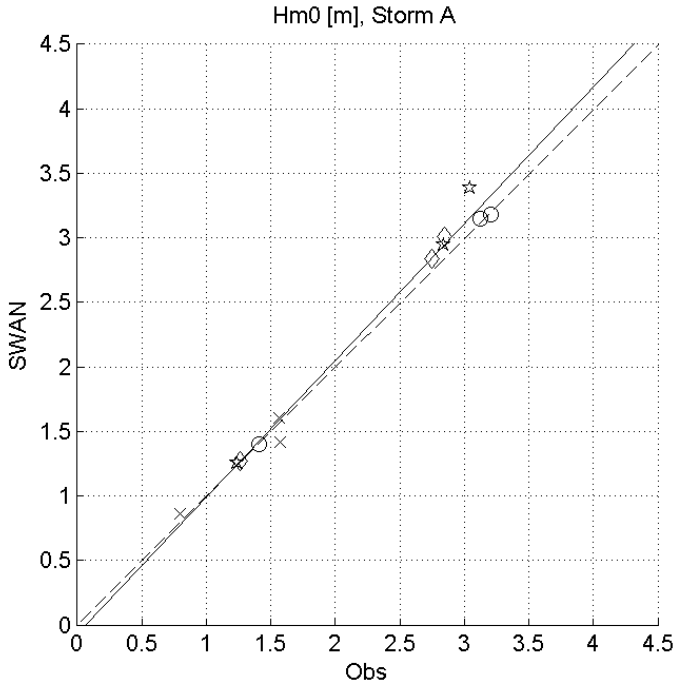
Hm0 [m], Storm A
SWAN
Obs
0
0.5
1
1.5
2
2.5
3
3.5
4
4.5
SWAN =1.06* Obs -0.07
r = 0.99

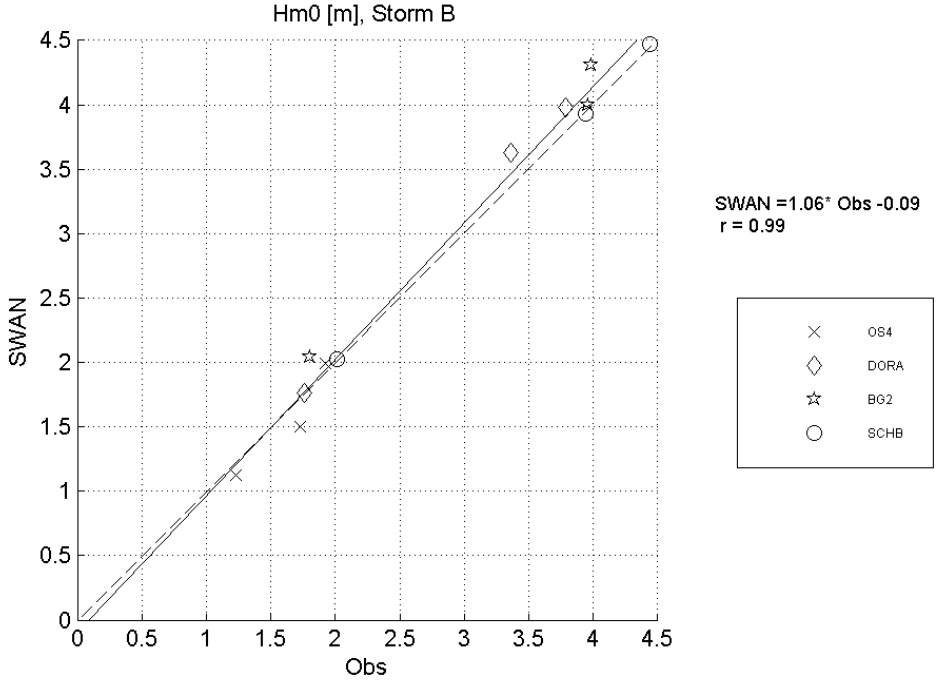
Hm0 [m], Storm B
SWAN
Obs
0
0.5
1
1.5
2
2.5
3
3.5
4
4.5
SWAN =1.06* Obs -0.09
r = 0.99
OS4
DORA
BG2
SCHB

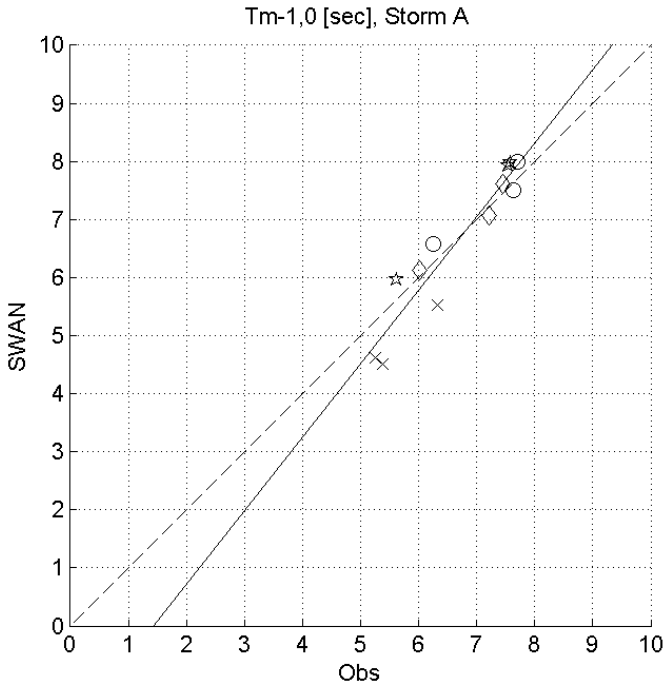

SWAN =1.26* Obs -1.81
r = 0.95

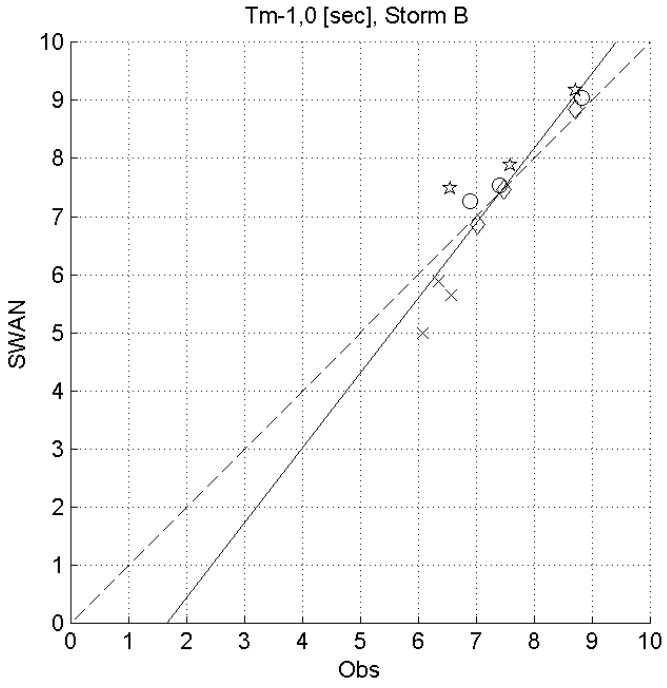

SWAN =1.29* Obs -2.15
r = 0.93

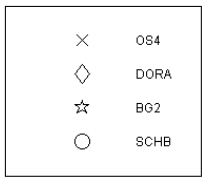

Scatterplots Storm A en Storm B

parameter Tm-1,0, layout versie g

APPENDIX 7.2.b
1461
07-Dec-2007

Storm A, version g

Parameter	Hm0	Tp	Tm-1,0	Tm02
n	12	12	12	12
BIAS %	2.7	-9.9	-0.7	-2.4
St dev %	5.3	20.6	8	6.4
MAE %	4.1	15.3	6.2	6
r	0.99	0.23	0.95	0.96
a	1.06	0.44	1.26	0.98
b	-0.07	3.45	-1.81	0

Storm B, version g

Parameter	Hm0	Tp	Tm-1,0	Tm02
n	12	12	12	12
BIAS %	2.5	-7.8	0	-0.3
St dev %	7	23.7	8.8	8.1
MAE %	5.1	15.6	6.4	5.6
r	0.99	0.36	0.93	0.95
a	1.06	0.43	1.29	1.02
b	-0.09	4.68	-2.15	-0.15

Storm A & B, version g

Parameter	Hm0	Tp	Tm-1,0	Tm02
n	24	24	24	24
BIAS %	2.6	-8.7	-0.4	-1.3
St dev %	6.1	21.8	8.3	7.2
MAE %	4.6	15.5	6.3	5.8
r	0.99	0.49	0.94	0.96
a	1.05	0.6	1.25	1.02
b	-0.07	2.67	-1.79	-0.16

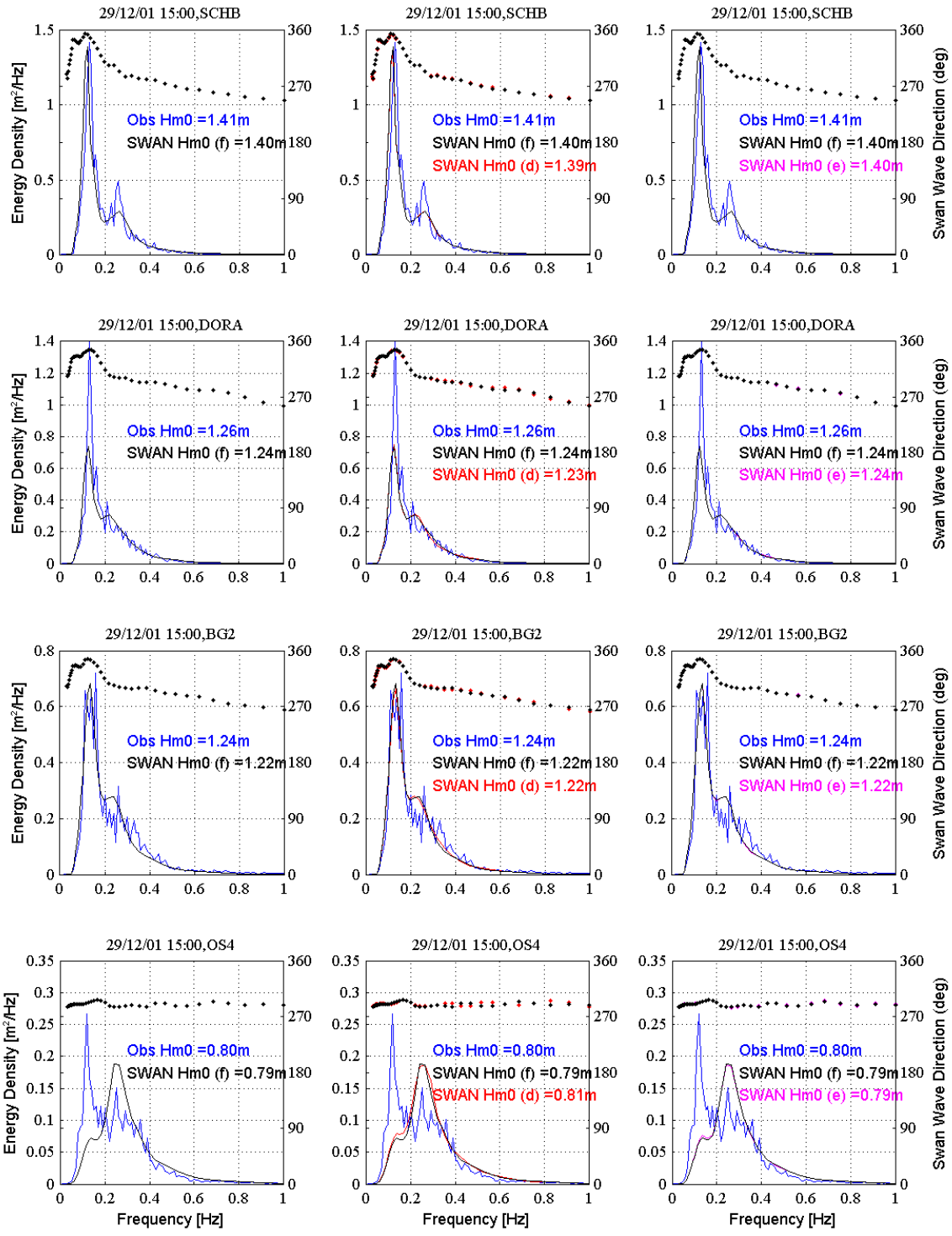

Comparison additional computations with the observations f (base case), d (directional resolution of 4^0), e (no triads)

Storm A t3 (=29-Dec-2001 15:00:00)

APPENDIX 7.4
1461
11-Dec-2007